UNIVERSIDADE DE SÃO PAULO
INSTITUTO DE FÍSICA DE SÃO CARLOS

FLÁVIO DE OLIVEIRA NETO

Effective lasers and enhancement of the radiation-matter interaction via pseudo-Hermitian Hamiltonians

São Carlos

2022

FLÁVIO DE OLIVEIRA NETO

Effective lasers and enhancement of the radiation-matter interaction via pseudo-Hermitian Hamiltonians

Thesis presented to the Graduate Program in Physics at the Instituto de Física de São Carlos da Universidade de São Paulo, to obtain the degree of Doctor in Science.

Concentration area: Theoretical Physics
Advisor: Prof. Dr. Miled Hassan Youssef Moussa

Corrected version

(original version available on the Program Unit)

São Carlos

2022

Oliveira Neto, Flávio
Effective lasers and enhancement of the radiation-matter interaction via pseudo-Hermitian Hamiltonians / Flávio Oliveira Neto; advisor Miled Hassan Youssef Moussa - corrected version -- São Carlos 2022.
104 p.

Thesis (Doctorate - Graduate Program in Basic Physics) -- Instituto de Física de São Carlos, Universidade de São Paulo - Brasil , 2022.

1. Quantum optics. 2. Laser theory. 3. Non-Hermitian quantum mechanics. I. Hassan Youssef Moussa, Miled, advisor. II. Title.

HERE'S TO MY FAMILY AND FRIENDS WHO HAVE ALWAYS SUPPORTED ME

ACKNOWLEDGMENTS

So many things happened during my doctorate. It feels like from a certain age life just goes by faster. Important things happen more often, suddenly a week is not so long and you change a lot of priorities. Social life, carrier, health, money... it all comes to time. I guess it is interesting how such different concepts, definitely not related to physics, can be resume to a single physical parameter. Perhaps the most important parameter in the universe, whose understanding fascinates because of its simplicity and also due to its complexity. If electrical impulses must travel through our nerves to our brain and even light itself takes a time to reach our eyes and be processed, everything we feel or see is in the past. Our responses are, therefore, delayed. Can we say we are always late? Like chasing something that we shall never reach? I think we can say that. We are always late, until we are not. Until there is no more time even to be late. No more time to take that travel, to eat that food, to be with that person. Time seems to be the one thing we are never getting back. It is our ultimate currency, the one that holds the absolute value of a certain matter. And yet we deal with it so brazenly. In the same planet, in the same country, in the same state, in the same city, in the very same neighborhood/block there are people whose hours have completely different values, according to our society. I believe this is the kind of issue you start noticing and being bothered about after some age, after some... time. How is that possible that one our of, let's say, a street sweeper, has so less value compared to a medical or a judge? Regardless of the impact of one's profession, we all live around the same amount of time and it seems extremely unfair that so many people spend so much of their time working only to have access to the basics to live by. And let's not be mistaken, all we buy we pay with some amount of our lifetime, and as I said, time is the one thing we are never getting back. Perhaps some social questions would be simpler if we understood that. The difference between a newborn and an old man is time. The difference between two people born in the same place but in different times can be gigantic. Long time ago we didn't have basic sanitation, no hygiene at all and medicine was so undeveloped that it was basically healerism. And probably in a long time we will be able to cure a great part of the diseases that today we can't, much more people will have access to basic sanitation and education and what to say about the new achievements in science? It may be like nowadays scientific fiction. And these people from this future might look back at us with the same pity we look at the people from a millennium ago. If we think that way we may start to see our time as a bad time to live, but quoting some

gray wizard: *"... that is not for us to decide. All we have to decide is what to do with the time that is given us"*.

For my time spent on this earth I am really grateful for so many things... Starting from the beginning, I am grateful for having had the best education available in my city, what was not easy for my parents, I know. But that definitely opened my mind in many ways and certainly had great influence on who I am. I am also grateful for have been well taken care of during my childhood.

Here I express my special thanks to my advisor, Miled, my colleagues Pedro, Gentil and Victor, all my teachers through the years, my most beloved friends; Luiz (Jão) and Bruno (Valjão), my grandfather (who's name I carry), my father, my sister and my mother. Finally, I would like to thank my wife, Bruna.

O presente trabalho foi realizado com o apoio da coordenação de aperfeiçoamento de Pessoal de Nível Superior - Brasil (CAPES) - Código de Financiamento 001

"There is no knowledge that is not power."

- Mortal Kombat

Abstract

OLIVEIRA NETO, F. *Effective lasers and enhancement of the radiation-matter interaction via pseudo-Hermitian Hamiltonians*. 2022. 104 p. Thesis (Doctor in Science) - Instituto de Física de São Carlos, Universidade de São Paulo, São Carlos, 2022.

In this work we propose a method using atom-field effective interactions along with reservoir engineering techniques into laser theory. Our proposal consists of creating generalized operators with which we can re-write the Hamiltonian in the Jaynes-Cummings bilinear form allowing us to build an isomorphism, between the conventional field operators and those of our effective laser, that guarantees the stationary solution in this new basis to be that of the usual theory. Mapping this steady state into the Fock basis we have a new laser state, different from the coherent state, that depends on the choosing of the generalized operator, having no diffusion from cavity losses due to a particular reservoir engineering technique. Moreover, we present a strategy for strengthening the atom-field interaction through a pseudo-Hermitian Jaynes-Cummings Hamiltonian. Apart from the engineering of an effective non-Hermitian Hamiltonian, our method also relies on the accomplishment of short-time measurements on canonically conjugate variables. The resulting fast Rabi oscillations may be used for many quantum optics purposes and specially to shorten the processing time of quantum information.

Keywords: Quantum optics. Laser theory. Non-Hermitian quantum mechanics.

Resumo

OLIVEIRA NETO, F. *Lasers efetivos e fortalecimento da interação radiação-matéria via Hamiltonianos pseudo-Hermitianos*. 2022. 104 p. Tese (Doutorado em Ciências) - Instituto de Física de São Carlos, Universidade de São Paulo, São Carlos, 2022.

Neste trabalho propomos um método fazendo uso de interações efetivas átomo-campo, juntamente com técnicas de engenharia de reservatório, aplicadas na teoria do laser. Nossa proposta consiste em criar operadores generalizados com os quais reescrevemos o Hamiltoniano na forma bilinear de Jaynes-Cummings, de forma que possamos construir um isomorfismo entre os operadores de campo convencionais e aqueles de nosso laser efetivo, que garanta que a solução estacionária nessa nova base seja igual à da teoria usual. Mapeando esse estado estacionário na base de Fock nós obtemos um novo estado para o laser, diferente do estado coerente, que depende da escolha do operador generalizado e é livre de processos de difusão, oriundos das perdas da cavidade, devido à uma técnica específica de engenharia de reservatório. Nós também apresentamos uma estratégia para fortalecer o acoplamento átomo-campo através de um Hamiltoniano de Jaynes-Cummings pseudo-Hermitiano. Além da engenharia de um Hamiltoniano não-Hermitiano, nosso método também conta com medições de curto tempo de variáveis canonicamente conjugadas. As oscilações de Rabi resultantes podem ser utilizadas para vários propósitos em ótica quântica, especialmente para encurtar o tempo de processamento em informação quântica.

Palavras-chave: Ótica quântica. Teoria do laser. Mecânica quântica não-Hermitiana.

LIST OF FIGURES

CONTENTS

CHAPTER 1

INTRODUCTION

1.1 About Quantum Mechanics and Laser Theory

Quantum theory has provided us satisfactory explanations about many phenomena, although even a century later we still have no consensus on its fundamental concepts and interpretations when it comes to certain idealized questions. Part of this conceptual barrier is due to the fact that coherent superpositions of different states of a system do occur in quantum mechanics, requiring a certain measurement process, which has many interpretations, such as the projection postulate, also known as the wave function collapse. This measurement issue is still open, and even the most widely accepted interpretation, of Copenhagen, counts with different points of view on the mechanism through which a certain state is determined, among all the possible outcomes of an observation, given that the Schrödinger's equation time evolution of a wave function is unitary and reversible, as opposed to what happens with the measurement process that, one may say, changes suddenly and discontinuously the wave function.

In order to enlighten quantum features of a system, which means capturing a small number of particles, atomic schemes were developed allowing a single ion to be trapped (1) making possible tests about the fundamental concepts of quantum mechanics, such as the coherence loss (2) of quantum states. The radiation-matter interaction was studied widely over the last few decades, counting on both theoretical and experimental works in contexts such as trapped ions,(3) as remarked above, and Cavity Quantum Electrodynamics (Cavity QED). (4) We can mention the works of preparing a Schrödinger cat-like superposition of states ($|\psi\rangle \propto \left(\left|\alpha e^{i\phi}\right\rangle + \left|\alpha e^{-i\phi}\right\rangle\right)$) with $|\alpha|^2 \approx 10$ in high quality factor cavities (2) and trapped ions, (5) which makes possible to investigate mesoscopic quantum coherence. Furthermore, the preparation of a variety of non-classical states has been reported in the context of QED (2,6) and trapped ions, (5,7,8) as well as the experimental demonstration

of generation and detection of Fock states. (9) Besides that, Rabi oscillations in circular Rydberg states atoms (10) were measured, unravelling the quantum nature of the radiation field. (11)

One of the central developments in the physics of radiation-matter interaction is the laser theory. Based on the theoretical framework provided by Townes and Schawlow, (12) the first laser, built by Maiman, (13) dates back to the 1960s, and has since played a major role both in basic and applied physics, with applications in many technical aspects of modern society. The quantum theory of laser was built basically from contributions led by H. Haken, (14) W. E. Lamb, (15, 16) and M. Lax, (17) from which are derived the more realistic models in which a transmitting window (18) and the pumping statistics of the lasing atoms (19–22) are included.

Among many others, we mention the uses of lasers for cooling and trapping atoms, (23–25) for Bose-Einstein condensation in dilute gases of alkali atoms, (26, 27) for the development of optical tweezers and their application in biological and physical sciences, (28–31) for many protocols for the implementation of quantum logic operation devices (32) and for generating ultrashort high-intensity laser pulses extensively used across physics and chemistry. (33, 34) These achievements draw a broader picture of the unique progress that quantum optics has undergone since the 1980s. In the addition to this picture we mention the generations of squeezed states of the radiation field, (35) essential for enhancing interferometric sensitivity, (36) and today a critical challenge for the development of gravitational wave interferometry. (36–38) Squeezed states of light have also being applied in optical waveguide tap, (39) quantum nondemolition measurements, (37) quantum information processing, (40, 41) and quantum metrology. (42, 43) We finally mention the progress made in the development of different sources for generating entangled photon states, used for investigating fundamentals of quantum mechanics. (44, 45)

Parallel to the developments of quantum optics, we witnessed the emergence of quantum communication and computation, which resulted in the new and promising field of quantum information theory. (32) The need for implementation of quantum logic operations demanded new techniques for engineering nonclassical states, (46–52) effective interactions (53–59) and reservoirs (49–52, 60–62) for phase coherence control. These demands have pushed the physics of the radiation-matter interaction to a new level through platforms such as cavity QED, (4) trapped ions, (3) circuit QED, (63) and all related topics.

Regarding coherence control, many methods have been designed. (64) However, the reservoir engineering (60) is of particular interest here. Its basic idea is to submit the system of interest, say a dissipative cavity mode (described by the creation and annihilation

operators $a^\dagger$ and a, and whose particular state $|\Psi\rangle$ we intend to protect from the action of the environment), to an interaction with an auxiliary strongly dissipative system as, for example, a two-level atom (described by the Pauli raising and lowering operators σ_+ and σ_-). This interaction must then be engineered so that it takes the bilinear form

$$\chi \left(A S_+ + A^\dagger S_- \right) \tag{1.1}$$

with χ being an effective atom-field coupling and $A^\dagger, A$ (S_+, S_-) defined by a canonical transformation on the original operators for the cavity mode: $a^\dagger, a$ (auxiliary atom: σ_+, σ_-), with the central requirement $A|\Psi\rangle = 0$. The master equation for the cavity mode, coming from reservoir engineering, is given by

$$\dot{\rho} = (\Gamma/2)\left(2A\rho A^\dagger - A^\dagger A\rho - \rho A^\dagger A\right) + (\gamma/2)\left(2a\rho a^\dagger - a^\dagger a\rho - \rho a^\dagger a\right) \tag{1.2}$$

with the assumption $\Gamma \propto \chi \gg \gamma$. It is therefore clear that the Lindbladian for $a^\dagger, a$ acts as a perturbation over that for $A^\dagger, A$, causing the fidelity of the protected state, necessarily an eigenstate of A with null eigenvalue (60) ($A|\Psi\rangle = 0$), to be slightly less than unity, since $\mathcal{F} \propto 1 - \gamma/\Gamma$.

1.2 About Pseudo-Hermitian Quantum Mechanics

Since the inspiring framework presented by Bender and Boettcher (65), where it its shown that a parity-time ($\mathcal{PT}$) transformation invariant Hamiltonian disposes real spectrum, non-Hermitian quantum mechanics has been earning notoriety over the last two decades. It is said that an invariant Hamiltonian preserves the $\mathcal{PT}$-symmetry when it shares its eigenstates with the $\mathcal{PT}$ operator, yet that symmetry is broken when the Hamiltonian stops sharing the same eigenstates with the $\mathcal{PT}$ operator. (66) A few years after Bender and Boettcher's contribution, Mostafazadeh (67) focused on the problem of the unitarity of the time evolution of a pseudo-Hermitian Hamiltonian, i.e., a Hamiltonian which enjoys real spectrum and unitary evolution in a new metric operator. The solution proposed was the construction of a Hilbert space based on a metric operator where the non-Hermitian Hamiltonian enjoys self-adjointness. Since then $\mathcal{PT}$-symmetric Hamiltonians have been studied widely in many fields of physics, from low to high energies, in part due to the $\mathcal{PT}$-symmetry condition, that is weaker than Hermiticity, and therefore increases the possibilities of the Hamiltonian description of physical systems, counting with real eigenvalues (65) and the normalization conservation (67).

Regarding $\mathcal{PT}$-symmetry, many contributions have been presented recently, such as the experimental realizations of Floquet $\mathcal{PT}$-symmetric systems (68) and $\mathcal{PT}$-symmetric flat bands, (69) besides enhanced sensing based on $\mathcal{PT}$-symmetric electronic circuits (70) and $\mathcal{PT}$-symmetric topological edge-gain effect. (71)

Finally, among many contributions from Mostafazadeh, (72) we mention a theorem of his, (73) formulated for time independent non-Hermitian Hamiltonians, symmetries and metric operators, that asserts that a diagonalizable (non-Hermitian) Hamiltonian is pseudo-Hermitian if and only if it has an antilinear symmetry, i.e., a symmetry generated by an invertible antilinear operator. In addition, it was shown that a non-Hermitian Hamiltonian can have a real spectrum not only when invariant under $\mathcal{PT}$-symmetry, but also under any antiunitary operator I satisfaying $I^{2k} = 1$, with k odd.

This thesis is organized as follows: In Chapter 2 we shall review the main concepts necessary to fully understand this work, starting with the laser theory and also a brief introduction of the non Hermitian quantum mechanics. In chapter 3 we present the squeezed vacuum state laser with zero diffusion from cavity losses. (74) Next, in chapter 4, we have the Schrödinger cat-like state laser with zero diffusion from cavity losses. In chapter 5 we study the pseudo-Hermitian work. Finally, in chapter 6, we set out our conclusions.

CHAPTER 2

QUANTUM LASER THEORY: MASTER EQUATION APPROACH

Semiclassical description may be adequate to describe quantities such as threshold, steady-state intensity, etc. Nonetheless, in order to be able to determine quantum quantities, such as photon statistics, we need to consider a fully quantized description, i.e., field and matter are quantized.

The knowledge of the photon statistical distribution of a laser is important for many reasons. Chronologically, it was thought that the steady state of a laser would be given by a Bose-Einstein distribution, although this result is impossible since a laser operating regime is far from thermodynamic equilibrium. Another point of view says that many atoms oscillating in phase produce what is essentially a classical current, and this would generate a coherent state, leading to a Poissonian statistics (which we shall see that is true, in the far from threshold regime)

There are many approaches by which we can study the Laser Theory. In this chapter we follow the master equation approach for the Scully-Lamb model, using two equivalent methods.

2.1 Method I

Let us consider the Jaynes-Cummings Hamiltonian, where a single mode of the field (cavity mode) interacts with a two-level atom, and the atomic sample is in resonance with the cavity, within the dipole and rotating-wave approximations

$$\mathcal{H} = \frac{\hbar\omega}{2}\sigma_z + \hbar\omega a^\dagger a + \hbar g\left(a\sigma_+ + a^\dagger\sigma_-\right) \tag{2.1}$$

In the interaction picture we have

$$V = g\left(a\sigma_+ + a^\dagger\sigma_-\right) \tag{2.2}$$

where we set $\hbar = 1$. Using Pauli matrices for the atomic operators we can write the time evolution operator

$$\begin{aligned} U(\tau) &= e^{-iV\tau} = \sum_{n=0}^{\infty} \frac{(-i\tau)^n}{n!} \begin{pmatrix} 0 & ga \\ ga^\dagger & 0 \end{pmatrix}^n \\ &= \sum_{n=0}^{\infty} \left[\frac{(-i\tau)^{2n}}{(2n)!} \begin{pmatrix} 0 & ga \\ ga^\dagger & 0 \end{pmatrix}^{2n} + \frac{(-i\tau)^{2n+1}}{(2n+1)!} \begin{pmatrix} 0 & ga \\ ga^\dagger & 0 \end{pmatrix}^{2n+1} \right] \end{aligned} \tag{2.3}$$

where we have, for the even order matrices

$$\begin{pmatrix} 0 & ga \\ ga^\dagger & 0 \end{pmatrix}^{2n} = \begin{pmatrix} \left[g^2 aa^\dagger\right]^n & 0 \\ 0 & \left[g^2 a^\dagger a\right]^n \end{pmatrix} \tag{2.4}$$

and for the odd order matrices

$$\begin{pmatrix} 0 & ga \\ ga^\dagger & 0 \end{pmatrix}^{2n+1} = \begin{pmatrix} 0 & g\left[g^2 aa^\dagger\right]^n a \\ ga^\dagger\left[g^2 aa^\dagger\right]^n & 0 \end{pmatrix} \tag{2.5}$$

We can identify these matrices as trigonometric functions. The even matrices can be written as

$$\sum_n \frac{(-i\tau)^{2n}}{(2n)!} \left(\sqrt{g^2 aa^\dagger}\right)^{2n} = \cos\left(\sqrt{aa^\dagger} g\tau\right) \tag{2.6}$$

and for the odd matrices we have

$$ga^\dagger \sum_n \frac{(-i\tau)^{2n+1}}{(2n+1)!} \frac{\left(\sqrt{g^2 aa^\dagger}\right)^{2n+1}}{\sqrt{g^2 aa^\dagger}} = ga^\dagger \frac{\sin\left(\sqrt{aa^\dagger} g\tau\right)}{\sqrt{g^2 aa^\dagger}} \tag{2.7}$$

Next we simplify the reading of the time evolution operator by writing $U = \begin{pmatrix} A & C \\ D & B \end{pmatrix}$, where the coefficients are

$$A = \cos\left(\sqrt{aa^\dagger}g\tau\right) \tag{2.8a}$$

$$B = \cos\left(\sqrt{a^\dagger a}g\tau\right) \tag{2.8b}$$

$$C = -ig\frac{\sin\left(\sqrt{aa^\dagger}g\tau\right)}{\sqrt{g^2aa^\dagger}}a \tag{2.8c}$$

$$D = -iga^\dagger\frac{\sin\left(\sqrt{aa^\dagger}g\tau\right)}{\sqrt{g^2aa^\dagger}} \tag{2.8d}$$

Considering that the atom is initially in the upper state, we can write the initial atom-field density matrix as

$$\rho(0) = \rho_f(0) \otimes \begin{pmatrix} 1 & 0 \\ 0 & 0 \end{pmatrix} \tag{2.9}$$

After an interaction time τ, we shall have

$$\rho(\tau) = U(\tau)\rho(0)U^\dagger(\tau) = U(\tau)\rho_f(0) \otimes \begin{pmatrix} 1 & 0 \\ 0 & 0 \end{pmatrix} U^\dagger(\tau) \tag{2.10}$$

leading to

$$\rho(\tau) = \begin{pmatrix} A & C \\ D & B \end{pmatrix}\rho_f(0) \otimes \begin{pmatrix} 1 & 0 \\ 0 & 0 \end{pmatrix}\begin{pmatrix} A^\dagger & D^\dagger \\ C^\dagger & B^\dagger \end{pmatrix} = \begin{pmatrix} A & C \\ D & B \end{pmatrix}\rho_f(0) \otimes \begin{pmatrix} A^\dagger & D^\dagger \\ 0 & 0 \end{pmatrix} \tag{2.11}$$

So we can write the atom-field density matrix at a time τ as

$$\rho(\tau) = \begin{pmatrix} A\rho_f(0)A^\dagger & A\rho_f(0)D^\dagger \\ D\rho_f(0)A^\dagger & D\rho_f(0)D^\dagger \end{pmatrix} \tag{2.12}$$

We are interested in the field, so we shall perform the trace over the atom, in order to eliminate the atomic dependence in the density matrix. Thus we find

$$Tr\Big[\rho(\tau)\Big]_{atom} = \rho_f(\tau) = A\rho_f(0)A^\dagger + D\rho_f(0)D^\dagger \tag{2.13}$$

using Eqs (2.8a) and (2.8d) we obtain

$$\rho_f(\tau) = \cos\left(\sqrt{aa^\dagger}g\tau\right)\rho_f(0)\cos\left(\sqrt{aa^\dagger}g\tau\right) + a^\dagger\frac{\sin\left(\sqrt{aa^\dagger}g\tau\right)}{\sqrt{aa^\dagger}}\rho_f(0)\frac{\sin\left(\sqrt{aa^\dagger}g\tau\right)}{\sqrt{aa^\dagger}}a$$

$$\equiv M(\tau)\rho_f(0) \tag{2.14}$$

and then we have an equation exclusively for the field density matrix, where M is a superoperator acting on ρ_f.

Let us assume that a dense flux of atoms, here considered all being in the upper state, arrives at the cavity. These atoms will interact with the mode of the cavity for a time interval during which they may stimulatingly decay emitting a photon with the same phase, momentum and polarization. Each of theses atoms, and their respective emitted photons, contribute to the construction of the laser state. We also assume that the beam has a regular distribution, so the number K of atoms that have crossed through the cavity during a time Δt is given by $K = r\Delta t$, where r is the injection rate and Δt is much larger than the time interval between consecutive atoms.

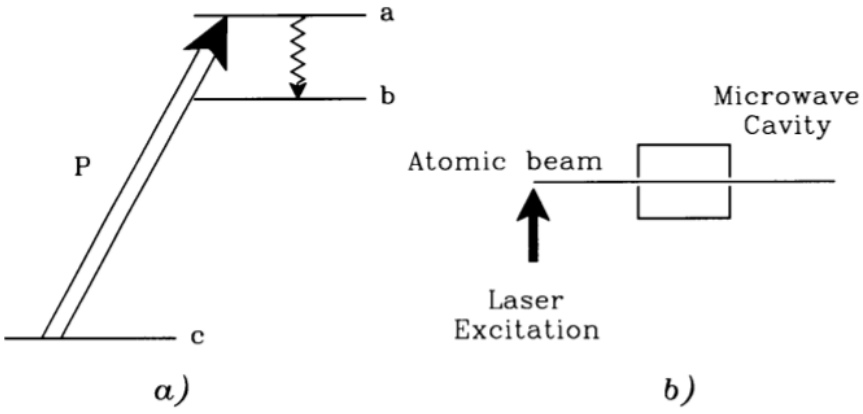

Figure 2.1 – **(a)** An atom is excited from a lowest level c to the upper level. The lasing transition occurs between the a and b levels. **(b)** An atomic beam arrives to the excitation region where excited states are participating in the laser action.
Source: ORSZAG (75)

Considering the interaction time between the atom and the field to be τ and that the $k-th$ atom enters the cavity at the time t_k, then the field, after interacting with the $k-th$ atom, can be written as

$$\rho_f(t_k + \tau) = M(\tau)\rho_f(t_k) \tag{2.15}$$

From now on we shall skip the field subindex. If k atoms have entered the cavity, one can say that

$$\rho^{(k)}(k\tau) = M^k(\tau)\rho(0) \tag{2.16}$$

If we differentiate the above equation with respect to time, using the derivative relation $\frac{d}{dt}(b^u) = b^u \ln(b)\frac{du}{dt}$, with $b = M$ and $u = k = r\Delta t$, we get a generalized master equation

$$\frac{d\rho(t)}{dt} = r\ln(M)\rho(t) + \mathcal{L}\rho(t) \tag{2.17}$$

where we have added the cavity loss term, $\mathcal{L}\rho(t)$, following the quantum theory of damping, where the harmonic oscillator is our single mode field interacting with a reservoir, at zero temperature

$$\mathcal{L}\rho(t) = \frac{C}{2}\left(2a\rho a^\dagger - a^\dagger a\rho - \rho a^\dagger a\right) \tag{2.18}$$

with $C = 1/t_{cav} = \Omega/Q$, t_{cav} being the photon's lifetime inside the cavity and Q is the cavity quality factor.

If the average photon number is sufficiently large and the distribution narrow, one can expand the generalized master equation and get

$$\frac{d\rho(t)}{dt} = r(M-1)\rho(t) - \frac{1}{2}r(M-1)^2 + \mathcal{L}\rho(t) \tag{2.19}$$

Finally, using Eq (2.14) we obtain

$$\begin{aligned}
\frac{d\rho(t)}{dt} &= \mathcal{L}\rho(t) - \frac{3}{2}r\rho(t) + 2r\Bigg[\cos\left(\sqrt{aa^\dagger}g\tau\right)\rho(t)\cos\left(\sqrt{aa^\dagger}g\tau\right) \\
&+g^2a^\dagger\frac{\sin\left(\sqrt{aa^\dagger}g\tau\right)}{\sqrt{g^2aa^\dagger}}\rho(t)\frac{\sin\left(\sqrt{aa^\dagger}g\tau\right)}{\sqrt{g^2aa^\dagger}}a\Bigg] \\
&-\frac{r}{2}\Bigg[\cos^2\left(\sqrt{aa^\dagger}g\tau\right)\rho(t)\cos^2\left(\sqrt{aa^\dagger}g\tau\right) + \\
&g^2\cos\left(\sqrt{aa^\dagger}g\tau\right)a^\dagger\frac{\sin\left(\sqrt{aa^\dagger}g\tau\right)}{\sqrt{g^2aa^\dagger}}\rho(t)\frac{\sin\left(\sqrt{aa^\dagger}g\tau\right)}{\sqrt{g^2aa^\dagger}}a\cos\left(\sqrt{aa^\dagger}g\tau\right) \\
&+g^2a^\dagger\frac{\sin\left(\sqrt{aa^\dagger}g\tau\right)}{\sqrt{g^2aa^\dagger}}\cos\left(\sqrt{aa^\dagger}g\tau\right)\rho(t)\cos\left(\sqrt{aa^\dagger}g\tau\right)\frac{\sin\left(\sqrt{aa^\dagger}g\tau\right)}{\sqrt{g^2aa^\dagger}}a \\
&g^4a^\dagger\frac{\sin\left(\sqrt{aa^\dagger}g\tau\right)}{\sqrt{g^2aa^\dagger}}a^\dagger\frac{\sin\left(\sqrt{aa^\dagger}g\tau\right)}{\sqrt{g^2aa^\dagger}}\rho(t)\frac{\sin\left(\sqrt{aa^\dagger}g\tau\right)}{\sqrt{g^2aa^\dagger}}a\frac{\sin\left(\sqrt{aa^\dagger}g\tau\right)}{\sqrt{g^2aa^\dagger}}a\Bigg]
\end{aligned} \tag{2.20}$$

We can obtain the photon statistics and linewidth using the expression above by calculating ρ_{nn} and $\rho_{n,n+1}$, respectively. This generalized master equation was derived using approximations. Next we make a more realistic model.

The stimulated emission is essential for the laser mechanism, but still the excited atom has a probability to spontaneously decay inside the cavity. In order to include this phenomena we consider a distribution of time the atoms spend in the cavity where the two levels decay at a rate γ and the time distribution is

$$P(\tau) = \gamma e^{-\gamma\tau} \tag{2.21}$$

Defining a course time grain $\Delta t \gg \langle\tau\rangle$, we can write

$$\begin{aligned}
\left(\frac{d\rho}{dt}\right)_{gain} &\approx \frac{\rho(t+\Delta t)-\rho(t)}{\Delta t} = r\Big[\rho(t+\Delta t)-\rho(t)\Big] \\
&= -r\rho(t) + r\int_0^{\Delta t\to\infty} d\tau\; e^{-\gamma\tau}\Bigg[\cos\left(\sqrt{aa^\dagger}g\tau\right)\rho(t)\cos\left(\sqrt{aa^\dagger}g\tau\right) \\
&+a^\dagger\frac{\sin\left(\sqrt{aa^\dagger}g\tau\right)}{\sqrt{aa^\dagger}}\rho(t)\frac{\sin\left(\sqrt{aa^\dagger}g\tau\right)}{\sqrt{aa^\dagger}}a\Bigg]
\end{aligned} \tag{2.22}$$

Here we take the opportunity to show where the gain and saturation coefficients of the laser come from. This next step makes us analyze the time scales of the argument of the trigonometric functions. The average time for the atom-field interaction is $1/g$, where g is the coupling strength from the Hamiltonian in Eq. (2.1) and τ is the time the atom spends interacting with the cavity. To ensure the atom can properly interact with the mode we need that $\tau \approx 1/g$ leading to $\tau g \approx 1$. Next we present the expansion up to 4-th order of the trigonometric functions.

$$\cos\left(\sqrt{aa^\dagger}g\tau\right) \approx 1 - \frac{(g\tau)^2}{2}aa^\dagger + \frac{(g\tau)^4}{24}\left(aa^\dagger\right)^2 + \ ... \tag{2.23a}$$

$$\frac{\sin\left(\sqrt{aa^\dagger}g\tau\right)}{\sqrt{aa^\dagger}} \approx g\tau - \frac{(g\tau)^3}{6}aa^\dagger + \ ... \tag{2.23b}$$

It is also useful to calculate

$$\int \tau^2 \gamma e^{-\gamma\tau} d\tau = \frac{2}{\gamma^2} \tag{2.24a}$$

$$\int \tau^4 \gamma e^{-\gamma\tau} d\tau = \frac{24}{\gamma^4} \tag{2.24b}$$

Using the above expansions (2.23a) and (2.23b) and also the integrals (2.24a) and (2.24b) into the master equation we get

$$\begin{aligned}\frac{d\rho}{dt} \ = \ & -r\left(\frac{g}{\gamma}\right)^2\Bigg[aa^\dagger\left\{\rho - \left(\frac{g}{\gamma}\right)^2\left(aa^\dagger\rho + 3\rho aa^\dagger\right)\right\} \\ & + \left\{\rho - \left(\frac{g}{\gamma}\right)^2\left(\rho aa^\dagger + 3aa^\dagger\rho\right)\right\}aa^\dagger - 2a^\dagger\left\{\rho - 2\left(\frac{g}{\gamma}\right)^2\left(aa^\dagger\rho + \rho aa^\dagger\right)\right\}a\Bigg] \\ & + \frac{C}{2}\left(2a\rho a^\dagger - a^\dagger a\rho - \rho a^\dagger a\right)\end{aligned} \tag{2.25}$$

We can rewrite the above equation in a more convenient form, as following

$$\begin{aligned}\frac{d\rho}{dt} &= \frac{\mathcal{A}}{2}\Big(2a^\dagger\rho a - aa^\dagger\rho - \rho aa^\dagger\Big) \\ &\quad \frac{\mathcal{B}}{2}\Big[\frac{1}{4}\Big(aa^\dagger\Big)^2\rho + \frac{1}{4}\,\rho\Big(aa^\dagger\Big)^2 + 6aa^\dagger\rho aa^\dagger - 4a^\dagger aa^\dagger\rho a - 4a^\dagger\rho aa^\dagger a\Big] \\ &\quad + \frac{C}{2}\Big(2a\rho a^\dagger - a^\dagger a\rho - \rho a^\dagger a\Big) \qquad (2.26)\end{aligned}$$

where $\mathcal{A} \equiv 2r\left(\frac{g}{\gamma}\right)^2$, $\mathcal{B} \equiv 4\mathcal{A}\left(\frac{g}{\gamma}\right)^2$ and C are the gain, saturation and cavity loss coefficients, respectively. We shall discuss the role of the first two later.

Now we go back to the full non-linear theory. Taking the nm matrix element of Eq (2.22) we find the following time integrals

$$\gamma\int_0^\infty d\tau\; e^{-\gamma\tau}\cos\Big(\sqrt{n+1}g\tau\Big)\cos\Big(\sqrt{m+1}g\tau\Big) = \frac{1+2\Big(n+m+2\Big)\Big(g/\gamma\Big)^2}{1+2\Big(n+m+2\Big)\Big(g/\gamma\Big)^2+\Big(n-m\Big)^2\Big(g/\gamma\Big)^4} \qquad (2.27a)$$

$$\gamma\int_0^\infty d\tau\; e^{-\gamma\tau}\sin\Big(\sqrt{n+1}g\tau\Big)\sin\Big(\sqrt{m+1}g\tau\Big) = \frac{2\Big(g/\gamma\Big)^2\sqrt{(n+1)(m+1)}}{1+2\Big(n+m+2\Big)\Big(g/\gamma\Big)^2+\Big(n-m\Big)^2\Big(g/\gamma\Big)^4} \qquad (2.27b)$$

Then, using the following coefficients

$$\mathcal{N}'_{nm} = \frac{1}{2}(n+m+2) + \frac{\frac{1}{8}(n-m)^2\mathcal{B}}{\mathcal{A}} \qquad (2.28a)$$

$$\mathcal{N}_{nm} = \frac{1}{2}(n+m+2) + \frac{\frac{1}{16}(n-m)^2\mathcal{B}}{\mathcal{A}} \qquad (2.28b)$$

we can write the master equation for the field density matrix

$$\left(\frac{d\rho}{dt}\right)_{nm} = -\frac{\mathcal{N}'_{nm}\mathcal{A}}{1+\mathcal{N}_{nm}\frac{\mathcal{B}}{\mathcal{A}}}\,\rho_{nm} + \frac{\sqrt{nm}\mathcal{A}}{1+\mathcal{N}_{n-1,m-1}\frac{\mathcal{B}}{\mathcal{A}}}\,\rho_{n-1,m-1} - \frac{C}{2}(n+m)\rho_{nm} + C\sqrt{(n+1)(m+1)}\rho_{n+1,m+1} \tag{2.29}$$

If we are interested in the photon statistics we take the diagonal elements, i.e., $m = n$. Next we shall use $\rho_{nn} = p_n$ since the diagonal elements of the density matrix can be interpreted as the population of photons. Thus, we get

$$\left(\frac{dp}{dt}\right)_n = -\frac{\mathcal{A}(n+1)}{1+(n+1)\frac{\mathcal{B}}{\mathcal{A}}}\,p_n + \frac{\mathcal{A}n}{1+n\frac{\mathcal{B}}{\mathcal{A}}}\,p_{n-1} + C(n+1)p_{n+1} - C(n)p_n \tag{2.30}$$

To give a physical meaning to the dynamics of the photon number probability we can expand the terms in the denominators using $\frac{1}{1+x} = 1 - x + x^2 - x^3 + \ldots$ where we shall consider terms only up to second order. Therefore we get

$$\dot{p}_n = -\mathcal{A}(n+1)\,p_n + \mathcal{B}(n+1)^2\,p_n + \mathcal{A}n\,p_{n-1} - \mathcal{B}n^2\,p_{n-1} + C(n+1)\,p_{n+1} - C(n)\,p_n \tag{2.31}$$

Below we have a probability flow diagram where we can see the flow in and out of the $|n\rangle$ state from and to the neighboring $|n-1\rangle$ and $|n+1\rangle$ states. We interpret the $-\mathcal{A}(n+1)p_n$ term as the gain due to the photon emitted via stimulated emission, the minus sign means the probability flows out of the $|n\rangle$ state into the $|n+1\rangle$ state. In the same way the term $\mathcal{A}n\,p_{n-1}$ represents the gain owing to the emitted photon, leading the population flow from $|n-1\rangle$ to $|n\rangle$, and therefore it is positive. We also have terms of saturation, for example the term $\mathcal{B}(n+1)^2 p_n$, which we can rewrite as $\mathcal{A}(n+1)\left[\frac{\mathcal{B}}{\mathcal{A}}(n+1)\right]p_n$ corresponding to the process in which photons are emitted and then reabsorbed, the reabsorption rate being $\frac{\mathcal{B}}{\mathcal{A}}(n+1)$. Similar explanations exist for the other saturation terms. Finally we have the cavity losses, where the term $C(n+1)p_{n+1}$ is due to the loss from p_{n+1} to p_n, while the last term, $C(n)p_n$, refers to a photon loss leading from p_n to p_{n-1}.

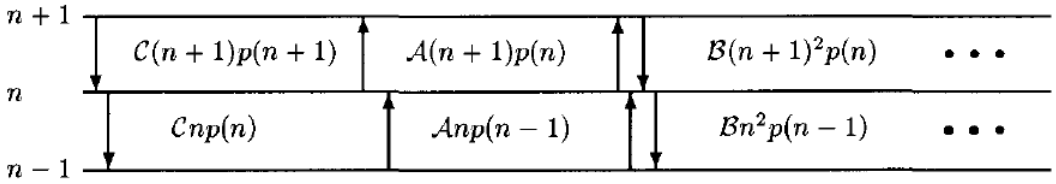

Figure 2.2 – Probability flow diagram for the field states of a laser.

Source: SCULLY (76)

Forward we seek a solution for the master equation. Naturally the dynamics of the laser mechanism is complicated and difficult do describe, but our interest lies in the stationary solution which we can find looking at Eq. (2.30) and imposing $\dot{p} = 0$, meaning that the population of the $|n\rangle$ state is not changing anymore. Next we say that, in this steady-state, the flow out of a state, e.g. the $|n\rangle$ state, is equal to the flow in, so it remains unchanged. This method of analysis is called detailed balance.

First let us focus on the linear approximation, i.e. $\mathcal{B} = 0$. In this case the steady state leads us to

$$-\mathcal{A}(n+1)\ p_n + \mathcal{A}n\ p_{n-1} + C(n+1)\ p_{n+1} - C(n)\ p_n = 0 \tag{2.32}$$

Equalizing the flows in and out we get

$$\mathcal{A}(n+1)p_n = C(n+1)\ p_{n+1} \tag{2.33a}$$

$$\mathcal{A}n\ p_{n-1} = C(n)\ p_n \tag{2.33b}$$

From this equations we can get the recursive relation

$$p_n = \left(\frac{\mathcal{A}}{C}\right) p_{n-1} \tag{2.34}$$

which leads us to

$$p_n = \left(\frac{\mathcal{A}}{C}\right)^n p_0 \tag{2.35}$$

The constant p_0 can be obtained from the normalization condition, $\sum_{n=0}^{\infty} p_n = 1$. For $\mathcal{A} < C$ we obtain

$$p_0 = 1 - \frac{\mathcal{A}}{C} \tag{2.36}$$

thus

$$p_n = \left(1 - \frac{\mathcal{A}}{C}\right)\left(\frac{\mathcal{A}}{C}\right)^n \tag{2.37}$$

Since there is no physical solution for $\mathcal{A} \geq C$ in the linear approximation ($\mathcal{B} = 0$), which we can see in the above equation (otherwise we would not be able to normalize the photon distribution), we can interpret $\mathcal{A} = C$ as a threshold condition. Hence, below threshold, the photon distribution indicates that the steady state solution is essentially that of a black body cavity

$$p_n = \left[1 - e^{\left(-\hbar\nu/k_b T\right)}\right] e^{\left(-n\hbar\nu/k_b T\right)} \tag{2.38}$$

that is, the laser below threshold behaves like an incandescent lamp, with the effective temperature defined by

$$e^{\left(-\hbar\nu/k_b T\right)} = \frac{\mathcal{A}}{C} \tag{2.39}$$

Now we shall study the other regime, where $\mathcal{A} \gg C$, that is, far above the threshold. In this regime the detailed balance gives us

$$p_n = \frac{\mathcal{A}/C}{1 + n\,\frac{\mathcal{B}}{\mathcal{A}}}\, p_{n-1} \tag{2.40}$$

and the solution is known as

$$\begin{aligned} p_n &= p_0 \left(\frac{\mathcal{A}}{C}\right)^n \prod_{k=0}^{n} \left(1 + \frac{k\mathcal{B}}{\mathcal{A}}\right)^{-1} = p_0 \left(\frac{\mathcal{A}}{C}\right)^n \left(\frac{\mathcal{A}}{\mathcal{B}}\right)^n \prod_{k=1}^{n} \left(\frac{\mathcal{A}}{\mathcal{B}} + k\right)^{-1} \\ &= p_0 \left(\frac{\mathcal{A}^2}{\mathcal{B}C}\right)^n \prod_{k=1}^{n} \left(\frac{\mathcal{A}}{\mathcal{B}} + k\right)^{-1} \end{aligned} \tag{2.41}$$

We calculate the average photon number

$$\begin{aligned}\langle n\rangle &= \sum_n n p_n = p_0 \sum_{n=1}\left(n+\frac{\mathcal{A}}{\mathcal{B}}-\frac{\mathcal{A}}{\mathcal{B}}\right)\left(\frac{\mathcal{A}^2}{\mathcal{B}C}\right)^n \prod_{k=1}^{k=n}\left[\frac{1}{\left(k+\frac{\mathcal{A}}{\mathcal{B}}\right)}\right] \\ &= p_0 \sum_{n=1}\left(n+\frac{\mathcal{A}}{\mathcal{B}}\right)\left(\frac{\mathcal{A}^2}{\mathcal{B}C}\right)^n \prod_{k=1}^{k=n}\left[\frac{1}{\left(k+\frac{\mathcal{A}}{\mathcal{B}}\right)}\right] - \frac{\mathcal{A}}{\mathcal{B}}\, p_0 \sum_{n=1}\left(\frac{\mathcal{A}^2}{\mathcal{B}C}\right)^n \prod_{k=1}^{k=n}\left[\frac{1}{\left(k+\frac{\mathcal{A}}{\mathcal{B}}\right)}\right]\end{aligned} \tag{2.42}$$

pulling out the last term of the first product

$$\begin{aligned}\langle n\rangle &= \left(\frac{\mathcal{A}^2}{\mathcal{B}C}\right) p_0 \sum_{n=1}\left(n+\frac{\mathcal{A}}{\mathcal{B}}\right)\left(\frac{\mathcal{A}^2}{\mathcal{B}C}\right)^{n-1}\left[\frac{1}{\left(n+\frac{\mathcal{A}}{\mathcal{B}}\right)}\right] \prod_{k=1}^{k=n-1}\left[\frac{1}{\left(k+\frac{\mathcal{A}}{\mathcal{B}}\right)}\right] \\ &\quad -\frac{\mathcal{A}}{\mathcal{B}} \sum_{n=1} p_0 \left(\frac{\mathcal{A}^2}{\mathcal{B}C}\right)^n \prod_{k=1}^{k=n}\left[\frac{1}{\left(k+\frac{\mathcal{A}}{\mathcal{B}}\right)}\right] \\ &= \left(\frac{\mathcal{A}^2}{\mathcal{B}C}\right) \sum_{n=1} p_0 \left(\frac{\mathcal{A}^2}{\mathcal{B}C}\right)^{n-1} \prod_{k=1}^{k=n-1}\left[\frac{1}{\left(k+\frac{\mathcal{A}}{\mathcal{B}}\right)}\right] - \frac{\mathcal{A}}{\mathcal{B}} \sum_{n=1} p_n\end{aligned} \tag{2.43}$$

The first sum is equivalent to the normalizing condition, while the second one misses the first term, p_0, which allows us to write

$$\begin{aligned}\langle n\rangle &= \left(\frac{\mathcal{A}^2}{\mathcal{B}C}\right) \sum_{n=1} p_{n-1} - \frac{\mathcal{A}}{\mathcal{B}} \sum_{n=1} p_n = \left(\frac{\mathcal{A}^2}{\mathcal{B}C}\right) - \frac{\mathcal{A}}{\mathcal{B}}\left(1-p_0\right) \\ &= \frac{\mathcal{A}}{\mathcal{B}}\left(\frac{\mathcal{A}}{C}-1\right) + \frac{\mathcal{A}}{\mathcal{B}} p_0\end{aligned} \tag{2.44}$$

Well over the threshold, i.e. $\dfrac{\mathcal{A}}{C} \gg 1$, we have

$$\langle n\rangle \approx \frac{\mathcal{A}}{\mathcal{B}}\left(\frac{\mathcal{A}}{C}\right) + \frac{\mathcal{A}}{\mathcal{B}} p_0 = \frac{\mathcal{A}}{\mathcal{B}}\left(\frac{\mathcal{A}}{C}+p_0\right) \approx \frac{\mathcal{A}}{\mathcal{B}}\left(\frac{\mathcal{A}}{C}\right) \tag{2.45}$$

Considering the well saturated regime, where $\mathcal{B} \gg \mathcal{A}$, we can write the photon distribution as

$$p_n \approx \left(\frac{\mathcal{A}^2}{\mathcal{B}C}\right)^n \frac{1}{n!}\, p_0 \tag{2.46}$$

whose normalization easily gives us $p_0 = e^{-\frac{\mathcal{A}^2}{\mathcal{B}C}}$. Using the relation $\langle n\rangle = \dfrac{\mathcal{A}^2}{\mathcal{B}C}$ we can

write the photon distribution as

$$p_n \approx e^{-\langle n \rangle} \frac{(\langle n \rangle)^n}{n!} \tag{2.47}$$

i.e., the same form as the Poisson distribution, which is a characteristic of a coherent state.

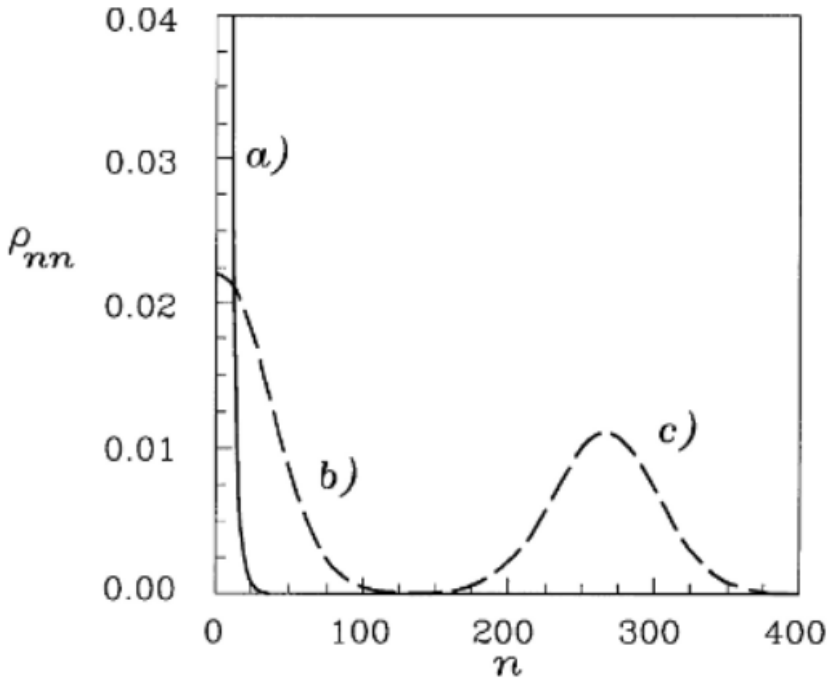

Figure 2.3 – Steady-state photon statistics versus n, for the cases below **(a)**, at **(b)** and above **(c)** threshold.

Source: ORSZAG (75)

The Mandel Q parameter can be calculated by

$$Q = \frac{\langle n^2 \rangle - \langle n \rangle^2}{\langle n \rangle} - 1 = \frac{C}{\mathcal{A} - C} \tag{2.48}$$

where we see that above the threshold ($\mathcal{A} > C$) we have $Q > 0$, which means the field is Super Poissonian. However, very far above threshold ($\mathcal{A} \gg C$) then Q approaches zero, which is expected from a poissonian distribution.

This is the Scully-Lamb Laser model, where we have an atomic pump that stands for the source of excitation for the atoms that, through the Hamiltonian, works as a pumping in the field as well.

2.2 Method II

Next we present a different method, still using the density matrix approach, where we have an atomic sample that is subjected to a pump with rate r and a serie of decay processes.

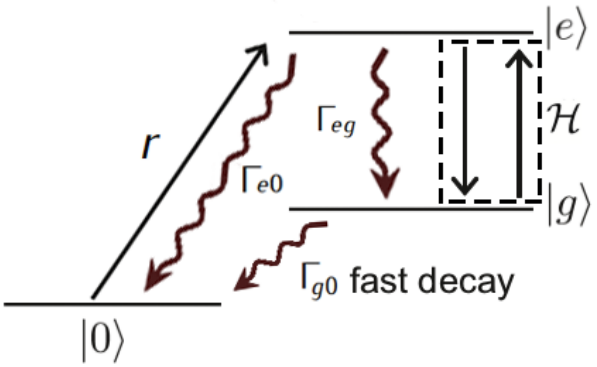

Figure 2.4 – A three-level atom, in which the pump r excites the atom from $|0\rangle$ to $|e\rangle$. The excitation exchange is managed through the Hamiltonian $\mathcal{H}$ and a series of decay processes
Source: Adapted from YAMAMOTO(77)

We consider the atomic sample shown in Figure 2.4, where the lowest level $|0\rangle$ simply serves the purpose of being subject to an incoherent pumping with rate r that leads it to the $|e\rangle$ state, not being coupled by the Hamiltonian. Meanwhile the other states, $|g\rangle$ and $|e\rangle$, are the lasing levels and we select the frequency of the mode to be equal to the frequency between these two levels of the atom, i.e. $\omega_c = \omega_e - \omega_g$. Choosing $\hbar = 1$ we can write the atom-field interaction Hamiltonian that describes the system as

$$\mathcal{H} = g\left(a\sigma_+ + a^\dagger\sigma_-\right) \tag{2.49}$$

where $\sigma_+ = |e\rangle\langle g|$ and $\sigma_- = |g\rangle\langle e|$ are the atomic raising and lowering operators. Our goal is to build a master equation that completely describes the system, containing all the main phenomena.
The first one considered is the linear photon loss due to output coupling through a cavity mirror, with rate C

$$\mathcal{L}_c\rho = \frac{C}{2}\left(2a\rho a^\dagger - a^\dagger a\rho - \rho a^\dagger a\right) \tag{2.50}$$

We also consider the pumping from $|0\rangle\, to\, |e\rangle$, mentioned before, which contributes to the master equation in the following way

$$\mathcal{L}_p\rho = \frac{r}{2}\left(2\sigma_{e0}\rho\sigma_{0e} - \sigma_{0e}\sigma_{e0}\rho - \rho\sigma_{0e}\sigma_{e0}\right) \tag{2.51}$$

where $\sigma_{e0} = |e\rangle\langle 0|$.

Although the construction of a laser is based on stimulated emission, the excited state, $|e\rangle$ is also subject to spontaneously decay into the $|g\rangle$ state. The master equation for this dissipation process is given by

$$\mathcal{L}_{eg}\rho = \frac{\Gamma_{eg}}{2}\left(2\sigma_-\rho\sigma_+ - \sigma_+\sigma_-\rho - \rho\sigma_+\sigma_-\right) \tag{2.52}$$

where Γ_{eg} is a Fermi's golden-rule decay rate for spontaneous emission.

The spontaneously decay may also occur in two more situations. The atom has a chance to decay to the lowest level, $|0\rangle$, from the $|g\rangle$ and $|e\rangle$ states. We include these processes in the equation below

$$\mathcal{L}_{sd}\rho = \frac{\Gamma_{e0}}{2}\left(2\sigma_{0e}\rho\sigma_{e0} - \sigma_{e0}\sigma_{0e}\rho - \rho\sigma_{e0}\sigma_{0e}\right) + \frac{\Gamma_{g0}}{2}\left(2\sigma_{0g}\rho\sigma_{g0} - \sigma_{g0}\sigma_{0g}\rho - \rho\sigma_{g0}\sigma_{0g}\right) \tag{2.53}$$

where $\sigma_{0g} = |0\rangle\langle g|$.

We may also consider the dephasing of the atomic dipole moment caused by an energy-conserving scattering of atoms by external degrees of freedom, beyond the fundamental decoherence limit imposed by the spontaneous decay rate Γ_{eg}. Such a process can be expressed in the master equation as follows

$$\mathcal{L}_d\rho = -\frac{\gamma}{2}\left(\sigma_{ee}\rho\sigma_{gg} + \sigma_{gg}\rho\sigma_{ee}\right) \tag{2.54}$$

Finally, summing all the contributions along with the Liouville-von Neumann term, we have the master equation for the combined atomic-field density matrix ρ

$$\begin{aligned}\dot{\rho}(t) &= ig\left(\rho a^\dagger\sigma_- + \rho a\sigma_+ - a^\dagger\sigma_-\rho - a\sigma_+\rho\right) + \frac{C}{2}\left(2a\rho a^\dagger - a^\dagger a\rho - \rho a^\dagger a\right) \\ &\quad + \frac{r}{2}\left(2\sigma_{e0}\rho\sigma_{0e} - \sigma_{0e}\sigma_{e0}\rho - \rho\sigma_{0e}\sigma_{e0}\right) + \frac{\Gamma_{eg}}{2}\left(2\sigma_-\rho\sigma_+ - \sigma_+\sigma_-\rho - \rho\sigma_+\sigma_-\right) \\ &\quad + \frac{\Gamma_{e0}}{2}\left(2\sigma_{0e}\rho\sigma_{e0} - \sigma_{e0}\sigma_{0e}\rho - \rho\sigma_{e0}\sigma_{0e}\right) + \frac{\Gamma_{g0}}{2}\left(2\sigma_{0g}\rho\sigma_{g0} - \sigma_{g0}\sigma_{0g}\rho - \rho\sigma_{g0}\sigma_{0g}\right) \\ &\quad - \frac{\gamma}{2}\left(\sigma_{ee}\rho\sigma_{gg} + \sigma_{gg}\rho\sigma_{ee}\right)\end{aligned} \tag{2.55}$$

Our interest lies in the cavity field, whose density matrix can be obtained by tracing

over the atomic coordinates

$$\frac{d}{dt}\rho_f = Tr_{atom}\left[\frac{d}{dt}\rho\right] = \sum_{i=0,g,e}\left\langle i\left|\left[\frac{d}{dt}\rho\right]\right|i\right\rangle \tag{2.56}$$

We start calculating the non-diagonal terms

$$\dot{\rho}_{ge} = ig\left(\rho_{gg}a^{\dagger} - a^{\dagger}\rho_{ee}\right) - \frac{\Gamma_{eg}}{2}\rho_{ge} - \frac{\Gamma_{g0}}{2}\rho_{ge} - \frac{\Gamma_{e0}}{2}\rho_{ge} - \frac{\gamma}{2}\rho_{ge} \tag{2.57}$$

We can define the total decay rate of the atomic dipole

$$\gamma_t = \gamma + \Gamma_{eg} + \Gamma_{g0} + \Gamma_{e0} \tag{2.58}$$

Substituting the total atomic decay into Eq. (2.57) we obtain

$$\dot{\rho}_{ge} = ig\left(\rho_{gg}a^{\dagger} - a^{\dagger}\rho_{ee}\right) - \frac{\gamma_t}{2}\rho_{ge} \tag{2.59}$$

Naturally we can find its adjoint counterpart by making

$$\dot{\rho}_{eg} = \left(\dot{\rho_{ge}}\right)^{\dagger} = ig\left(\rho_{ee}a - a\rho_{gg}\right) - \frac{\gamma_t}{2}\rho_{ge} \tag{2.60}$$

The other equations of motion can be obtained through the same method and are given below

$$\dot{\rho}_{0g} = ig\rho_{0e}a - \frac{\left(\Gamma_{g0} + r\right)}{2}\rho_{0g} \tag{2.61}$$

$$\dot{\rho}_{g0} = -iga^{\dagger}\rho_{e0} - \frac{\left(\Gamma_{g0} + r\right)}{2}\rho_{g0} \tag{2.62}$$

$$\dot{\rho}_{0e} = ig\rho_{0g}a^{\dagger} - \frac{\left(r + \Gamma_{e0} + \Gamma_{eg}\right)}{2}\rho_{0e} \tag{2.63}$$

$$\dot{\rho}_{e0} = -iga\rho_{g0} - \frac{\left(r + \Gamma_{e0} + \Gamma_{eg}\right)}{2}\rho_{e0} \tag{2.64}$$

Here we assume the photon decay rate C is the slowest decay process. In such a case, the atomic variables can be adiabatically eliminated and the system is described by only field variables. This is called a slaving principle. In the limit $\gamma_t \gg C$, we can adiabatically eliminate the operator ρ_{ge} from Eq. (2.59) by substituting their steady-state solution

$$\rho_{ge} = \frac{2ig}{\gamma_t}\left(\rho_{gg}a^\dagger - a^\dagger\rho_{ee}\right) \tag{2.65}$$

Analogously we have

$$\rho_{eg} = \frac{2ig}{\gamma_t}\left(\rho_{ee}a - a\rho_{gg}\right) \tag{2.66}$$

$$\rho_{0g} = \frac{2ig}{\Gamma_{g0} + r}\,\rho_{0e}a \tag{2.67}$$

$$\rho_{g0} = -\frac{2ig}{\Gamma_{g0} + r}\,a^\dagger\rho_{e0} \tag{2.68}$$

$$\rho_{0e} = \frac{2ig}{\Gamma_{e0} + \Gamma_{eg} + r}\,\rho_{0g}a^\dagger \tag{2.69}$$

$$\rho_{e0} = -\frac{2ig}{\Gamma_{e0} + \Gamma_{eg} + r}\,a\rho_{g0} \tag{2.70}$$

Now we get back to Eq (2.56) and calculate the diagonal terms

$$\dot{\rho_{00}} = \Gamma_{e0}\rho_{ee} + \Gamma_{g0}\rho_{gg} - r\rho_{00}\rho_{00} \tag{2.71}$$

$$\dot{\rho}_{gg} = ig\left(\rho_{ge}a - a^\dagger\rho_{eg}\right) + \Gamma_{eg}\rho_{ee} - \Gamma_{g0}\rho_{gg} \tag{2.72}$$

$$\dot{\rho_{ee}} = ig\left(\rho_{eg}a^\dagger - a\rho_{ge}\right) + r\rho_{00} - \left(\Gamma_{e0} + \Gamma_{eg}\right)\rho_{ee} \tag{2.73}$$

Summing Eqs (2.71), (2.72) and (2.73) we form the total density matrix master equation, i.e. $\dot{\rho_f}(t) = \dot{\rho}_{00}(t) + \dot{\rho}_{gg}(t) + \dot{\rho}_{ee}(t)$

$$\dot{\rho_f}(t) = ig\left(\rho_{ge}a + \rho_{eg}a^\dagger - a\rho_{ge} - a^\dagger\rho_{eg}\right) \tag{2.74}$$

Finally we substitute Eqs (2.65) and (2.66) into Eq. (2.74) and add the cavity decay

$$\begin{aligned}\dot{\rho}_f(t) &= \frac{2g^2}{\gamma_t}\Big(2a^\dagger\rho_{ee}a - aa^\dagger\rho_{ee} - \rho_{ee}aa^\dagger\Big) \\ &\quad -\frac{2g^2}{\gamma_t}\Big(2a\rho_{gg}a^\dagger - a^\dagger a\rho_{gg} - \rho_{gg}a^\dagger a\Big) \\ &\quad +\frac{C}{2}\Big(2a\rho_f a^\dagger - a^\dagger a\rho_f - \rho_f a^\dagger a\Big)\end{aligned} \tag{2.75}$$

The master equation of Eq. (2.75) includes saturation to all orders. Unfortunately, it still depends on the atomic operators ρ_{gg} and ρ_{ee}. To find an analytical expression we shall consider saturation to only second order. Also we consider that most atoms are in the ground state $|0\rangle$ at all times, i.e. $\rho_f = \rho_{00} + \rho_{gg} + \rho_{ee} \approx \rho_{00}$, and the lower lasing level $|g\rangle$ decays very fast to the ground state $|0\rangle$ so we can say that

$$\rho_{gg} \approx 0 \tag{2.76}$$

Thus Eq. (2.73) becomes

$$\dot{\rho_{ee}} = r\rho_{00} - \Big(\Gamma_{eg} + \Gamma_{e0}\Big)\rho_{ee} - \frac{2g^2}{\gamma_t}\Big(aa^\dagger\rho_{ee} + \rho_{ee}aa^\dagger\Big) \tag{2.77}$$

and we use perturbation technique to the second order to obtain

$$\rho_{ee} \approx \frac{r}{\Gamma_{eg} + \Gamma_{e0}}\rho_f - \frac{2g^2 r}{\gamma_t\Big(\Gamma_{eg} + \Gamma_{e0}\Big)^2}\Big(aa^\dagger\rho_f + \rho_f aa^\dagger\Big) \tag{2.78}$$

Substituting Eq. (2.78) into Eq. (2.75) we can finally write

$$\begin{aligned}\frac{d}{dt}\rho_f &= \frac{2rg^2}{\gamma_t\Big(\Gamma_{eg} + \Gamma_{e0}\Big)}\Big(2a^\dagger\rho_f a - aa^\dagger\rho_f - \rho_f aa^\dagger\Big) \\ &\quad +\frac{4rg^4}{\gamma_t^2\Big(\Gamma_{eg} + \Gamma_{e0}\Big)^2}\Big(aa^\dagger aa^\dagger\rho_f + \rho_f aa^\dagger aa^\dagger \\ &\quad + 2aa^\dagger\rho_f aa^\dagger - 2a^\dagger aa^\dagger\rho_f a - 2a^\dagger\rho_f aa^\dagger a\Big) \\ &\quad +\frac{C}{2}\Big(2a\rho_f a^\dagger - a^\dagger a\rho_f - \rho_f a^\dagger a\Big)\end{aligned} \tag{2.79}$$

This is the master equation for the reduced field density matrix. The first and the last terms stand for the linear gain and the cavity loss, respectively, while the second term is

call the gain saturation. The saturation is a nonlinear process that can be understood as a system acting back on the reservoir, and it is responsible for the laser having a stationary solution even far from the equilibrium condition.

Now, let us define the linear gain as

$$\mathcal{A} = \frac{4rg^2}{\gamma_t\left(\Gamma_{eg} + \Gamma_{e0}\right)} \tag{2.80}$$

And the gain saturation is

$$\mathcal{B} = \frac{32rg^4}{\gamma_t^2\left(\Gamma_{eg} + \Gamma_{e0}\right)^2} = 8\mathcal{A}\,\frac{g^2}{\gamma_t\left(\Gamma_{eg} + \Gamma_{e0}\right)} \tag{2.81}$$

Substituting Eqs (2.80) and (2.81) into Eq (2.79) we obtain

$$\begin{aligned}\frac{d}{dt}\rho_f &= \frac{\mathcal{A}}{2}\left(2a^\dagger\rho_f a - aa^\dagger\rho_f - \rho_f aa^\dagger\right)\\ &+\frac{\mathcal{B}}{2}\left[\frac{1}{4}aa^\dagger aa^\dagger\rho_f + \frac{1}{4}\,\rho_f aa^\dagger aa^\dagger\right.\\ &\left.+\,\frac{1}{2}aa^\dagger\rho_f aa^\dagger - \,\frac{1}{2}a^\dagger aa^\dagger\rho_f a - \,\frac{1}{2}a^\dagger\rho_f aa^\dagger a\right]\\ &+\frac{C}{2}\left(2a\rho_f a^\dagger - a^\dagger a\rho_f - \rho_f a^\dagger a\right)\end{aligned} \tag{2.82}$$

Here we take some time to unify our atomic decay rates so the next step is simpler. These decay rates are: Γ_{eg}, for the $|e\rangle \to |g\rangle$ decay, Γ_{e0}, for the $|e\rangle \to |0\rangle$ decay, Γ_{g0}, for the $|g\rangle \to |0\rangle$ decay and finally γ, for the dephasing process. The first two decay rates, Γ_{eg} and Γ_{e0}, must be much smaller than the coupling of the Hamiltonian, i.e. $\Gamma_{eg}, \Gamma_{e0} \ll g$, which means that the atom is much more likely to exchange excitation with the cavity through the Hamiltonian, stimulatingly emitting a photon, than to emit a photon via spontaneous emission. Moreover, after the atom emitted a photon and decayed to the $|g\rangle$ state, we need it to go to the $|0\rangle$ state for the atomic pumping lead it back to the $|e\rangle$ state, so the process continues. In this case we have $\Gamma_{g0} \gg \Gamma_{eg}, \Gamma_{e0}$. The dephasing process does not play an important role, so we shall make $\gamma \ll \Gamma_{g0}$.

After all this analysis, let us say that $\gamma_t\left(\Gamma_{eg} + \Gamma_{e0}\right) = 2\Gamma^2$ so we can write $\mathcal{A} = 2rg^2/\Gamma^2$ and $\mathcal{B} = 4\mathcal{A}g^2/\Gamma^2$.

In possession of the master equation for the reduced field we aim for the steady state

by making a coarse grained time approximation

$$\dot{\rho}_{nn} = \frac{\rho_{nn}(t+\Delta t) - \rho_{nn}(t)}{\Delta t} = r \int_0^\infty d\tau\, \Gamma e^{-\Gamma t} \left[\sum_\alpha \rho_{\alpha n,\alpha n}(t+\tau) - \rho_{nn}(t) \right] \tag{2.83}$$

where r is the rate of excited state atom injection into the cavity, Γ stands for a general decay rate for the atom inside the cavity, $\rho_{nn}(t)$ is the diagonal density matrix element with $\alpha = g, e$ at a time t and $\rho_{\alpha n,\alpha n}(t+\tau)$ is the straightforward diagonal matrix element evolved from $\rho_{nn}(t)$ though the unitary time evolution operator

$$U(\tau) = e^{iV\tau} \tag{2.84}$$

Following we assume that the system at a time t is in a pure state, for simplicity. The final master equation is independent of the choice of an initial state and we obtain the identical result if we start with a mixed state. We shall express this state as

$$|\psi(t)\rangle = \sum_n C_n(t)\, |e\rangle \otimes |n\rangle \tag{2.85}$$

By applying the time evolution operator of Eq (2.84) into the state given above we get

$$\begin{aligned} |\psi(t+\tau)\rangle &= \sum_n C_n(t) \sum_j \frac{(ig\tau)^j}{j!} \left(a^\dagger \sigma_- + a\sigma_+ \right)^j |e\rangle \otimes |n\rangle \\ &= \sum_n \Big[C_{en}(t+\tau)\, |e\rangle\, |n\rangle + C_{g,n+1}(t+\tau)\, |g\rangle \otimes |n+1\rangle \Big] \end{aligned} \tag{2.86}$$

where

$$C_{en}(t+\tau) = C_n(t) \cos\left(g\tau\sqrt{n+1} \right) \tag{2.87}$$

$$C_{g,n+1}(t+\tau) = iC_n(t) \sin\left(g\tau\sqrt{n+1} \right) \tag{2.88}$$

which enable us to write the matrix elements

$$\begin{aligned} \rho_{en}(t+\tau) &= C_{en}(t+\tau) C^*_{en}(t+\tau) \\ &= \rho_{nn}(t) \cos^2\left(g\tau\sqrt{n+1} \right) \end{aligned} \tag{2.89}$$

and

$$\begin{aligned}\rho_{gn+1}(t+\tau) &= C_{gn}(t+\tau)C^{*}_{gn}(t+\tau) \\ &= \rho_{nn}(t)\sin^2\left(g\tau\sqrt{n+1}\right)\end{aligned} \tag{2.90}$$

However in Eq. (2.83) we established the number of photons as n, meaning that the matrix element we should use is the one coming from ρ_{n-1}, i.e. we make $n \to n-1$ on Eq. (2.90). Using this updated equation together with Eq. (2.89) into Eq. (2.83) we obtain

$$\begin{aligned}\dot{\rho}_{nn} &= r\left[\int_0^\infty d\tau\,\Gamma e^{-\Gamma\tau}\rho_{nn}(t)\cos^2\left(g\tau\sqrt{n+1}\right)\right. \\ &\quad \left.+\int_0^\infty d\tau\,\Gamma e^{-\Gamma\tau}\rho_{n-1,n-1}(t)\sin^2\left(g\tau\sqrt{n}\right)-\int_0^\infty d\tau\,\Gamma e^{-\Gamma\tau}\rho_{nn}(t)\right]\end{aligned} \tag{2.91}$$

where the integrals are given by

$$\int_0^\infty d\tau\,\Gamma e^{-\Gamma\tau}\cos^2\left(g\tau\sqrt{n+1}\right) = \frac{\Gamma^2+2g^2(n+1)}{\Gamma^2+4g^2(n+1)} \tag{2.92a}$$

$$\int_0^\infty d\tau\,\Gamma e^{-\Gamma\tau}\sin^2\left(g\tau\sqrt{n}\right) = \frac{2g^2n}{\Gamma^2+4g^2n} \tag{2.92b}$$

Next we substitute the results from the integrals (2.92a) and (2.92b) together with adding the matrix elements of the cavity photon loss Liouvillian into the master equation of Eq. (2.91)

$$\begin{aligned}\dot{\rho}_{nn} &= \frac{r+2r\left(\frac{g}{\Gamma}\right)^2\left(n+1\right)}{1+4\left(\frac{g}{\Gamma}\right)^2\left(n+1\right)}\rho_{nn}-r\rho_{nn}-\frac{2r\left(\frac{g}{\Gamma}\right)^2 n}{1+4\left(\frac{g}{\Gamma}\right)^2 n}\rho_{n-1,n-1} \\ &\quad +\frac{C}{2}\langle n|\left(2a^\dagger\rho a-aa^\dagger\rho-\rho aa^\dagger\right)|n\rangle\end{aligned} \tag{2.93}$$

where we can see that naturally the linear gain and gain saturation coefficients (Eqs (2.80) and (2.81)) appear. A straightforward calculation gives us

$$\dot{\rho}_{nn} = \frac{\mathcal{A}n}{1+n\frac{\mathcal{B}}{\mathcal{A}}}\,\rho_{nn} - \frac{\mathcal{A}(n+1)}{1+(n+1)\frac{\mathcal{B}}{\mathcal{A}}}\,\rho_{n-1,n-1} + Cn\,\rho_{n-1,n-1} - C(n+1)\,\rho_{nn} \quad (2.94)$$

that is equivalent to Eq. (2.30) and the same treatment of finding the steady state solutions can be applied.

We have shown that these two methods give the same results and each of them has its own advantages. The first one is more intuitive and the hand calculation is easier, however it is not quite simple to simulate in a computational program, whereas the second method allows us to include much more phenomena, making a more complete description of the laser, such as all the decay rates. Besides, although the second one is more complicated it is a lot easier to simulate.

At last, let us show that we can obtain the mean photon number directly from the Master Equation of Eq. (2.55), calculating equations of motion for the average value of a desired operator by multiplying on one side of the equation by this operator and taking the partial trace over the density matrix variables. The relevant equations of motion are:

$$\frac{d}{dt}\langle a^\dagger a\rangle = ig\left(\langle a\sigma_+\rangle - \langle a^\dagger\sigma_-\rangle\right) - C\langle a^\dagger a\rangle \quad (2.95a)$$

$$\frac{d}{dt}\langle a\rangle = -ig\langle\sigma_-\rangle - \frac{C}{2}\langle a\rangle \quad (2.95b)$$

$$\frac{d}{dt}\langle\sigma_-\rangle = ig\langle a\rangle\left(\langle\sigma_+\sigma_-\rangle - \langle\sigma_-\sigma_+\rangle\right) - \frac{\left(\Gamma_{eg}+\Gamma_{e0}+\Gamma_{g0}+\gamma\right)}{2}\langle\sigma_-\rangle \quad (2.95c)$$

$$\frac{d}{dt}\langle\sigma_+\sigma_-\rangle = ig\left(\langle a^\dagger\sigma_-\rangle - \langle a\sigma_+\rangle\right) + r\langle|0\rangle\langle 0|\rangle - \left(\Gamma_{eg}+\Gamma_{e0}\right)\langle\sigma_+\sigma_-\rangle \quad (2.95d)$$

$$\frac{d}{dt}\langle\sigma_-\sigma_+\rangle = ig\left(\langle a\sigma_+\rangle - \langle a^\dagger\sigma_-\rangle\right) + \Gamma_{eg}\langle\sigma_+\sigma_-\rangle - \Gamma_{g0}\langle\sigma_-\sigma_+\rangle \quad (2.95e)$$

$$\frac{d}{dt}\langle|0\rangle\langle 0|\rangle = -r\langle|0\rangle\langle 0|\rangle + \Gamma_{e0}\langle\sigma_+\sigma_-\rangle + \Gamma_{g0}\langle\sigma_-\sigma_+\rangle \quad (2.95f)$$

Since we are looking for a solution in the steady-state we can set all the derivatives of expected values equal to zero. Using these equations, together with the closure relation for the atomic basis,

$$\mathbb{I} = |0\rangle\langle 0| + |g\rangle\langle g| + |e\rangle\langle e| \tag{2.96}$$

where $|g\rangle\langle g| = \sigma_-\sigma_+$ and $|e\rangle\langle e| = \sigma_+\sigma_-$, we can solve this linear system finding

$$\langle a^\dagger a\rangle = \frac{r/C}{2r+\Gamma_{g0}+\Gamma_{e0}}\left[\Gamma_{g0}\left(1-\frac{\gamma_t C}{4g^2}\right)-\Gamma_{eg}\right] - \frac{\gamma_t\left[\Gamma_{eg}\left(r+\Gamma_{g0}\right)+\Gamma_{e0}\Gamma_{g0}\right]}{4g^2\left(2r+\Gamma_{g0}+\Gamma_{e0}\right)} \tag{2.97}$$

In order to verify this method consistency, below we have a simulation where we plot the distributions of probability in the Fock basis for the laser generated by Eq. (2.55) and a coherent state distribution with $|\alpha|^2$ given by Eq. (2.97).

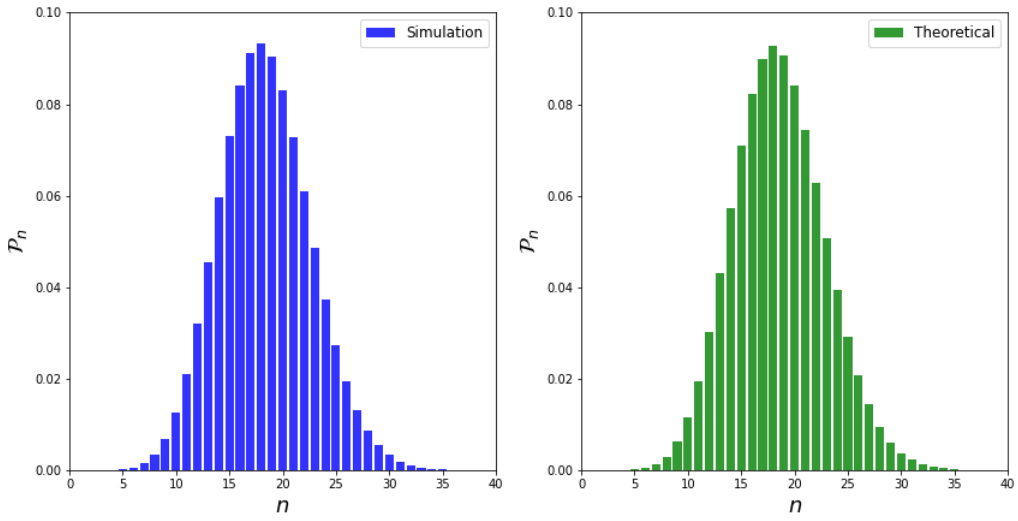

Figure 2.5 – Occupation probability in the Fock space. The blue histogram comes from the laser obtained through the Master Equation 2.55 and the green one refers to the theoretical prediction from Eq.(2.97)

Source: By the author.

Described in units of g, the parameters used were: $r = 0.1$, $\Gamma_{g0} = 7.5$, $\Gamma_{eg} = \Gamma_{e0} = \gamma = 0.1$ and $C = 0.005$. From Eq. (2.97) we expect the mean photon number to be around 18.6, which is satisfactorily accurate in comparison with the laser obtained by simulating Eq. (2.55), that gives us the mean photon number of 18.4.

As said in the beginning of this chapter, there are many methods of studying laser light, and each one has its own advantages. Here we tried to show how to extract the best of them, in terms of phenomena understanding and also computational simulation.

2.3 The Fokker-Planck Equation: Laser Linewidth

So far we have focused on the probability distribution for the laser, calculated by using the density matrix, but there is another important feature we can analyse: the dynamics of the laser linewidth.

Once we have obtained the master equation for the reduced field density matrix (2.83) we can introduce the diagonal $P(\alpha)$ representation of coherent states for ρ_f

$$\rho_f = \int P(\alpha) \left|\alpha\right\rangle\!\left\langle\alpha\right| \frac{d^2\alpha}{\pi} \tag{2.98}$$

through which we can obtain the quantum mechanical Fokker-Planck equation for a laser

$$\frac{d}{dt}P(\alpha) = -\frac{1}{2}\left\{\frac{\partial}{\partial\alpha}\left[\left(\mathcal{A} - C - \mathcal{B}\alpha^2\right)\alpha P(\alpha)\right] + c.c.\right\} + \mathcal{A}\,\frac{\partial^2}{\partial\alpha\partial\alpha^*}P(\alpha) \tag{2.99}$$

Rewriting the above equation using polar coordinates with $\alpha = re^{i\theta}$

$$\begin{aligned}\frac{d}{dt}P(r,\theta) = -\frac{1}{2}\frac{1}{r}\frac{\partial}{\partial r}\left[r^2\left(\mathcal{A} - C - \mathcal{B}r^2\right)P(r,\theta)\right] \\ \frac{1}{4}\mathcal{A}\left(\frac{\partial^2}{\partial r^2} + \frac{1}{r}\frac{\partial}{\partial r} + \frac{1}{r^2}\frac{\partial^2}{\partial\theta^2}\right)P(r,\theta)\end{aligned} \tag{2.100}$$

We see that the first term of the above equation is the drift term and the second one is the diffusion term. In the steady state we set $\frac{d}{dt}P(r,\theta) = 0$. Assuming an average amplitude r_0, the drift term disappears at $r = r_0$ and we obtain

$$\mathcal{A} - C - \mathcal{B}r_0^2 = 0 \tag{2.101}$$

Introducing a small amplitude noise by

$$\Delta r = r - r_0 \tag{2.102}$$

we have

$$r^2\left(\mathcal{A} - C - \mathcal{B}r^2\right) = -2r\left(\mathcal{B}r_0^2\right)(r - r_0) \tag{2.103}$$

Subtituting Eq. (2.103) into Eq. (2.100) together with $\frac{d}{dt}P(r,\theta) = 0$ and using the ansatz $P(r,\theta) = P(r)\Phi(\theta)$ we have

$$\frac{1}{2}\frac{1}{r}\frac{\partial}{\partial r}\left[2r\mathcal{B}r_0^2(r - r_0)P(r)\right] + \frac{\mathcal{A}}{4}\frac{1}{r}\frac{\partial}{\partial r}\left[r\frac{\partial}{\partial r}P(r)\right] = 0 \tag{2.104}$$

which leads to

$$\frac{\partial}{\partial r}P(r) = -\frac{4\mathcal{B}r_0^2}{\mathcal{A}}(r - r_0)P(r) \tag{2.105}$$

The solution is given by the Gaussian distribution

$$P(r) = \frac{1}{\sqrt{2\pi\sigma^2}}\, e^{\left[-\frac{(r - r_0)^2}{2\sigma^2}\right]} \tag{2.106}$$

where the variance in the amplitude is given by

$$\sigma^2 = \frac{\mathcal{A}}{4\mathcal{B}r_0^2} \tag{2.107}$$

Looking far above threshold, the average amplitude r_0 satisfies

$$r_0^2 = \frac{\mathcal{A} - C}{\mathcal{B}} \approx \frac{\mathcal{A}}{\mathcal{B}} \tag{2.108}$$

Therefore, the variance is reduced to

$$\sigma^2 = \frac{1}{4} \tag{2.109}$$

That is the well known amplitude noise of a coherent state, corresponding to the Poisson photon statistics.

The steady state solution for the angular distribution function $\Phi(\theta)$ from Eq. (2.100) leads to

$$\frac{d}{d\theta}\Phi(\theta) = 0 \tag{2.110}$$

The above result suggests that the laser phase is uniformly distributed in $[0, 2\pi]$ under the steady state condition. This conclusion originates from the fact that a laser has a restoring force only for the amplitude r and does not have a restoring force for the phase

θ. The gain saturation term $\mathcal{B}r^2$ in Eq. (2.100) only depends on the amplitude r, so that a laser is a phase insensitive oscillator. Nevertheless, the field emitted by a laser has a distinct feature from a thermal field not only in the amplitude (or photon number) distribution but also in the phase noise. The time dependent phase distribution function satisfies

$$\frac{d}{dt}\Phi(\theta) = \frac{\mathcal{A}}{4}\frac{1}{r_0^2}\frac{\partial^2}{\partial\theta^2}\Phi(\theta) \equiv \frac{D}{2}\frac{\partial^2}{\partial\theta^2}\Phi(\theta) \tag{2.111}$$

where D is the phase diffusion constant and corresponds precisely to the Schawlow-Townes laser linedwidth, when $\mathcal{A} \approx C$, that is not far from the threshold. The fourth-order expansion used to obtain Eq. (2.83) loses its validity well above threshold. It is interesting to observe that C is the empty cavity linewidth, thus the formula

$$D = \frac{C}{2\langle n\rangle} \tag{2.112}$$

shows that the linewidth is decreased by a factor $\langle n\rangle^{-1}$.

These results were also calculated by Lax,(78) Gordon (79) and Haken. (80)

2.4 Pseudo-Hermitian Quantum Mechanics

A system governed by an Hermitian Hamiltonian has real spectra and unitary evolution. This is so common that this hermiticity is usually implicit. The unitary evolution ensures that, if we have a normalized state at a time t_0, the states coming from the time evolution operator from the Schrödinger equation are normalized at all times $t > t_0$ and the real spectra means that the expectation values for the energies of the system are real values, i.e. they can be measured and interpreted as usually. Therefore is clear the preference of using Hermitian Hamiltonians. The main idea of a pseudo-Hermitian quantum theory is to shed light on Hamiltonians that would have been ignored due to its non-Hermitian nature by replacing the Hermiticity condition with a weaker condition showing space-time reflection symmetry. These new Hamiltonians may have interesting mathematical features and may prove themselves very adequate in describing the physical world. Naturally we should not discard any of the key physical properties presented in a quantum theory, as we will show, as long as a pseudo-Hermitian Hamiltonian exhibits all of the properties of a Hermitian quantum theory in a new metric.

Let us consider a system with a non-Hermitian Hamiltonian $\mathcal{H}$. The Schrödinger

equation reads

$$i\hbar\frac{\partial}{\partial t}\left|\psi(t)\right\rangle = \mathcal{H}\left|\psi(t)\right\rangle \tag{2.113}$$

Now we introduce the (time independent) Dyson map η, a non unitary operator, as follows

$$i\hbar\frac{\partial}{\partial t}\Big(\eta\left|\psi(t)\right\rangle\Big) = \eta\,\mathcal{H}\,\eta^{-1}\Big(\eta\left|\psi(t)\right\rangle\Big) \tag{2.114}$$

We can rewrite the above equation in the form of the Schrödinger equation

$$i\hbar\frac{\partial}{\partial t}\left|\phi(t)\right\rangle = h\left|\phi(t)\right\rangle \tag{2.115}$$

where we have

$$h = \eta\,\mathcal{H}\,\eta^{-1} \tag{2.116a}$$

$$\left|\phi\right\rangle = \eta\ \left|\psi\right\rangle \tag{2.116b}$$

We impose this new Hamiltonian to be Hermitian, i.e. $h = h^\dagger$, so Eq (2.116a) leads to the pseudo-Hermiticity relation

$$\Theta\,\mathcal{H} = \mathcal{H}^\dagger\,\Theta \tag{2.117}$$

where $\Theta = \eta^\dagger\eta$ is the metric operator.

We can apply the result from Eq.(2.116a) to obtain the same relation as in Eq.(2.117) for any observable $\mathcal{O}(X,P)$ of the non-Hermitian system associated with the observables $o(x,p)$ of the Hermitian system, such that

$$\mathcal{O} = \ \eta^{-1}o\ \eta \tag{2.118}$$

Therefore, all observables become pseudo-Hermitian ($\mathcal{O}^\dagger\,\Theta = \Theta\,\mathcal{O}$) and, depending on the observable of interest, as momentum or position for example, the choice of the metric can be made so that this observable is Hermitian. (81)

Using Eq. (2.116b) we can demonstrate that the time evolution is unitary, using the

metric to calculate the inner product.

$$\left\langle \psi(t)\middle|\tilde{\psi}(t)\right\rangle_{\Theta} \equiv \left\langle \psi(t)\middle|\Theta\middle|\tilde{\psi}(t)\right\rangle = \left\langle \phi(t)\middle|\tilde{\phi}(t)\right\rangle \tag{2.119}$$

We can also demonstrate that the Hamiltonians $\mathcal{H}$ and h have the same spectrum. Let us consider a system governed by the Hermitized Hamiltonian h whose eigenvalues and eigenstates are given by

$$h\,|\phi_n\rangle = \mathcal{E}_n\,|\phi_n\rangle \tag{2.120}$$

Using Eq (2.116a) and Eq (2.116b) into the above equation we show that $\mathcal{H}$ and h have the same spectrum:

$$\mathcal{H}\,|\psi_n\rangle = \mathcal{E}_n\ \ |\psi_n\rangle \tag{2.121}$$

At last we calculate the expected values associated with the evolution governed by $\mathcal{H}$

$$\left\langle \psi(t)\middle|\mathcal{O}\middle|\tilde{\psi}(t)\right\rangle_{\Theta} \equiv \left\langle \psi(t)\middle|\Theta\ \mathcal{O}\middle|\tilde{\psi}(t)\right\rangle = \left\langle \phi(t)\middle|o\middle|\tilde{\phi}(t)\right\rangle \tag{2.122}$$

CHAPTER 3

SQUEEZED VACUUM STATE LASER WITH ZERO DIFFUSION FROM CAVITY LOSSES

3.1 Introduction and motivation

It is well-known that squeezed states are most efficiently generated from optical parametric down-conversion in a non-linear $\chi^{(2)}$ crystal. (76, 82, 83) We also mention the generation of squeezed states by four wave mixing in an optical cavity. (76, 83, 84) However, our purpose here is to demonstrate the possibility of generating squeezed state of light through the laser mechanism, with the required nonlinearity being constructed through the atom-field interaction itself. The squeezing of cavity-field states through their effective interaction with atoms have been systematically pursued in cavity quantum electrodynamics. (85–88) The most distinctive characteristic of our laser method for building a steady squeezed state is exactly that the required nonlinearity for light squeezing is here replaced by the same atom-field effective interaction that coherently pumps the cavity.

A laser with reduced linewidth is most useful for a variety of applications, among which we mention optical sensing, metrology, higher order coherent communication, high-precision detection, and laser spectroscopy. (89) Therefore, the method here presented can contribute to or inspire the design of lasers with exceedingly small diffusion and linewidth, with broad technological applications.

Our proposal for the construction of a squeezed vacuum state laser with zero phase diffusion due to cavity losses is based on the construction of an effective atom-field inter-

actions from the usual Jaynes-Cummings Hamiltonian (JCH)

$$\lambda \left(a^{\dagger} \sigma_{-} + a \sigma_{+} \right), \tag{3.1}$$

where λ is the Rabi frequency, $a^{\dagger}$ and a are the cavity photon creation and annihilation operators, while σ_{+} and σ_{-} are the Pauli raising and lowering operators for the two-level atom. The engineering of the effective interaction must obey two conditions:

i) First, this interaction must present the same bilinear form of the JCH, i.e.,

$$\chi \left(A^{\dagger} \sigma_{-} + A \sigma_{+} \right) \tag{3.2}$$

where χ is the effective atom-field coupling while $A^{\dagger}$ and A are generalized photon creation and annihilation operator constructed from $a^{\dagger}$ and a. This bilinear form allows us to establish an isomorphism between the cavity field operators in our effective laser $(A^{\dagger}, A)$ and in the conventional coherent state laser $(a^{\dagger}, a)$. This isomorphism, mapping the field operators $a \leftrightarrow A$ and $a^{\dagger} \leftrightarrow A^{\dagger}$, allows us to derive the equations of the effective laser directly from those of the conventional laser, and consequently, the steady state of the effective laser automatically from the coherent state of the usual theory. To this end, we must complete the construction of such an isomorphism by deriving, from the vector basis of the conventional laser, $\{|n\rangle\}$, another vector basis for the cavity field of the effective laser, $\left\{ |n\rangle^{A} \right\}$. The action of our generalized operators $\left(A^{\dagger}, A \right)$ on the basis state $\left\{ |n\rangle^{A} \right\}$ must emulate that of the usual creation and annihilation operators $\left(a^{\dagger}, a \right)$ on the Fock space $\{|n\rangle\}$. Consequently, the master equation describing the effective laser will be exactly that following from the conventional laser through the map $a \leftrightarrow A$ and $a^{\dagger} \leftrightarrow A^{\dagger}$. In the above-threshold regime, the steady state of the effective laser will be exactly the coherent state written in the new basis $\left\{ |n\rangle^{A} \right\} : |\alpha\rangle^{A} = e^{-|\alpha|^{2}/2} \sum_{n=0}^{\infty} \left(\alpha^{n} / \sqrt{n!} \right) |n\rangle^{A}$, which leads to the desired laser state when mapped into the conventional Fock basis.

ii) The second condition ensures the quantum coherence of the effective laser state, say $|\Psi\rangle$, to be minimally affected by cavity losses, the main source of laser noise. For this, the laser state $|\Psi\rangle$ must be an unique eigenstate of A with null eigenvector, i.e., $A|\Psi\rangle = 0$. This condition is the same used in Ref. (60) for the proposition of a reservoir engineering method for the protection of a particular state $|\Psi\rangle$, again the unique eigenstate of a generalized cavity field operator A with null eigenvalue. As discussed in the introduction, the operator A takes place on the bilinear interaction $\tilde{\chi} \left(A^{\dagger} S_{-} + A S_{-} \right)$ which must be engineered between the system whose state must be protected, as a cavity field, and an

auxiliary system described by the operators S_+ and S_-, an atom or an atomic sample. This engineered interaction, under the condition of a sufficiently strong coupling $\tilde{\chi}$, leads to the master equation for the cavity mode

$$\dot{\rho} = (\Gamma/2)\left(2A\rho A^\dagger - A^\dagger A\rho - \rho A^\dagger A\right) + (\gamma/2)\left(2a\rho a^\dagger - a^\dagger a\rho - \rho a^\dagger a\right), \tag{3.3}$$

with $\Gamma \propto \tilde{\chi} \gg \gamma$. Therefore, the Lindbladian for $a^\dagger, a$ acts as a perturbation over that for $A^\dagger, A$, causing the fidelity of the protected state, given by $\mathcal{F} \propto 1 - \gamma/\Gamma$, to be slightly less than unity. However, in our protocol for building the effective laser, the isomorphism between the field operators $(a^\dagger, a)$ and $(A^\dagger, A)$ automatically results in the engineered Lindbladian $(\Gamma/2)\left(2A\rho A^\dagger - A^\dagger A\rho - \rho A^\dagger A\right)$, without the need for the approximations required to obtain this engineered superoperator from Eq. (3.3). Furthermore, we have the advantage of eliminating the unwanted Lindbladian for $a^\dagger, a$ which, acts as a perturbation over that for $A^\dagger, A$. We have thus considered here a particular reservoir engineering technique which, however, keeps all the main ingredients of the method in Ref. (60): the engineering of the effective atom–field interaction and, consequently, of the associated Lindbladian, however with the advantage of eliminating the unwanted Lindbladian for $a^\dagger, a$.

This chapter is organized as follows: In Section 2 we present a scheme, based on the adiabatic elimination of fast variables, for the construction of the effective Hamiltonian required for the operation of the squeezed vacuum laser. In Section 3 we construct the isomorphism between the cavity field operators in the effective and the Jaynes-Cummings interactions, and in Section 4 we present the master equation for the squeezed vacuum laser and the numerical analysis demonstrating the effectiveness of our method. Finally, in Section 5 we present our conclusions.

3.2 The effective atom-field interaction

The first step for achieving our goal is to engineer the atom-field interaction through which we implement the amplification-saturation mechanism building up and sustaining our squeezed vacuum state. The effective interaction follows from considering the transitions induced by quantum and classical fields in a three-level Lambda-type configuration, as depicted in Figure. 3.1. The intermediate (more-excited) atomic level $|i\rangle$ must be considered apart from the lasing levels $|g\rangle$ and $|e\rangle$. The cavity mode (ω) is used to promote the Raman-type transitions $g \longleftrightarrow i$ and $e \longleftrightarrow i$, with detunings $\Delta_g = \omega_i - \omega$ and

$\Delta_e = \omega_0 + \omega - \omega_i$, and coupling strengths λ_g and λ_e. Two pairs of laser beams ($\omega_{g\ell}$ and $\omega_{e\ell}$, $\ell = 1, 2$) help to excite the same atomic transitions with detunings $\delta_{g1} = \omega_{g1} - \omega_i$, $\delta_{g2} = \omega_i - \omega_{g2}$, $\delta_{e1} = \omega_i - \omega_0 - \omega_{e1}$ and $\delta_{e2} = \omega_0 + \omega_{e2} - \omega_i$ and coupling strengths $\Omega_{g\ell}$ and $\Omega_{e\ell}$.

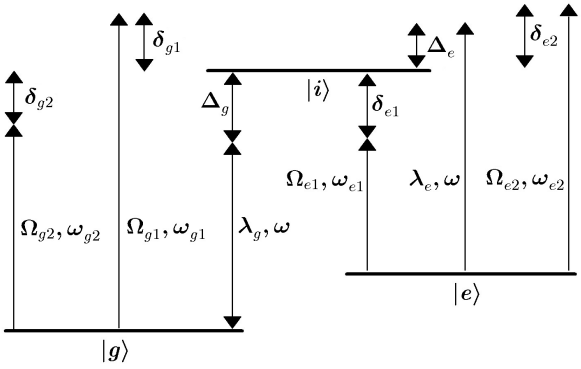

Figure 3.1 – Sketch of the Λ configuration to engineer the effective interaction for building up the squeezed vacuum laser

Source: By the author.

The Hamiltonian describing the process is given by $\mathcal{H}(t) = \mathcal{H}_0 + V(t)$, where ($\hbar = 1$)

$$\mathcal{H}_0 = \omega a^\dagger a + \omega_0 \sigma_{ee} + \omega_i \sigma_{ii} \tag{3.4a}$$

$$V(t) = \lambda_g a \sigma_{ig} + \lambda_e a \sigma_{ie} + \sum_\ell \left(e^{-i\omega_{g\ell} t} \Omega_{g\ell} \sigma_{ig} + e^{-i\omega_{e\ell} t} \Omega_{e\ell} \sigma_{ie} \right) + h.c. \tag{3.4b}$$

using the Pauli operators $\sigma_{rs} = |r\rangle\langle s|$, with r, s denoting the atomic levels. In what follows we assume $\lambda_g = \lambda_e = \lambda$, $\Omega = \Omega_{g1} = \Omega_{g2} = -\Omega_{e1} = -\Omega_{e2}$, $\delta_{g1} = \delta_{g2} = \delta_{e1}/\kappa = \delta_{e2}/\kappa$, $\Delta_g = \delta_{e1}$ and $\Delta_e = \delta_{g1}$. Then, under the set of parameters $\delta_{r\ell} \gg \Omega \gg \bar{n}\lambda$, with $\bar{n}$ being the average photon number in the cavity, we verify that, in the interaction picture, the non-diagonal Hamiltonian $\mathcal{H}_I(t)$ consists of highly oscillatory terms such that, to a good approximation, we obtain the second-order effective Hamiltonian (54–56, 90–92)

$$H_{eff} = -i\mathcal{H}_I(t) \int_0^t d\tau \mathcal{H}_I(\tau) = g \left(A\sigma_+ + A^\dagger \sigma_- \right) \tag{3.5}$$

where $\sigma_+ = |e\rangle\langle g|$, $\sigma_- = |g\rangle\langle e|$, the coupling strength is given by $g = \sqrt{1-\kappa^2}\lambda\Omega^*/\delta_{e1}$, with $\kappa = \delta_{e1}/\delta_{g1}$, and the generalized operators read

$$A = \frac{a + \kappa a^\dagger}{\sqrt{1-\kappa^2}}, \quad A^\dagger = \frac{a^\dagger + \kappa a}{\sqrt{1-\kappa^2}} \tag{3.6}$$

with $\left[A, A^\dagger\right] = \left[a, a^\dagger\right] = 1$. The squeezed vacuum, to be defined below, with squeezing factor $r = \tanh^{-1}\kappa$, is an eigenstate of A with null eigenvalue, as required by the

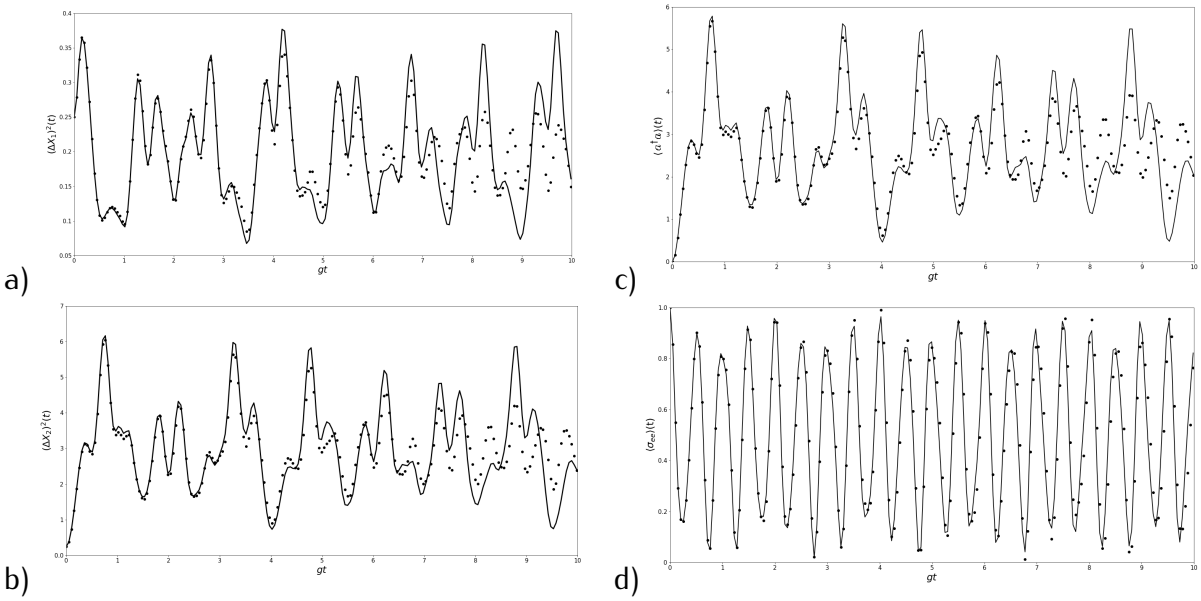

Figure 3.2 – Plot, against gt, of the variances **(a)**, $(\Delta X_1)^2(t)$ and **(b)**, $(\Delta X_2)^2(t)$, and the excitations **(c)**, $\langle a^\dagger a\rangle(t)$ and **(d)**, $\langle \sigma_{ee}\rangle(t)$ in function of gt, for the field states generated by the effective and full Hamiltonians (straight and dotted lines, respectively). We have started with the atom and the cavity mode in the excited and the vacuum state, $|e\rangle|0\rangle$, considering, in units of the Rabi frequency λ, the parameters $\delta_{g1} = 10^3$, $\delta_{e1} = 6\times 10^2$, $\Omega_{g1} = 40$, and $g = 0.05$, such that $\kappa = 0.6$.

Source: By the author.

engineering reservoir technique.

In order to verify the validity of the approximations leading from $V(t)$ to H_{eff}, we plot in Figures 3.2(a) and (b) the variances of the quadratures $X_1 = \left(a^\dagger + a\right)/2$ and $X_2 = \left(a - a^\dagger\right)/2i$, against gt, for the field states generated by both the full and the effective Hamiltonians in Eqs. (3.4) and (3.5). Here we remind that gt is a convenient dimensionless parameter frequently used to indicate the time evolution in atom-field interaction processes. We start with the atom in the excited state $|e\rangle$ and the cavity mode in the vacuum state $|0\rangle$, considering, in units of the Rabi frequency λ, the parameters $\delta_{g1} = 10^3$, $\delta_{e1} = 6\times 10^2$, $\Omega = 40$, and $g = 0.05$, such that $\kappa = 0.6$. In Figures 3.2(a) and (b) the straight and dotted lines refer to the effective and full Hamiltonians, respectively, showing a good agreement between both curves until $gt \approx 7$. We have also plotted in Figures 3.2(c) and (d) the excitations $\langle a^\dagger a\rangle(t)$ and $\langle \sigma_{ee}\rangle(t)$ against gt, and we again see a very good agreement between the curves generated by the full and the effective Hamiltonians until the same $gt \approx 7$. Since our squeezed state laser is built from the effective interaction (3.5), its operating time is then limited to the time interval of the validity of the effective Hamiltonian, $t \approx 7/g = 7\delta_{e1}/\sqrt{1-\kappa^2}\lambda\Omega$, and must be restarted whenever this time interval has elapsed.

Regarding the engineering of the effective atom-field interaction (3.5), a detailed account on Raman transition in cavity quantum electrodynamics can be found in Ref. (93). We note that the atomic level configuration we have used to engineer the required interaction is certainly not unique; it can be engineered from other level configuration using more or less classical fields. Finally, we stress that in engineering the effective Hamiltonian (3.5) we have not take into account the usually small amplitude and phase fluctuations of the required laser beams, which would indeed result in some phase diffusion of our squeezed vacuum laser.

We finally stress that another proposal for building a squeezed lasing has been reported in which the cavity is parametric driven using a non-linear $\chi^{(2)}$ crystal inside the cavity. (94) Our engineered atom-field interaction thus replaces the parametric driven process in Ref. (94), dispensing the non-linear crystal inside the cavity and the coherent drive of the cavity mode. However, since our laser requires the effective atom-field interaction, it has an operating timescale after which it must be restarted.

3.3 The isomorphism between the $A^\dagger, A$ and $a^\dagger, a$ algebras

Having engineered the required interaction (3.5), we now start to construct the vector basis $\{|n\rangle_A\}$ for the cavity field, in whose states $|n\rangle_A$ the action of operators $A^\dagger A$, $A^\dagger$ and A, must lead to the same relations as those resulting from the actions of $a^\dagger a$, $a^\dagger$ and a on the Fock basis $\{|n\rangle\}$, i.e.:

$$A^\dagger A\,|n\rangle_A = n\,|n\rangle_A \tag{3.7a}$$

$$A^\dagger\,|n\rangle_A = \sqrt{n+1}\,|n+1\rangle_A \tag{3.7b}$$

$$A\,|n\rangle_A = \sqrt{n}\,|n-1\rangle_A \tag{3.7c}$$

All the basis states $\{|n\rangle_A\}$ are constructed from the vacuum state $|0\rangle_A$, starting from the relation

$$A\,|0\rangle_A = 0 \tag{3.8}$$

which enables us to determine the probability amplitudes c_n defining the superposition $|0\rangle_A = \sum_n c_n\,|n\rangle$. Considering the operator A as given by Eq. (3.6), we first compute the vacuum state from Eq. (3.8) and then, using the relation $\left(A^\dagger\right)^n |0\rangle_A/\sqrt{n!}$, we derive all the

even and odd generalized excitations, given by

$$|2m\rangle_A = \frac{\left(1-\kappa^2\right)^{1/4}}{\sqrt{(2m)!}} \sum_{n=0}^{\infty} (-\kappa)^{n-m} \sqrt{\frac{(2n-1)!!}{(2n)!!}} \times \sum_{\ell=0}^{m} \binom{m}{\ell} \left(-\kappa^2\right)^{\ell} \frac{(2n)!!}{[2(n+\ell-m)]!!} \frac{[2(n+\ell)-1]!!}{(2n-1)!!} |2n\rangle \tag{3.9a}$$

$$|2m+1\rangle_A = \frac{\left(1-\kappa^2\right)^{3/4}}{\sqrt{(2m+1)!}} \sum_{n=0}^{\infty} (-\kappa)^{n-m} \sqrt{\frac{(2n+1)!!}{(2n)!!}} \times \sum_{\ell=0}^{m} \binom{m}{\ell} \left(-\kappa^2\right)^{\ell} \frac{(2n)!!}{[2(n+\ell-m)]!!} \frac{[2(n+\ell)+1]!!}{(2n+1)!!} |2n+1\rangle \tag{3.9b}$$

The basis defined by the even and odd number states given by Eqs. (3.9), thus establishes the isomorphism between the fields in the squeezed vacuum and the coherent state lasers. Knowing that the steady state of the conventional laser is the coherent state $|\alpha\rangle$ (owing to the Jaynes-Cummings atom-field interaction), it is then automatic to derive the steady state of our laser, which results from the effective Hamiltonian (3.5). Once the isomorphism is established, all we have to do is to describe the coherent state in the vector basis $\{|n\rangle_A\}$, i.e., $|\alpha\rangle_A = D_A(\alpha)|0\rangle_A = \exp\left(\alpha A^\dagger - \alpha^* A\right)|0\rangle_A = e^{-|\beta|^2/2} e^{\beta a^\dagger} e^{-\beta^* a}|0\rangle_A$, with $\beta = (\alpha - \kappa\alpha^*)/\sqrt{1-\kappa^2}$. We obtain, expanded in the usual Fock basis $\{|n\rangle\}$, the state

$$|\alpha\rangle_A = (1-\kappa^2)^{1/4} e^{\left(\kappa\alpha^2 - |\alpha|^2\right)/2} \sum_{n=0}^{\infty} \sqrt{n!} \left(\sum_{\ell=0}^{n} \left(\frac{\kappa}{2}\right)^{\ell/2} \frac{\beta^{n-\ell}}{(n-\ell)!\ell!} H_\ell(x) \right) |n\rangle \tag{3.10}$$

where the argument of the Hermite Polynomials is given by $x = \kappa(\beta^*)^2/2$.

We note that for $\kappa = 0$ we immediately recover the usual Fock basis states from Eq. (3.9) and the usual coherent state from Eq. (3.10). In Figure 3.3(a) we show the photon number distribution $\mathcal{P}_n$ and a phase-space plot of the uncertainties of the laser state given by Eq. (3.10), using $\alpha = 0.18$ and $r = \mathrm{Tanh}^{-1}\kappa = 0.69$, and considering $\kappa = 0.6$ as in Figure 3.2. This produced squeezed vacuum displays a good agreement with the ideal squeezed vacuum $S(r = 0.69)|0\rangle$, whose photon distribution and projection of the Wigner distribution in phase space is shown in Figure 3.3(b), and where S stands for the well-known squeeze operator

$$S(\xi) = \exp\left[\xi^* a^2 - \xi\left(a^\dagger\right)^2\right] \tag{3.11}$$

with $\xi = re^{i\varphi}$, r being the degree of squeezing and φ the squeezing direction in phase

space (76, 83), here with $\varphi = 0$. The produced laser state deviates slightly from the ideal squeezed vacuum as indicated by the populations of the odd Fock states. We finally note that the squeezed vacuum $S(\xi)\,|0\rangle$, with squeezing factor $r = \tanh^{-1}\kappa$, is an eigenstate of A with null eigenvalue, as required by the engineering reservoir technique.

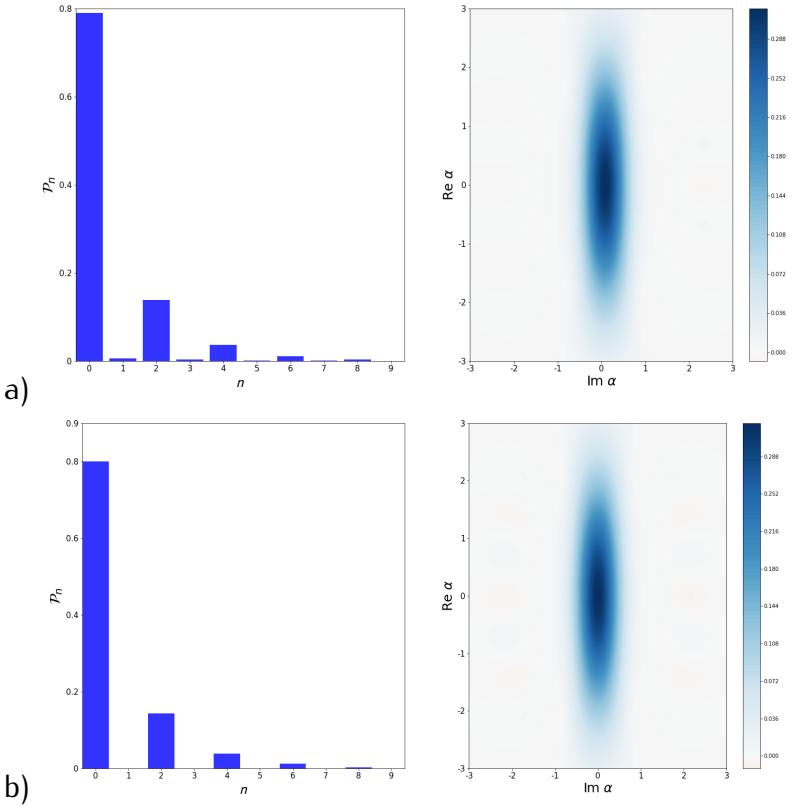

Figure 3.3 – The photon number distribution $\mathcal{P}_n$ and the uncertainties of the squeezed vacuum state in phase-space generated by the **(a)** effective Hamiltonian for $\alpha = 0.18$ and $r = 0.69$, and **(b)** the ideal squeezed vacuum $S(r = 0.69)\,|0\rangle$.
Source: By the author.

3.4 The master equation for the squeezed vacuum laser

From the isomorphism we have established, we automatically derive from the conventional laser theory the master equation describing the dynamics of the cavity field when interacting with a pumped atomic sample, through the effective Hamiltonian (3.5), and the environment. This master equation is given by

$$\dot{\rho} = \mathcal{L}_{\mathcal{A}}\rho + \mathcal{L}_{\mathcal{B}}\rho + \mathcal{L}_{\mathcal{C}}\rho \tag{3.12}$$

where the Lindbladians accounting for gain, saturation and cavity loss, obey the expressions

$$\mathcal{L}_{\mathcal{A}}\rho = \frac{\mathcal{A}}{2}\left(2A^{\dagger}\rho A - AA^{\dagger}\rho - \rho AA^{\dagger}\right) \tag{3.13a}$$

$$\mathcal{L}_{\mathcal{B}}\rho = \frac{\mathcal{B}}{2}\left[\frac{1}{4}AA^{\dagger}\left(AA^{\dagger}\rho + 3\rho AA^{\dagger}\right) + \frac{1}{4}\left(\rho AA^{\dagger} + 3AA^{\dagger}\rho\right)AA^{\dagger} - A^{\dagger}\left(AA^{\dagger}\rho + \rho AA^{\dagger}\right)A\right] + \ldots \tag{3.13b}$$

$$\mathcal{L}_{\mathcal{C}}\rho = \frac{\mathcal{C}}{2}\left(2A\rho A^{\dagger} - A^{\dagger}A\rho - \rho A^{\dagger}A\right) \tag{3.13c}$$

The coefficients for gain $\mathcal{A} = 2R\,(g/\gamma)^2$, saturation $\mathcal{B} = 4\mathcal{A}\,(g/\gamma)^2$, and loss $\mathcal{C} = \omega/Q$, are defined from the atomic pumping rate $R = Kp$, K being the total atomic injection rate, p the probability for the atomic laser excitation, g the Rabi frequency, γ the effective atomic decay rate, and Q the cavity quality factor. The Lindbladian for saturation in Eq. (3.13b) is given only up to 4-th order in g. The isomorphism then assures us that the squeezed vacuum state in Eq. (3.10) follows directly from the competition between amplification ($\mathcal{A}$) and dissipation ($\mathcal{C}$), mediated by the the saturation of the cavity field excitation ($\mathcal{B}$), described by the master equation (3.12). Far above threshold, when $\mathcal{A} \gg \mathcal{C}$, the far from equilibrium steady state of the cavity field is given by Eq. (3.10).

As anticipated above, we note that unlike what happens with engineered reservoirs, we do not have a term in Eq. (3.12) (similar to the Lindbladian for $a^{\dagger}, a$ in Eq. (3.3)), that acts to introduce error in the laser mechanism. This is indeed a remarkable bonus for our method, in which the only source of errors stems from the engineering of the effective Hamiltonian (3.5). By limiting the time interval of the laser operation such that $gt = 7$, the errors coming from the engineered protocol must, however, be small as we have seen from Figure 3.2.

To strengthen our result coming from the isomorphism —that the laser resulting from the atom-field interaction described by the effective Hamiltonian (3.5) is indeed the squeezed vacuum—, in what follows we numerically analyze the construction, step by step, of such a cavity field steady state. For this we numerically simulate the successive passage of N atoms through the cavity, at the rate R, considering the atom-field interaction (3.5), the cavity field starting in the vacuum and all the atoms in their excited states. The first atom finds the field in its initial vacuum state $\rho(0)$, leading it to the state $\rho(t)$, with $t = 1/R$. After its passage through the cavity, we compute the reduced density operator for the field state by tracing over the atomic degrees of freedom. The second atom then finds the cavity in this reduced state, leading it to another reduced state at time $2t$, and so on until the

time Nt, each step being described by the equation

$$\begin{aligned}\dot{\rho}_{i+1}(t) = r\left[\rho(t_{i+1}) - \rho(t_i)\right] = -i\left[H_{eff}(t_i), \rho(t_i)\right] \\ + (C/2)\left[2A\rho(t_i)A^\dagger - A^\dagger A\rho(t_i) - \rho(t_i)A^\dagger A\right] \\ + (\gamma/2)\left(2\sigma_-\rho(t_i)\sigma_+ - \sigma_+\sigma_-\rho(t_i) - \rho(t_i)\sigma_+\sigma_-\right)\end{aligned} \tag{3.14}$$

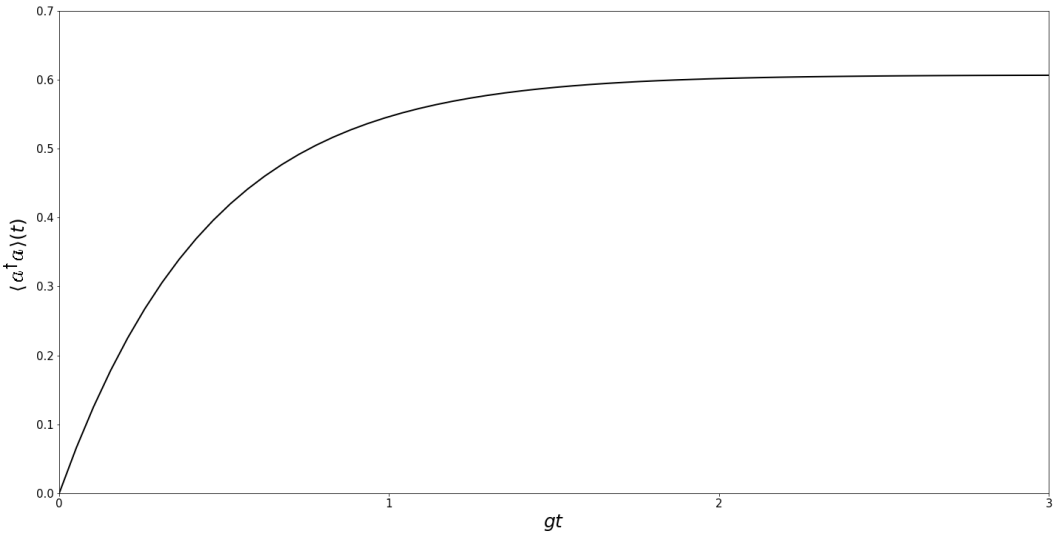

Figure 3.4 – The mean occupation number $\left\langle a^\dagger a \right\rangle(t)$, considering the same parameters used in Figure 3.2, together with $C/g = 0.35$, $r/g = 92$ and $\gamma/g = 0.5$, leading to $\mathcal{A}/g = 736$. We consider the cavity initially in the vacuum state and the atoms prepared in their excited states.

Source: By the author.

3.5 The construction and characterization of the squeezed vacuum state

We next analyze the laser state derived from Eq. (3.14), by comparing it with the squeezed vacuum state defined in Eq. (3.10), which by its turn comes from Eq. (3.12). All the following figures consider the same parameters used in Figure 3.2 to validate the effective interaction in Eq. (3.5), together with the choices $C/g = 0.35$, $r/g = 92$ and $\gamma/g = 0.5$, which lead to the rate $\mathcal{A}/g = 736$.

In Figure 3.4 we plot the mean occupation number $\left\langle a^\dagger a \right\rangle(t)$ of the laser state resulting from Eq. (3.14) against gt. We verify that the mean occupation number reaches the steady value $\left\langle a^\dagger a \right\rangle(t) = 0.62$ for $gt \approx 3$, long before the validity of the effective Hamiltonian is

compromised, for $gt \approx 7$. This steady excitation is in good agreement with that predicted by Eq. (3.10), given by $\langle a^\dagger a \rangle = 0.56$, about 10% less than the numerical simulation. The value $gt \approx 3$ follows after the passage of 1734 atoms through the cavity.

In Figure 3.5(a) we present the photon number distribution $\mathcal{P}_n$ and the phase space projection of the Wigner function of the laser state following from Eq. (3.14), for $gt = 4$. We again verify a good agreement with the ideal squeezed vacuum state as it becomes clear from Figure 3.5(b) where the fidelity $\mathcal{F} = \mathrm{Tr}\,\rho S(\xi)\,|0\rangle\langle 0|\,S^\dagger(\xi)$ of the state ρ coming from Eq. (3.14) is plotted against gt, regarded to the ideal squeezed vacuum $S(\xi)\,|0\rangle$ in Eq. (3.10). We note that the fidelity already starts from a high value due to the large population of the ground state in the squeezed vacuum field. The plot in Figure 3.5(a) also indicates that our laser has no diffusion due to cavity losses; if we had non-zero diffusion, the elliptical projection should circulate around the origin of the phase space, as occurs with the coherent state of the conventional laser theory (76, 83). In Figure 3.5(c), we plot the photon number distribution $\mathcal{P}_n$ and the phase space projection of the Wigner function of the conventional laser state for the same time interval $gt = 4$ ($\lambda t = 7.5 \times 10^{-2}$) considered in Figure 3.5(a). We clearly observe the occurrence of phase diffusion in the coherent state of the conventional laser, which is absent from our squeezed vacuum state laser, as shown in Figure 3.5(a).

In Figure 3.6 we plot the variances $(\Delta X_1)^2(t)$ (solid line) and $(\Delta X_2)^2(t)$ (dotted line), against gt, of the laser state coming from Eq. (3.14), showing that these variances approaches the values $(\Delta X_1)^2(t) = e^{-2r}/4 \approx 0.062$ and $(\Delta X_2)^2(t) = e^{2r}/4 \approx 0.993$ computed from the squeezed vacuum state in Eq. (3.10). In Figure 3.7 we plot the Mandel parameter $Q_M = \left(\langle n^2 \rangle - \langle n \rangle^2\right)/\langle n \rangle - 1$ for the laser state against gt, showing that for $gt \approx 2$ we reach a stationary value around $Q_M = 2\cosh^2|r| - 1 \approx 2.113$, as expected for the ideal squeezed vacuum state. Finally, in Figure 3.8 we plot the off-diagonal matrix elements $\rho_{0,8}(t)$ and $\rho_{4,6}(t)$, against gt, which demonstrate, together with Figure 3.5(a), that the phase coherence is preserved due to the absence of phase diffusion of our squeezed vacuum laser, since $A\,|\alpha\rangle_A \to 0$; otherwise these matrix elements would decay to zero.

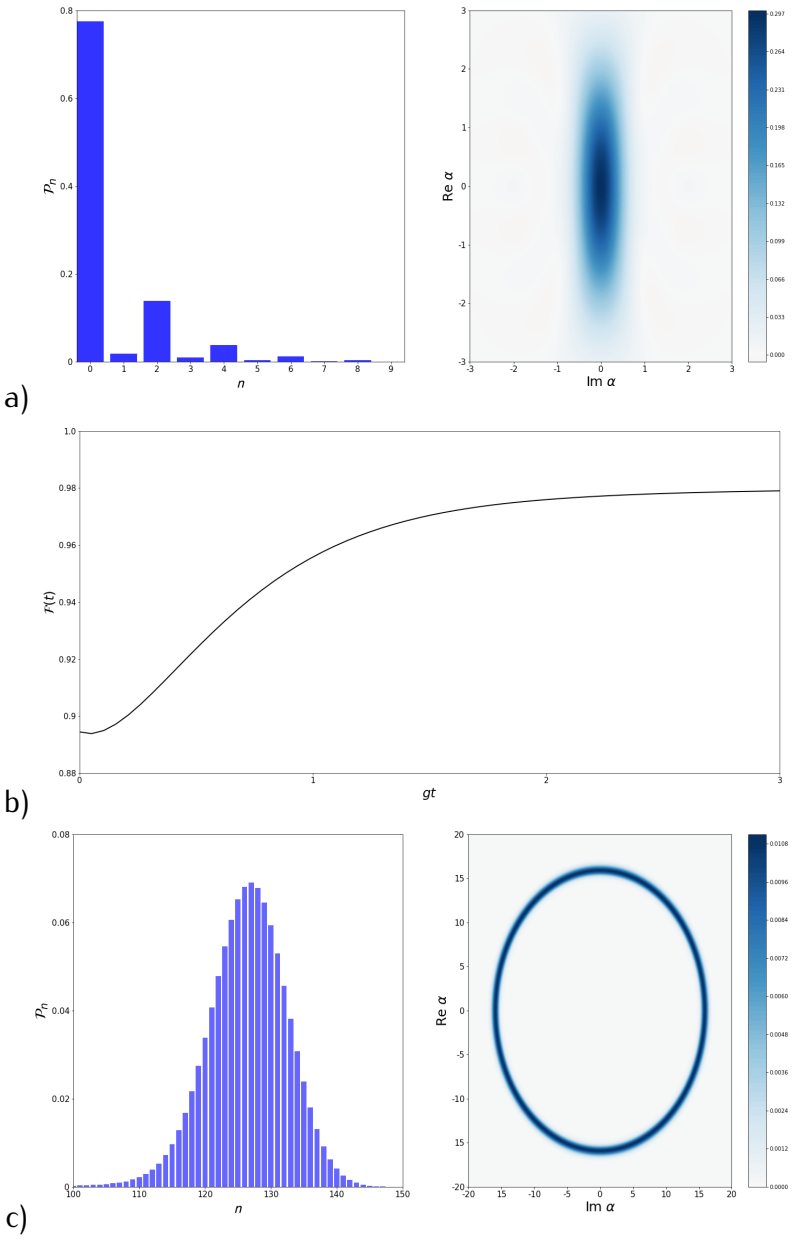

Figure 3.5 – **(a)** The photon number distribution $\mathcal{P}_n$ and the phase space projection of the Wigner function of the produced laser state for $gt = 4$, and **(b)** the fidelity of the evolved laser state against gt. **(c)** we plot the photon number distribution $\mathcal{P}_n$ and the phase space projection of the Wigner function in phase space for the conventional coherent state laser. We use the same parameters of Figure 3.4.

Source: By the author.

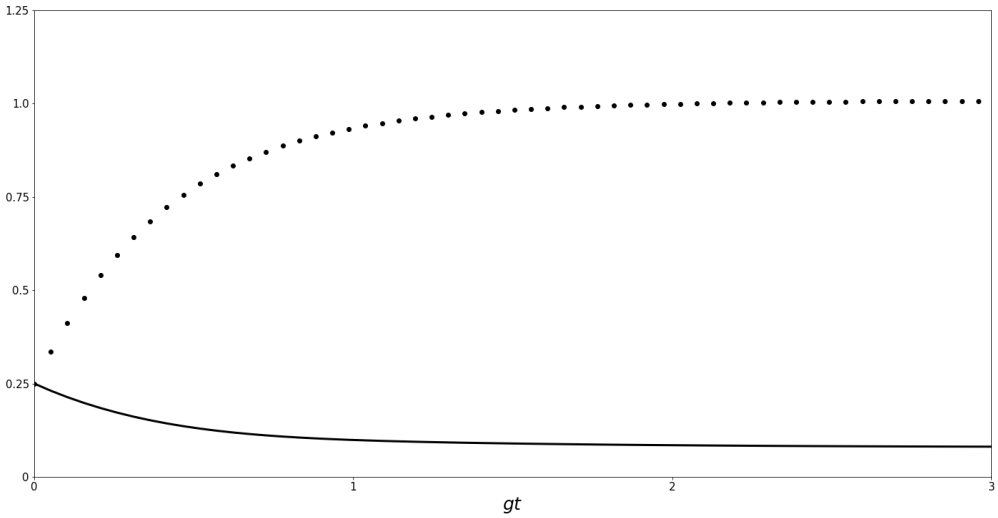

Figure 3.6 – The variances $(\Delta X_1)^2(t)$ (solid line) and $(\Delta X_2)^2(t)$ (dotted line) of the generated laser state against gt, using the same parameters of Figure 3.4.
Source: By the author.

3.6 Conclusion

We have presented a method to produce a squeezed vacuum laser with zero diffusion due to cavity losses. This method is based on merging together a particular reservoir engineering technique with the laser theory. The reservoir engineering demands us to build up an effective interaction between the system whose state we want to protect (the cavity field) and an auxiliary system (the laser active medium), of the form of Eq. (3.2), $\chi\left(A\sigma_+ + A^\dagger\sigma_-\right)$, with the laser steady state being an eigenstate of A with null eigenvalue: $A|\Psi\rangle = 0$. We stress that we have not take into account the usually small amplitude and phase fluctuations of the laser beams required for engineering the effective interaction; these fluctuations would result in some phase diffusion of our squeezed vacuum laser.

The effective interaction must enable the construction of an isomorphism between the field operators in the effective $\left(A^\dagger, A\right)$ and the Jaynes-Cummings $\left(a^\dagger, a\right)$ Hamiltonians. The isomorphism is carried out by building a basis state $\{|n\rangle_A\}$ for the operators $A^\dagger, A$ similar to the Fock basis state $\{|n\rangle\}$ for $a^\dagger, a$. The laser theory, by its turn, provides the mechanism by which the cavity mode is fed by the stimulated emission of the active medium when subjected to linear amplification, in addition to inducing a saturation which results in a far-from-equilibrium steady state.

Our method has an advantage over the reservoir engineering, in which we cannot, evidently, eliminate the environment (described by the Lindbladian for $a^\dagger, a$ in Eq. (3.3)) that acts to introduce errors in the action of the artificially constructed reservoir (described by

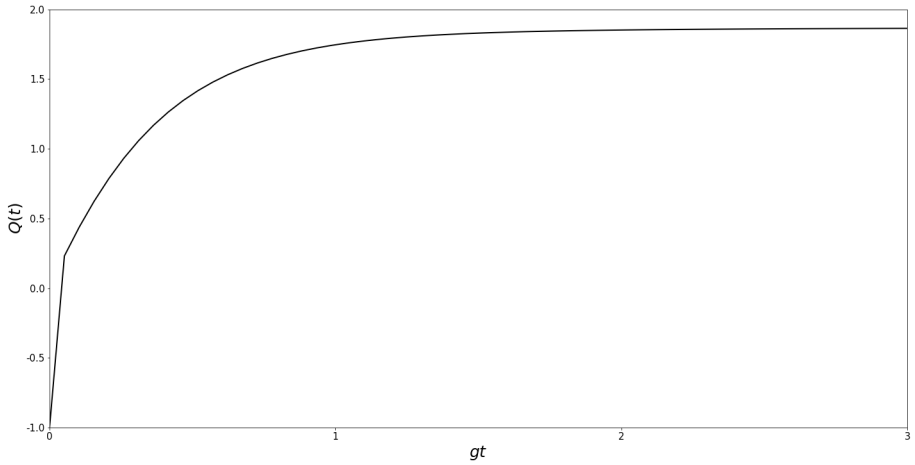

Figure 3.7 – The Mandel Q_M parameter for the laser state against gt, using the same parameters of Figure 3.4

Source: By the author.

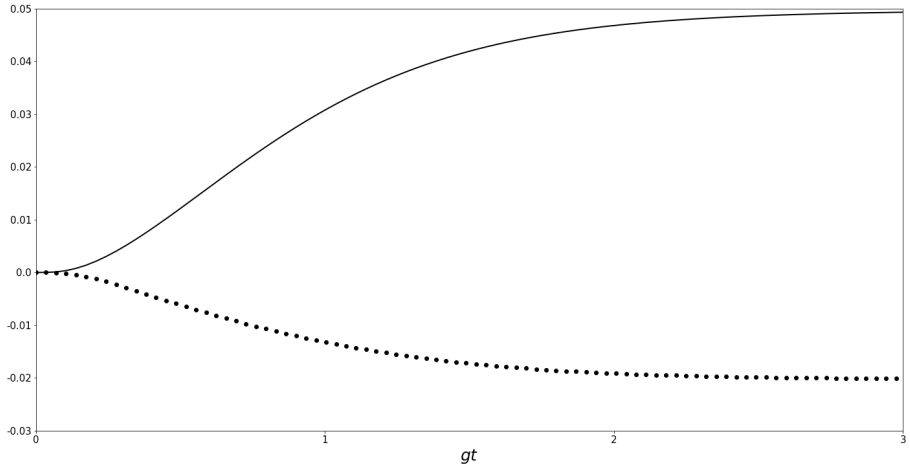

Figure 3.8 – Off-diagonal matrix elements $\rho_{0,8}(t)$ (solid line) and $\rho_{4,6}(t)$ (dotted line) against gt, using the same parameters of Figure 3.4.

Source: By the author.

the Lindbladian for $A^{\dagger}, A$). This does not occur in our method, in which the only source of errors comes from the protocol for building up the effective interaction, based on the adiabatic elimination of fast variables, which is also present in the reservoir engineering. This is a very unique aspect of our method, which shows that the association of reservoir engineering with the laser mechanism results in both a more robust protocol than the reservoir engineering (due to the absence of the Lindbladian for $a^{\dagger}, a$) and also an unconventional laser field described by a nonclassical coherence-preserving state.

It is important to stress that we have not presented here a comparison between the efficiencies of our laser method and other methods for light squeezing in the literature. (51, 55, 76, 82–85, 90–92) This task is beyond our purposes of presenting a laser method for light squeezing where the required nonlinearity arises from the atom-field effective interaction itself, rather then the pumping of a $\chi^{(2)}$ crystal.

In addition to the many applications we have already listed for a reduced linewidth laser, we observe that a squeezed vacuum laser may be useful for high-resolution interferometry, a timely topic due to the newly emerging field of gravitational wave interferometry. Moreover, the present method challenges us to design effective interactions leading to other nonclassical laser states, as for example steady superposition states. This challenge can leads us to a new chapter regarding the preparation of nonclassical steady states, which could be useful for a variety of fundamental and technological applications.

CHAPTER 4

CAT-LIKE STATE LASER WITH ZERO DIFFUSION FROM CAVITY LOSSES

4.1 Introduction

Following the procedures of the previous chapter we can obtain a totally different state simply by engineering a different operator A in the effective atom-field interaction, in the bilinear form of the Jaynes-Cummings Hamiltonian, i.e.

$$\chi\left(A^{\dagger}\sigma_{-}+A\sigma_{+}\right) \tag{4.1}$$

This time we present the developments for building a Schroedinger cat-like state (SCLS) laser, also with zero diffusion due to cavity loss. While a squeezed vacuum state laser is useful for high-precision spectroscopy, (89,95) a SCLS laser can find applications to test fundamental phenomena of quantum mechanics. (3,4) Moreover, a laser with zero linewidth is useful for applications such as high-precision detection, metrology and optical sensing. (89,95)

This chapter is organized as follows: In section 2 we construct the isomorphism between the cavity field operators in the effective and the Jaynes-Cummings interactions. In section 3 we present the numerical analysis demonstrating the effectiveness of our method. In section 4 we give a blueprint, based on the adiabatic elimination of fast variables, for the construction of the effective Hamiltonian required for the operation of the SCLS laser. Finally, in section 5 we set out our conclusions.

4.2 The effective atom-field interaction for the Schrödinger cat-like state lasers

Deferring the derivation of the effective Hamiltonian to Section 4, here we restrict ourselves to discussing the properties of this Hamiltonian, similar to that in Eq. (4.1), given by

$$H_{\pm,N} = \chi \left(A^{\dagger}_{\pm,N}\sigma_{-} + A_{\pm,N}\sigma_{+} \right) \tag{4.2a}$$

with the generalized field operators

$$A_{\pm,N} = e^{i(2\pi/N)a^{\dagger}a}a + e^{\pm i\pi/N}\alpha \tag{4.3}$$

The particular case of the field operator with $N = 2$, was already anticipated in Ref. (96), where a detection feedback method for preserving quantum coherence is presented. The SCLS $|\Psi\rangle_{\pm,N}$ that are eigenstates of $A_{\pm,N}$, are of the form

$$|\Psi\rangle_{\pm,N} = \mathcal{N}_{\pm,N} \sum_{n=1}^{N} c_n \left| e^{i(n-1)2\pi/N}\alpha \right\rangle \tag{4.4}$$

$\mathcal{N}_{\pm,N}$ being the normalization factor. Given the difficulty to derive a general form for the coefficients c_n, below we present the states for $N = 2$, 3, and 4:

$$|\Psi\rangle_{\pm,2} = \mathcal{N}_{\pm,2} \left(|\alpha\rangle + e^{\pm i\pi/2} |-\alpha\rangle \right) \tag{4.5a}$$

$$|\Psi\rangle_{+,3} = \mathcal{N}_{+,3} \left(|\alpha\rangle + e^{i2\pi/3} \left| e^{i2\pi/3}\alpha \right\rangle + \left| e^{i4\pi/3}\alpha \right\rangle \right) \tag{4.5b}$$

$$|\Psi\rangle_{-,3} = \mathcal{N}_{-,3} \left(|\alpha\rangle + e^{-i2\pi/3} \left| e^{i2\pi/3}\alpha \right\rangle + e^{-i2\pi/3} \left| e^{i4\pi/3}\alpha \right\rangle \right) \tag{4.5c}$$

$$|\Psi\rangle_{+,4} = \mathcal{N}_{+,4} \left(|\alpha\rangle + e^{i3\pi/4} \left| e^{i\pi/2}\alpha \right\rangle + \left| e^{i\pi}\alpha \right\rangle + e^{-i\pi/4} \left| e^{i3\pi/2}\alpha \right\rangle \right) \tag{4.5d}$$

$$|\Psi\rangle_{-,4} = \mathcal{N}_{+,4} \left(|\alpha\rangle + e^{-i3\pi/4} \left| e^{i\pi/2}\alpha \right\rangle - \left| e^{i\pi}\alpha \right\rangle + e^{-i3\pi/4} \left| e^{i3\pi/2}\alpha \right\rangle \right) \tag{4.5e}$$

The Wigner functions for these SCLS: $|\Psi\rangle_{\pm,2}$, $|\Psi\rangle_{\pm,3}$, and $|\Psi\rangle_{\pm,4}$, are depicted in Figure 4.1 (a,b,c), respectively, considering $\alpha = 3e^{i\pi/4}$.

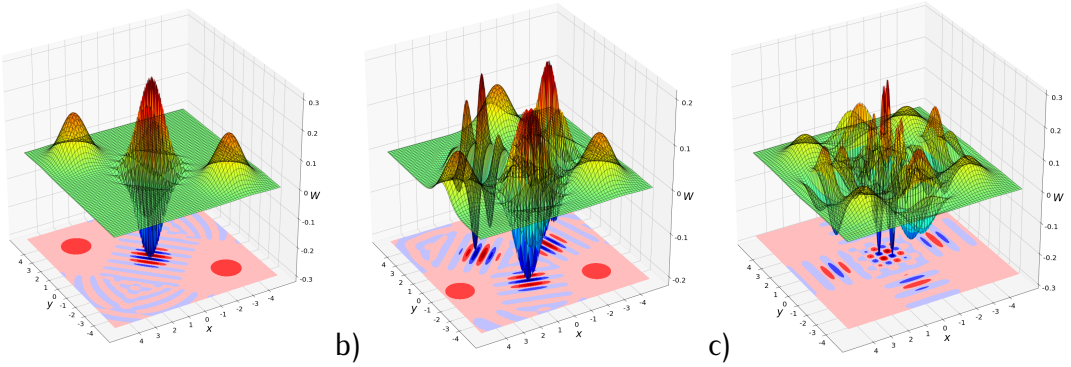

a) b) c)

Figure 4.1 – Wigner functions for the SCLS $|\Psi\rangle_{\pm,2}$, $|\Psi\rangle_{\pm,3}$, and $|\Psi\rangle_{\pm,4}$ (a,b and c, respectively), considering $\alpha = 3e^{i\pi/4}$.

Source: By the author.

4.3 Construction of the isomorphism between the $A^{\dagger}_{\pm,N}, A_{\pm,N}$ and $a^{\dagger}, a$ operators algebras

As anticipated in the Introduction, to set the isomorphism between the $A^{\dagger}_{\pm,N}, A_{\pm,N}$ and $a^{\dagger}, a$ algebras we must derive the vector basis $\left\{|n\rangle^{A}_{\pm,N}\right\}$ for the generalized field operators (4.3), in such a way that

$$A^{\dagger}_{\pm,N}A_{\pm,N}\,|n\rangle^{A}_{\pm,N} = n\,|n\rangle^{A}_{\pm,N} \tag{4.6a}$$

$$A^{\dagger}_{\pm,N}\,|n\rangle^{A}_{\pm,N} = \sqrt{n+1}\,|n\rangle^{A}_{\pm,N} \tag{4.6b}$$

$$A_{\pm,N}\,|n\rangle^{A}_{\pm,N} = \sqrt{n}\,|n\rangle^{A}_{\pm,N} \tag{4.6c}$$

To this end, we start from the relation $A_{\pm,N}\,|0\rangle^{A}_{\pm,N} = 0$ to compute the generalized vacuum state

$$|0\rangle^{A}_{\pm,N} = e^{-|\alpha|^2/2}\sum_{n=0}^{\infty}\frac{\left(e^{-i(\pi/N)(n+1\mp1)}\alpha\right)^n}{\sqrt{n!}}\,|n\rangle \tag{4.7}$$

and then, using the relation $\left(A^{\dagger}_{\pm,N}\right)^n|0\rangle^{A}_{\pm,N}/\sqrt{n!}$, all the generalized number states

$$|m\rangle^{A}_{\pm,N} = \frac{e^{-|\alpha|^2/2}}{\sqrt{m!}}\sum_{n=0}^{\infty}\frac{\left(e^{-i(\pi/N)(n+1\mp1)}\alpha\right)^n\left(e^{\pm i\pi/N}\alpha^*\right)^m}{\sqrt{n!}} \times\sum_{\ell=0}^{m}\left(-|\alpha|^{-2}\right)^{\ell}\binom{m}{\ell}\frac{(n)!}{(n-\ell)!}\,|n\rangle \tag{4.8a}$$

It is then automatic to derive the steady state of our laser: the coherent state in the vector basis $\left\{|n\rangle^A\right\}$, given by

$$|\beta\rangle^A_{\pm,N} = e^{\left(-|\alpha|^2-|\beta|^2\right)/2} \sum_{n=0}^{\infty} \frac{\left(e^{-i(\pi/N)(n+1\mp1)}\alpha\right)^n}{\sqrt{n!}} \times \sum_{k=0}^{\infty} \frac{\left(e^{\pm i\pi/N}\alpha^*\beta\right)^k}{k!} \sum_{\ell=0}^{k} \left(-|\alpha|^{-2}\right)^{\ell} \binom{k}{\ell} \frac{(n)!}{(n-\ell)!} |n\rangle \tag{4.9}$$

In order to have zero diffusion due to cavity losses, our SCLS laser must operate in the regime where $\beta = 0$, such that, as discussed in the Introduction, $A_{\pm,N}|\beta = 0\rangle^A_{\pm,N} = 0$. It is then immediate to concluded that the state of our laser will be $|\beta = 0\rangle^A_{\pm,N} = |0\rangle^A_{\pm,N} = |\Psi\rangle_{\pm,N}$. However, using the laser master equation, the best we can do is to consider the regime where β approaches zero, rendering $A_{\pm,N}|\beta \sim 0\rangle^A_{\pm,N} \sim 0$, and consequently a laser with approximately zero diffusion from cavity losses. With regard to the value of α, which defines the excitation of the SCLS, it follows completely from the engineering scheme of the effective interaction (4.2a). The same happens with the squeezed vacuum laser presented in Ref. (74) where the degree of squeezing also follows from the engineered Hamiltonian. The success of the engineering scheme is what leads to a substantial value for both the degree of squeezing and the excitation α in Eq. (4.9).

4.4 The master equation and the operating regime for the SCLS laser

The isomorphism we have established leads us automatically to the master equation describing the dynamics of the cavity field due to its interaction with a pumped atomic sample through the effective Hamiltonian (4.2a). From the conventional laser theory we thus obtain for the cavity field

$$\dot{\rho}_{\pm,N} = \mathcal{L}_{\mathcal{A}}\rho_{\pm,N} + \mathcal{L}_{\mathcal{B}}\rho_{\pm,N} + \mathcal{L}_{\mathcal{C}}\rho_{\pm,N} \tag{4.10}$$

where the Lindbladians accounting for gain ($\mathcal{L}_{\mathcal{A}}\rho_{\pm,N}$), saturation ($\mathcal{L}_{\mathcal{B}}\rho_{\pm,N}$) and loss ($\mathcal{L}_{\mathcal{C}}\rho_{\pm,N}$) of the cavity field are given by

$$\mathcal{L}_{\mathcal{A}}\rho_{\pm,N} = \frac{\mathcal{A}}{2}\left(2A^{\dagger}_{\pm,N}\rho_{\pm,N}A_{\pm,N} - A_{\pm,N}A^{\dagger}_{\pm,N}\rho_{\pm,N} - \rho_{\pm,N}A_{\pm,N}A^{\dagger}_{\pm,N}\right) \tag{4.11a}$$

$$\begin{aligned}\mathcal{L}_{\mathcal{B}}\rho_{\pm,N} = \frac{\mathcal{B}}{2}\Bigg[&\frac{1}{4}A_{\pm,N}A^{\dagger}_{\pm,N}\left(A_{\pm,N}A^{\dagger}_{\pm,N}\rho_{\pm,N} + 3\rho_{\pm,N}A_{\pm,N}A^{\dagger}_{\pm,N}\right)\\ &+\frac{1}{4}\left(\rho_{\pm,N}A_{\pm,N}A^{\dagger}_{\pm,N} + 3A_{\pm,N}A^{\dagger}_{\pm,N}\rho_{\pm,N}\right)A_{\pm,N}A^{\dagger}_{\pm,N}\\ &-A^{\dagger}_{\pm,N}\left(A_{\pm,N}A^{\dagger}_{\pm,N}\rho_{\pm,N} + \rho_{\pm,N}A_{\pm,N}A^{\dagger}_{\pm,N}\right)A_{\pm,N}\Bigg] + \ldots\end{aligned} \tag{4.11b}$$

$$\mathcal{L}_{\mathcal{C}}\rho = \frac{\mathcal{C}}{2}\left(2A_{\pm,N}\rho_{\pm,N}A^{\dagger}_{\pm,N} - A^{\dagger}_{\pm,N}A_{\pm,N}\rho_{\pm,N} - \rho_{\pm,N}A^{\dagger}_{\pm,N}A_{\pm,N}\right) \tag{4.11c}$$

The well-known coefficients for gain $\mathcal{A} = 2\Gamma(\lambda/\gamma)^2$, saturation $\mathcal{B} = 4\mathcal{A}(\lambda/\gamma)^2$, and loss $\mathcal{C} = \omega/Q$, are defined through the atomic pumping rate Γ, the Rabi frequency λ, the atomic decay rate γ, and the cavity quality factor Q. The saturation term $\mathcal{L}_{\mathcal{B}}\rho$ is presented only up to 4-th order in λ. As in the usual laser theory, the far from equilibrium steady state, which is an eigenvalue of the generalized operator $A_{\pm,N}$, follows from the condition $\mathcal{A} \gg \mathcal{C}$. However, for the zero diffusion condition to be observed, i.e.: for $A_{\pm,N}|\beta \sim 0\rangle^{A}_{\pm,N} \sim 0$, we must also ensure that $\mathcal{B} \gg \mathcal{A}$, leading to an average photon number for equilibrium state given by $\langle\beta\rangle^{A}_{\pm,N} = \mathcal{A}^2/\mathcal{B}\mathcal{C} \sim 0$. Therefore, the operating regime of our effective lasers —the present SCLS laser and the squeezing vacuum laser in Ref. (74)— is achieved far above threshold, under strong saturation, such that $\mathcal{B} \gg \mathcal{A} \gg \mathcal{C}$. When the strong saturation condition is not observed, we still have a steady state for $\mathcal{A} \gg \mathcal{C}$, given by $|\beta\rangle^{A}_{\pm,N}$ in Eq. (4.9) instead of $|\Psi\rangle_{\pm,N} \sim |0\rangle^{A}_{\pm,N}$. We stress that the zero diffusion condition, $\langle\beta\rangle^{A}_{\pm,N} = \mathcal{A}^2/\mathcal{B}\mathcal{C} \sim 0$, does not affect the excitation of the laser state in the conventional Fock basis $\{|n\rangle\}$, which, as remarked above, depends entirely on the engineering of the effective Hamiltonian. In the blueprint presented bellow for engineering the effective interaction (4.2a), it follows that the magnitude of α depends on that of the required amplification mechanism of the cavity mode.

Unlike what happens with engineered reservoirs, the master equation for the effective laser does not present the Lindbladian for $a^{\dagger}, a$ appearing in Eq. (1.2), and acting to introduce error in the laser mechanism. This interesting bonus coming from our isomorphism method shows that the only source of errors we have, comes from the engineering of the effective interaction.

Next we numerically analyze the construction of the steady SCLS of our laser, considering, in a similar way to what has been done in Ref. (97), the master equation

$$\begin{aligned}\dot{\rho}_{\pm,N} = &-\frac{i}{\hbar}[H_{\pm,N}, \rho_{\pm,N}] + \mathcal{L}_{\mathcal{C}}\rho_{\pm,N} \\ &+ \frac{\gamma}{2}\left(2\sigma_-\rho_{\pm,N}\sigma_+ - \sigma_+\sigma_-\rho_{\pm,N} - \rho_{\pm,N}\sigma_+\sigma_-\right) \\ &+ \frac{\Gamma}{2}\left(2\sigma_+\rho_{\pm,N}\sigma_- - \sigma_-\sigma_+\rho_{\pm,N} - \rho_{\pm,N}\sigma_-\sigma_+\right)\end{aligned} \tag{4.12}$$

where in addition to the von Neumann term accounting for effective atom-field interaction, we consider the relaxation of the cavity mode, $\mathcal{L}_{\mathcal{C}}\rho$, together with both the relaxation (γ) and the amplification (Γ) of the atomic system.

To analyse the SCLS produced by our laser, in Figure 4.2 we plot, against λt, the fidelity $\mathcal{F}_{\pm,N} = \mathrm{Tr}\,\rho_{\pm,N}|\Psi\rangle_{\pm,N}\langle\Psi|$ of the state $\rho_{\pm,N}$ coming from Eq. (4.12), regarded to the ideal SCLS $|\Psi\rangle_{\pm,N}$ in Eq. (4.4). We have fixed $\mathcal{C}/\lambda = 5\times10^{-1}$, $\gamma/\lambda = 10^{-3}$, $|\alpha| = 3$, and $\varphi = 0$ to derive the solid, dashed and dotted lines curves for $\Gamma/\lambda = 10^{-2}$, 10^{-1} and 1, respectively. While the fidelity of the solid line approaches unity, with $\langle\beta\rangle_{A,N} \sim 0.1$, those for the dashed and dotted lines exceeds 0.9 and 0.5, respectively, with $\langle\beta\rangle_{A,N} \sim 0.4$ and 1.0. We note that the average number $\langle\beta\rangle_{A,N}$ is only a quantity that scales in inverse proportion to the fidelity of the SCLS laser, whose excitation is in fact given by $|\alpha|^2 = 9$. Moreover, the curves shown in Figure 4.2 are exactly the same for any values of N exactly because the diffusion depends only on the magnitude of β.

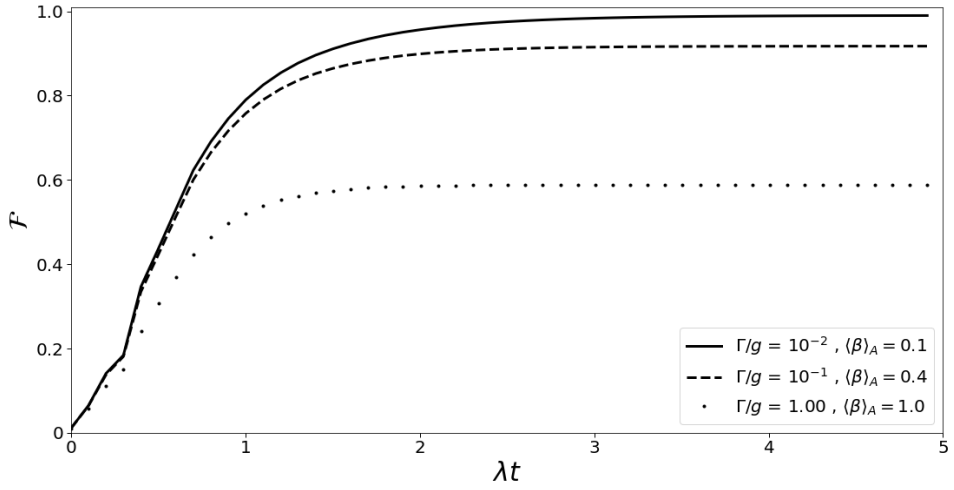

Figure 4.2 – Plot of the fidelities $\mathcal{F}_{\pm,N} = \mathrm{Tr}\,\rho_{\pm,N}|\Psi\rangle_{\pm,N}\langle\Psi|$, against λt, for the states $\rho_{\pm,N}$ coming from Eq. (4.12), regarded to the ideal SCLS $|\Psi\rangle_{\pm,N}$ in Eq. (4.4). We have considered $\mathcal{C}/\lambda = 5\times10^{-1}$, $\gamma/\lambda = 10^{-3}$, $|\alpha| = 3$, and $\varphi = 0$ to obtain the solid, dashed and dotted lines curves for $\Gamma/\lambda = 10^{-2}$, 10^{-1} and 1, respectively.
Source: By the author.

In Figure 4.3 (a, b and c) we plot the Wigner distributions for the steady laser states $\rho_{+,2}$, at $\lambda t = 5$, produced when considering the same parameters in Figure 4.2, with $\Gamma/\lambda = 10^{-2}$ (a), 10^{-1} (b) and 1 (c). These states must be compared with their ideal equivalents $|\Psi\rangle_{+,2}$ shown in Figure 4.4 for $|\alpha| = 3$, and $\varphi = 0$. As expected, the states produced by our laser clearly depart from their ideal equivalents as we increase Γ/λ and consequently the average number $\langle\beta\rangle_{A,2.}$.

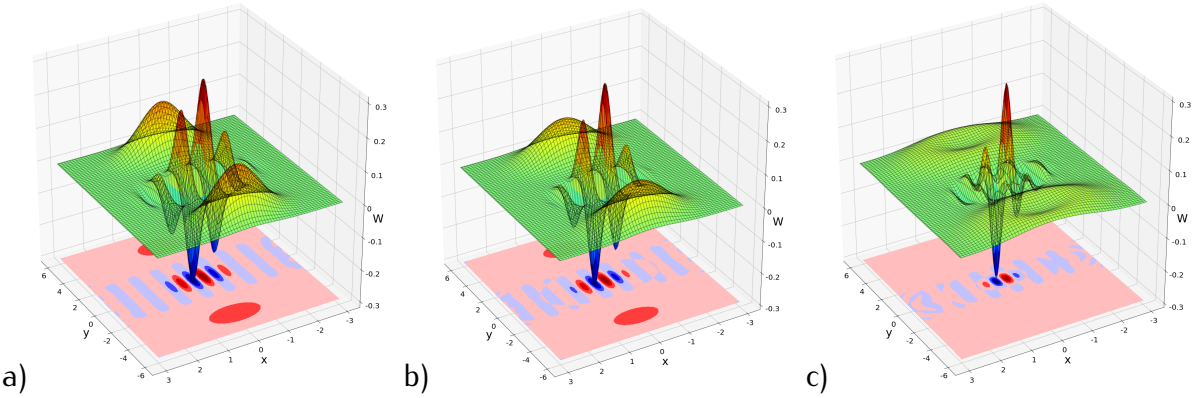

Figure 4.3 – Plots at $\lambda t = 5$, of the Wigner function for the steady laser states $\rho_{+,2}$, produced for the same parameters in Figure 4.2, with $\Gamma/\lambda = 10^{-2}$ (a), 10^{-1} (b) and 1 (c).
Source: By the author.

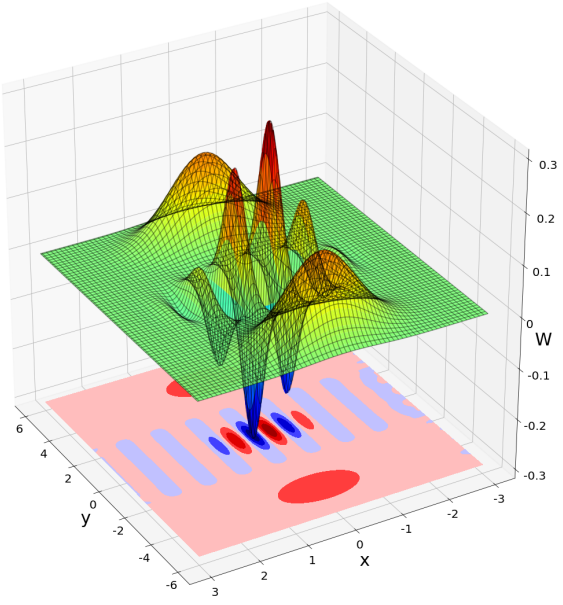

Figure 4.4 – Wigner function for the ideal state $|\Psi\rangle_{+,2}$, with $|\alpha| = 3$ and $\varphi = 0$.
Source: By the author.

In Figure 4.5, considering again the same parameters in Figure 4.2, with $\Gamma/\lambda = 10^{-2}$, we show the construction of the laser equilibrium state from the vacuum, presenting the Wigner functions for the cavity field, together with their projections, at 5 different instants: $t = 0$, $\lambda t = 0.25$, $\lambda t = 0.50$, $\lambda t = 1.0$ and $\lambda t = 5$, as illustrates Figure 4.5 (a) to 5

(e), respectively. We first observe that the vacuum, at $t = 0$, evolves to a superposition that presents interferences between low-excited Fock states, in the vicinity of the vacuum, around $\lambda t = 0.25$. Then, progressively, from around $\lambda t = 0.50$, we observe a continuous evolution to a superposition of coherent states, that becomes stationary around $\lambda t = 3$, as indicated by Figure 4.2.

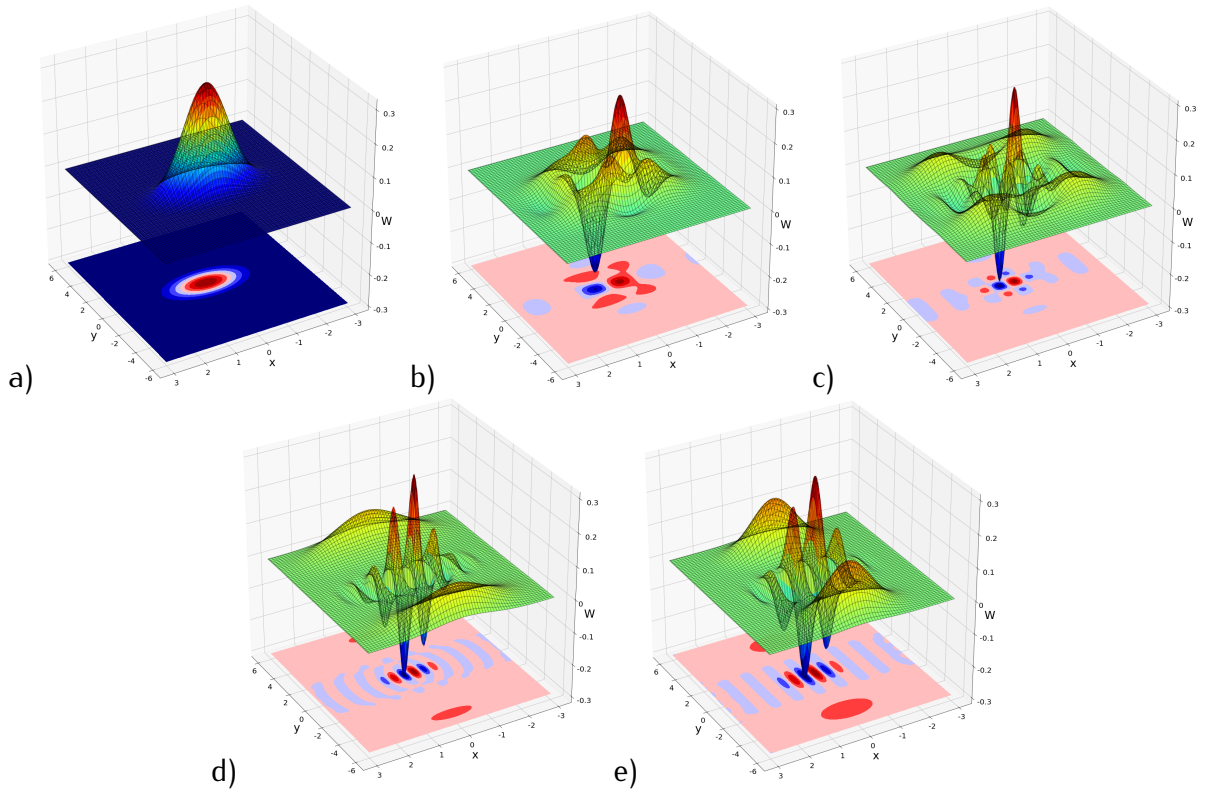

Figure 4.5 – Construction of the laser state for the same parameters used in Figure 4.2, with $\Gamma/\lambda = 10^{-2}$. We show the Wigner functions for the laser states at 5 different instants: $t = 0$ (a), $\lambda t = 0.25$ (b), $\lambda t = 0.50$ (c), $\lambda t = 1.0$ (d) and $\lambda t = 5$ (e).
Source: By the author.

Finally, in Figure 4.6 we present the construction of the laser state for the same parameters used in Figure 4.2, but now with $\Gamma/\lambda = 1$. We consider only the instants $t = 0$, $\lambda t = 0.5$, and $\lambda t = 5$, as illustrated from Figure 4.6 (a) to 6(c), respectively. These figures must be compared with those in Figure 4.7 where we have used the same parameters as in Figure 4.6 (a, b and c), but considering the usual JCH instead of the effective Hamiltonian in Eq. (4.2a). It is evident from the states in Figure 4.6 that an usual laser, based on the JCH, presents diffusion, while our effective laser has no diffusion irrespective of the fidelity of the produced state that decreases when we increase Γ/λ.

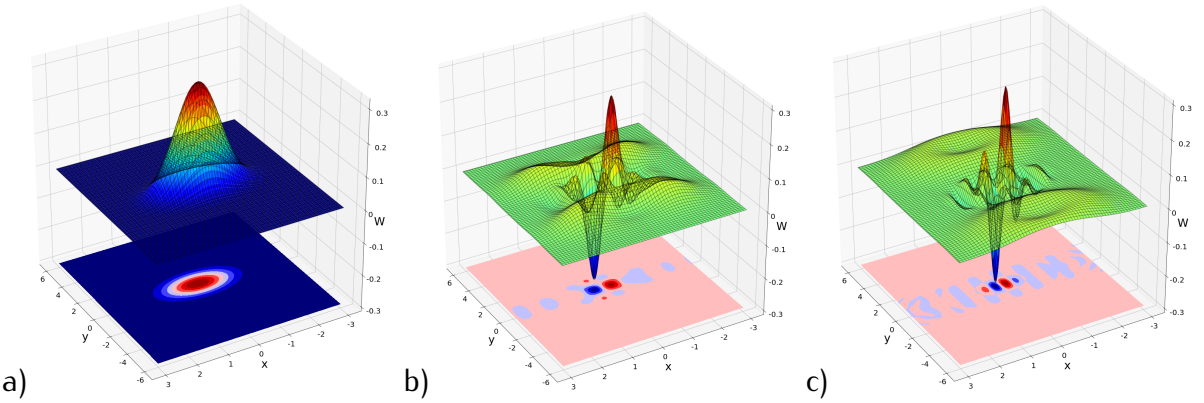

Figure 4.6 – Construction of the laser state for the same parameters used in Figure 4.2, but now with $\Gamma/\lambda = 1$. We plot the Wigner functions for the field states consider the instants $t = 0$ (a), $\lambda t = 0.5$ (b), and $\lambda t = 5$ (c).
Source: By the author.

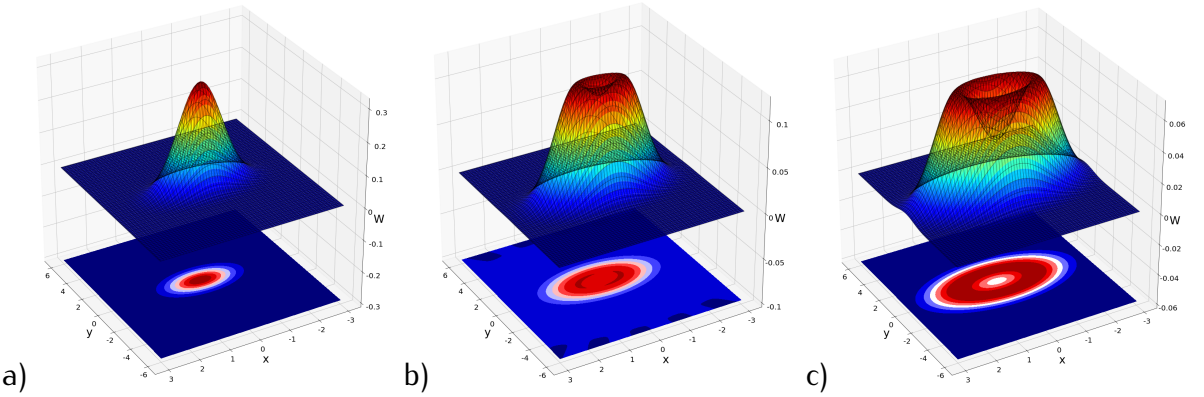

Figure 4.7 – Using the same parameters as in Figure 4.6 (a, b and c), we plot the Wigner functions for the field states generated under the usual JC atom-field interaction, instead of the effective Hamiltonian in Eq. (4.2a).
Source: By the author.

4.5 A blueprint for the engineering of the effective atom-field interaction

For the engineering of the effective atom-field interaction we consider a cavity mode (ω) —described by the creation ($a^\dagger$) and annihilation (a) operators— under linear amplification with a time-dependent coefficient $\xi(t)$, and interacting with two atomic samples, one for the laser active medium and another for building a necessary Kerr interaction. The laser active medium is composed by atoms in the ground $\left(|g\rangle_L\right)$ and excited $\left(|e\rangle_L\right)$ lasing (L) levels, with transition frequency ω_0. The auxiliary sample helps in building the Kerr interaction, and here we build on a scheme previously presented by S.-B. Zheng (98), considering the ground $\left(|g\rangle_K\right)$, intermediate $\left(|i\rangle_K\right)$ and excited $\left(|e\rangle_K\right)$ Kerr (K) states, in the ladder configuration depicted in Figure 4.8, where $\Delta = \omega - \omega_i$ and $\delta = \omega_e - 2\omega$. The

Hamiltonian modeling the system is given by $H(t) = H_0 + V(t)$, where

$$H_0 = \omega a^\dagger a + \frac{\omega_0}{2}\sigma_z^{(L)} + \omega_i \sigma_{ii}^{(K)} + \omega_e \sigma_{ee}^{(K)} \tag{4.13a}$$

$$V(t) = \lambda\left(a\sigma_+^{(L)} + a^\dagger \sigma_-^{(L)}\right) + \xi(t)a^\dagger + \xi^*(t)a + g_1\left(a\sigma_{ig}^{(K)} + a^\dagger \sigma_{gi}^{(K)}\right) + g_2(t)\left(a\sigma_{ei}^{(K)} + a^\dagger \sigma_{ie}^{(K)}\right) \tag{4.13b}$$

The Pauli operators $\sigma_{rs}^{(\ell)} = |r\rangle_{\ell\ell}\langle s|$, apply for the lasing ($\ell = L$) and Kerr ($\ell = K$) levels $r, s = g, e, i$. We have assumed a time-dependent Rabi frequency $g_2(t)$ for the coupling between the cavity mode and the Raman-type transition $|i\rangle_K \leftrightarrow |e\rangle_K$. Although this is a sensitive issue of our protocol, we believe that this time dependence can be achieved using the Stark effect on appropriately chosen atomic levels, so that only the $|i\rangle_K \leftrightarrow |e\rangle_K$ transition is effectively affected. More specifically, we assume that only the excited level $\left(|e\rangle_K\right)$ is effectively affected by the Stark shift, so that the Hamiltonian $H(t)$ properly describes the process.

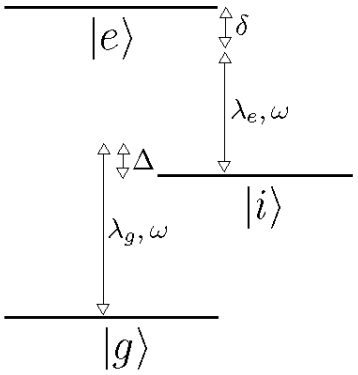

Figure 4.8 – Ladder configuration of the ground $\left(|g\rangle_K\right)$, intermediate $\left(|i\rangle_K\right)$ and excited $\left(|e\rangle_K\right)$ Kerr (K) states, used forengineering the Kerr interaction.
Source: By the author.

In the interaction picture, following from the unitary transformation $U_0 = e^{-iH_0 t}$, we obtain the Hamiltonian $\mathcal{H}(t) = \mathcal{V}(t) + \tilde{\mathcal{V}}(t)$, where

$$\mathcal{V}(t) = \lambda e^{-i\tilde{\delta}t} a^\dagger \sigma_-^{(L)} + \xi(t) e^{i\omega t} a^\dagger + H.c. \tag{4.14}$$

$$\tilde{\mathcal{V}}(t) = g_1 e^{i\Delta t} a^\dagger \sigma_{gi}^{(K)} + g_2(t) e^{-i(\Delta+\delta)t} a^\dagger \sigma_{ie}^{(K)} + H.c. \tag{4.15}$$

with the atom-field detuning $\tilde{\delta} = \omega_0 - \omega$. We next assume that the coupling between the mode and the Kerr levels, in $\tilde{\mathcal{V}}(t)$, oscillates strongly compared to that between the mode and the lasing levels and also the linear amplification, in $\mathcal{V}(t)$. In this case, assuming that $\Delta \gg g_1, g_2(t), \delta$ and $\delta \gg g_1 \langle g_2 \rangle / \Delta$, $\langle g_2 \rangle$ being a time average of $g_2(t)$ over the interval T

required for the laser to reach the steady state, we obtain to a good approximation (53,54), the Hamiltonian

$$\tilde{\mathcal{H}}(t) = \mathcal{V}(t) - i\tilde{\mathcal{V}}(t)\int_0^t dt_1\tilde{\mathcal{V}}(t_1) + i\tilde{\mathcal{V}}(t)\int_0^t dt_1\tilde{\mathcal{V}}(t_1)\int_0^{t_1} dt_2\tilde{\mathcal{V}}(t_2)\int_0^{t_2} dt_3\tilde{\mathcal{V}}(t_3) \tag{4.16}$$

where $\mathcal{V}(t)$ is added to a second- and a fourth-order corrections of $\tilde{\mathcal{V}}(t)$, the third-order correction being null. Assuming that the function $g_2(t)$ varies slowly compared to the exponential that multiplies it in $\tilde{\mathcal{V}}(t)$, we obtain

$$\tilde{\mathcal{H}}(t) = \left(\frac{g_1^2}{\Delta}a^\dagger a - \chi(t)a^{\dagger 2}a^2\right)\sigma_{gg}^{(K)} + \left(\lambda e^{i\tilde{\delta}t}a^\dagger\sigma_-^{(L)} + \xi(t)e^{i\omega t}a^\dagger + H.c.\right) \tag{4.17}$$

where $\chi(t) = g_1^2 g_2^2(t)/\Delta^2\delta$. We next assume that our Kerr medium is prepared in the ground state $|g\rangle_K$ and performing a second unitary transformation on the Schrödinger equation governed by $\tilde{\mathcal{H}}(t)$, using $U_1 = \exp\left[-i\left(g_1^2/\Delta\right)ta^\dagger a\right]$, we obtain the Hamiltonian

$$H_1(t) = -\chi(t)a^{\dagger 2}a^2 + \left(\lambda e^{-i\left(\tilde{\delta}-g_1^2/\Delta\right)t}a^\dagger\sigma_-^{(L)} + \xi(t)e^{i\left(\omega+g_1^2/\Delta\right)t}a^\dagger + H.c.\right) \tag{4.18}$$

By adjusting the atom-field detuning such that $\tilde{\delta} = g_1^2/\Delta$ and the coefficient of the amplification in the form $\xi(t) = \tilde{\xi}(t)e^{-i(\omega+g_1^2/\Delta)t}$, we obtain the simplified interaction

$$\tilde{H}_1(t) = -\chi(t)a^{\dagger 2}a^2 + \left(\lambda a^\dagger\sigma_-^{(L)} + \tilde{\xi}(t)a^\dagger + H.c.\right) \tag{4.19}$$

We next consider that $\tilde{\xi}(t) = \left|\tilde{\xi}(t)\right| e^{i(\varphi+\pi/2\pm\pi/N)}$, with the phase $\varphi + \pi/2 \pm \pi/N$ depending on a positive integer N, such that the pumping term in $\mathcal{V}(t)$, given by $\xi(t)e^{i\omega t} = \tilde{\xi}(t)e^{-i(g_1^2/\Delta)t}$, corroborates our assumption that $\tilde{\mathcal{V}}(t)$ oscillates strongly compared to $\mathcal{V}(t)$. We then perform a third unitary transformation, considering $U_2 = \exp\left(ia^{\dagger 2}a^2\int_0^t dt_1\chi(t_1)\right)$ and assuming the time-dependent Kerr coupling to be a Gaussian pulse of the form $\chi(t) = \chi_0\exp\left[-\left(N\chi_0 t\right)^2/4\pi\right]$. We also assume that the Gaussian width, around $1/N\chi_0$, is sufficiently smaller than the interval T for the laser to reach the steady state, i.e., $N\chi_0 \gg 1/T$. This assumption enables us to extend the upper limit of the integral in U_2 to infinity, to obtain $\int_0^t dt_1\chi(t_1) = \pi/N$, N being the same positive integer defining the phase of $\tilde{\xi}(t)$, such that

$$H_2(t) = \lambda e^{i(2\pi/N)a^\dagger a}a\sigma_+^{(L)} + \tilde{\xi}(t)e^{i(2\pi/N)a^\dagger a}a + H.c. \tag{4.20}$$

Finally, we perform the last unitary transformation,

$U_3 = \exp\left[i\int_0^t dt_1 \left|\tilde{\xi}(t_1)\right| \left(e^{i(\varphi+\pi/2+\pi/N)}a^\dagger e^{-i(2\pi/N)a^\dagger a} + e^{-i(\varphi+\pi/2+\pi/N)}e^{i(2\pi/N)a^\dagger a}a\right)\right]$, considering, as for the Kerr coupling, that $\left|\tilde{\xi}(t)\right|$ is a Gaussian pulse of the form $\left|\tilde{\xi}(t)\right| = \xi_0 \exp\left[-\left(\xi_0\sqrt{\pi}t\right)^2/4\alpha^2\right]$, with a sufficiently smaller width, such that $\int_0^t dt_1 \left|\tilde{\xi}(t_1)\right| \approx |\alpha|$. We then obtain the effective Hamiltonian

$$H_\pm(t) = \lambda\left(A_\pm^\dagger \sigma_-^{(L)} + A_\pm \sigma_+^{(L)}\right) \tag{4.21}$$

with the canonical operators anticipated in Eq. (4.3): $A_\pm = e^{i(2\pi/N)a^\dagger a}a + e^{\pm i\pi/N}\alpha$ and $A_\pm^\dagger = a^\dagger e^{-i(2\pi/N)a^\dagger a} + e^{\mp i\pi/N}\alpha^*$, where the magnitude of $\alpha = |\alpha|\, e^{i\varphi}$, which defines the excitation of our SCLS laser, follows from that of the pumping of the cavity mode, $\tilde{\xi}(t)$.

4.6 Conclusion

We have presented here a protocol for the construction of a SCLS laser based essentially on the engineering of an effective atom-field interaction in the Jaynes-Cummings form (4.2a): $H_{\pm,N} = \chi\left(A_{\pm,N}^\dagger \sigma_- + A_{\pm,N}\sigma_+\right)$. The generalized field operators $A_{\pm,N}^\dagger$ and $A_{\pm,N}$, follow from the usual creation and annihilation operators $a^\dagger$and a, being defined in Eq. (4.3): $A_{\pm,N} = e^{i(2\pi/N)a^\dagger a}a + e^{\pm i\pi/N}\alpha$. Our protocol also relies on the construction of an isomorphism between the algebras for $a^\dagger, a$ and $A_{\pm,N}^\dagger, A_{\pm,N}$, i.e., the construction of a vector basis $\left\{|n\rangle_{\pm,N}^A\right\}$ for the generalized field operators from Eq. (4.3), where the action of these operators on the basis states, described by Eq. (4.6), emulates that of the operators $a^\dagger, a$ on the Fock basis vectors $\{|n\rangle\}$. The isomorphism ensures that the steady state produced by our effective laser is the coherent state $|\beta\rangle_{\pm,N}^A$ in the generalized vector basis $\left\{|n\rangle_{\pm,N}^A\right\}$, eigenstate of the generalized annihilation operator: $A_{\pm,N}|\beta\rangle_{\pm,N}^A = \beta_{\pm,N}|\beta\rangle_{\pm,N}^A$. However, to ensure a laser state with zero diffusion due to cavity losses, our laser must operate in the regime where $\beta = 0$, such that, $A_{\pm,N}|\beta = 0\rangle_{\pm,N}^A = 0$. We must then consider the regime where β approaches zero, rendering a laser with approximately zero diffusion, $A_{\pm,N}|\beta \sim 0\rangle_{\pm,N}^A \sim 0$. This is achieved in a far above threshold regime, under strong saturation, where the laser coefficients for gain ($\mathcal{A}$), saturation ($\mathcal{B}$) and loss ($\mathcal{C}$) satisfy the relation $\mathcal{B} \gg \mathcal{A} \gg \mathcal{C}$.

As anticipated in the introduction, a SCLS laser can be used to test fundamental phenomena of quantum mechanics (3, 4). A laser with zero linewidth can also be useful for technological applications, such as high-precision detection, metrology and optical sensing (89, 95). Moreover, the method here presented challenges us to design effective interactions leading to other nonclassical laser states. After all, the spectacular development

we have witnessed within radiation–matter interaction from the 1900s onwards, indicates that quantum technology will increasingly demand the engineering design of nonclassical states, (46–49) reservoirs (60–62) and effective interactions. (50–52)

CHAPTER 5

STRENGTHENING THE ATOM-FIELD COUPLING THROUGH THE DEEP-STRONG REGIME VIA PSEUDO-HERMITIAN HAMILTONIANS

5.1 Introduction

At the beginning of the 1990s we witnessed remarkable developments in platforms of matter-field interactions, (3, 4) allowing the manipulation of the interplay between the matter and field block buildings. Essentially, these were due the achieved intensity of the matter-field coupling compared to the lifetimes of the involved electronic and field states. Concomitantly, there has been a breakthrough in the field of quantum computation and communication (32) triggered by the quantum algorithm for the factorization of integers presented by P. Shor. (99)

The symbiosis between the theoretical proposition of schemes for the implementation of quantum logical operations and their practical realization through the advances achieved in the area of mater-field interaction in the early 1990s, grounded the quantum information theory, giving this subject the current status of an independent and most prominent research area. In addition to experimentally established proofs-of-principles for quantum information processing, (3, 4, 32) the foundations on quantum mechanics (3, 4, 100) also benefited greatly from the dialogue between theory and experimentation that spread from the physics of matter-field interaction to nuclear magnetic resonance, cold atoms, and solid-state physics.

Apart from the computational gain afforded by quantum qubits and algorithms, it is

the goal of the present work to investigate, in the domain of matter-field interaction, the possibility of further increasing this gain by strengthening the hitherto achieved matter-field coupling. This strengthening should result in a shorter time for excitation exchange between matter and field, and then for quantum information processing. To attain it, we turn to another major advance that occurred in the late 1990s: The quantum mechanics of $\mathcal{PT}$-symmetric Hamiltonians. (65, 67, 101) Similarly to what happened with quantum information, the pseudo-Hermitian quantum mechanics is currently an independent research field benefiting from strong activity and interesting results. (102, 103)

The possibility of achieving faster than Hermitian quantum mechanics was long envisioned in Ref. (104). The challenge then posed is the quantum brachistochrone problem: the search for a Hamiltonian who governs the evolution of a given initial state to a given final state in the least time interval τ. The authors concluded that for Hermitian Hamiltonians τ has a nonzero lowerbound, whereas for pseudo-Hermitian Hamiltonians it can be made arbitrarily small. However, in contradiction to this remarkable conclusion, it was subsequently found (105) that an inconsistency in the method proposed in (104) actually prevents it from achieving faster than Hermitian evolutions. The protocol we present here is an alternative to achieve faster than Hermitian evolutions by strengthening the atom-field coupling through pseudo-Hermitian interactions. Furthermore, strengthening the atom-field coupling presents a wide range of practical applications in quantum optics. (106–108)

5.2 The effective pseudo-Hermitian Hamiltonian

Our scheme for enhancing the atom-field coupling begins with the construction of an effective non-Hermitian Hamiltonian H_{eff}, from the fundamental Jaynes-Cummings (JC) interaction ($\hbar = 1$)

$$H = \lambda \left(a\sigma_+ + a^\dagger \sigma_- \right), \tag{5.1}$$

where λ is the well-known Rabi frequency, the field ($\omega a^\dagger a$), of frequency ω, is described by the creation and the annihilation operators $a^\dagger$and a, and the two-level atom ($\omega_0 \sigma_z/2$), with frequency ω_0 and excited and ground states e and g, is described by the pseudo-spin operators $\sigma_z = |e\rangle\langle e| - |g\rangle\langle g|$, $\sigma_+ = |e\rangle\langle g|$ and $\sigma_- = |g\rangle\langle e|$. The engineering of the effective interaction is one of the main challenges of our protocol, and we address it through the method of the adiabatic elimination of fast variables. For now we start from

the premise of an effective non-Hermitian Hamiltonian for the atom-field interaction:

$$H_{eff} = \lambda \left(\alpha a \sigma_+ + \beta a^\dagger \sigma_- \right), \tag{5.2}$$

where α and β are assumed to be real and positive dimensionless parameters defined in the range $[0, 1]$ for a second-order effective interaction H_{eff}.

For treating the non-Hermitian Hamiltonian we follow the procedure in Ref. (67), by constructing an Hermitian counterpart of H_{eff} through a nonunitary Dyson map η, i.e,

$$h = \eta H_{eff} \eta^{-1}. \tag{5.3}$$

The pseudo-Hermiticity relation $\Theta H_{eff} = H_{eff}^\dagger \Theta$ ensures $h = h^\dagger$, and the metric operator $\Theta = \eta^\dagger \eta$ ensures the unitarity of the time-evolution of the state vector of the non-Hermitian H_{eff}. In fact, through the map η, the pseudo-Hermitian H_{eff}, governing the Schrödinger equation $i\hbar\partial_t |\Psi(t)\rangle = H_{eff} |\Psi(t)\rangle$, is transformed into its Hermitian counterpart h governing the equation $i\hbar\partial_t |\psi(t)\rangle = h |\psi(t)\rangle$, where $|\Psi(t)\rangle = \eta^{-1} |\psi(t)\rangle$. In the metric defined by operator $\Theta = \eta^\dagger \eta$, it is straightforward to verify the unitarity of the time-evolution of $|\Psi(t)\rangle$, defined by $\langle \Psi(t) | \Psi(t) \rangle_\Theta \equiv \langle \Psi(t) | \Theta | \Psi(t) \rangle = \langle \psi(t) | \psi(t) \rangle$. The computation of the matrix elements of the observables $\mathcal{O} = \eta^{-1} o \eta$ (67, 109) associated with H_{eff} are accordingly defined by

$$\left\langle \Psi(t) | \mathcal{O} | \tilde{\Psi}(t) \right\rangle_\Theta \equiv \langle \Psi(t) | \Theta \mathcal{O} | \Psi(t) \rangle = \langle \psi(t) | o | \psi(t) \rangle, \tag{5.4}$$

with o being the observables associated with the Hermitian h.

We next outline our protocol starting from the engineered Hamiltonian H_{eff} to construct its pseudo-Hermitian counterpart h through the nonunitary Dyson map

$$\eta = \exp\left[\epsilon \left(a^\dagger a + 1/2 \right) + \mu a^2 + \nu \left(a^\dagger \right)^2 \right] \otimes \mathbf{1}, \tag{5.5}$$

where the parameters ϵ, μ, and ν are assumed to be real and the identity operator $\mathbf{1}$ stands for the atomic subspace. The operator η is a positive non-Hermitian operator for $\epsilon^2 - 4\mu\nu > 0$. Defining $\Lambda_\pm = \theta \coth\theta \pm \epsilon$, with $\theta = \sqrt{\epsilon^2 - 4\mu\nu}$, we obtain from Eq. (5.3) the Hamiltonian

$$h = \lambda \frac{\sinh\theta}{\theta} \left[\alpha \left(\Lambda_- a - 2\nu a^\dagger \right) \sigma_+ + \beta \left(2\mu a + \Lambda_+ a^\dagger \right) \sigma_- \right]. \tag{5.6}$$

Assuming $\alpha = |\alpha| e^{i\varphi_\alpha}$ and $\beta = |\beta| e^{i\varphi_\beta}$ with $\varphi_\beta = -\varphi_\alpha$, the Hermiticity of h demands

the relations

$$\epsilon = sgn\left(|\alpha| - |\beta|\right) \frac{\ln \Upsilon}{2\sqrt{1+z^2}}, \tag{5.7a}$$

$$\mu = sgn\left(|\alpha| - |\beta|\right) \frac{z \ln \Upsilon}{4\sqrt{R}\sqrt{1+z^2}}, \tag{5.7b}$$

$$\nu = -sgn\left(|\alpha| - |\beta|\right) \frac{z\sqrt{R} \ln \Upsilon}{4\sqrt{1+z^2}}, \tag{5.7c}$$

$$\theta = sgn\left(|\alpha| - |\beta|\right) \frac{\ln \Upsilon}{2}, \tag{5.7d}$$

where we have defined the Hermiticity degree

$$R = \left(|\beta| / |\alpha|\right)^{sgn(|\alpha|-|\beta|)},$$

such that $0 \leq R \leq 1$ for $|\alpha| > |\beta|$ or $|\alpha| < |\beta|$. The ratio R thus decreases monotonically from unity as the Hamiltonian H_{eff} moves away from Hermiticity. We have also defined the quantity

$$\Upsilon = \frac{1 + R + (1-R)\sqrt{1+z^2}}{1 + R - (1-R)\sqrt{1+z^2}} = \frac{1}{z_{\max}^2 - z^2}\left(\frac{1+R}{2\sqrt{R}} z_{\max} + \sqrt{1+z^2}\right)^2, \tag{5.8}$$

and the only free parameter of the map, the positive real

$$z = \sqrt{-4\mu\nu/\epsilon^2} \leq z_{\max}, \tag{5.9}$$

which is bounded, for a given R, to the maximum $z_{\max} = \min\left[2\sqrt{R}/\left(1-R\right), 1\right] \leq 1$, since $z > z_{\max}$ leads to the forbidden $\theta < 0$ as well as $\Upsilon < 0$. For $z_{\max} = 1$ we obtain $R_{\max} \approx 0.17$, showing that the enhancement of the atom-field coupling, prevented for $R > R_{\max}$, demands Hamiltonians with a significantly small degree of Hermiticity. By fixing R and z we automatically obtain ϵ, μ, and ν from Eq. (5.7), and defining $\chi = 2z/z_{\max} \leq 2$, such that $0 < \chi \leq 2$, we end up with the Hermitian counterpart of H_{eff}:

$$h = G\left[a\sigma_+ + a^\dagger\sigma_- + \chi\left(a^\dagger\sigma_+ + a\sigma_-\right)\right]. \tag{5.10}$$

where the effective coupling strength is given by

$$G = \alpha\lambda\Lambda_- \sinh\theta/\theta. \tag{5.11}$$

The Rabi frequency G increases proportionally to θ, diverging when $\theta \to \infty$, what happens,

for a given R, when $1 + R - (1 - R)\sqrt{1 + z^2} \to 0$ or, equivalently, for z approaching the upper physical limit $z_{\max}$ and $\chi \to 2$. As expected, the counter-rotating terms inevitably contribute when the effective Rabi frequency starts to increase, from the neighborhood of the strong-coupling ($G \approx \omega \approx \omega_0$) through the deep-strong coupling regime ($G \gg \omega \approx \omega_0$). The growth of the effective coupling G relative to the Rabi frequency λ implies in a shortened period for the atomic inversion $\langle \sigma_z(t) \rangle$ or excitation exchange, proportional to $1/G$ instead of $1/\lambda$.

In Figure 5.1 we plot G/λ against z for distinct values of $R = \beta/\alpha$, assuming $\alpha = 10^{-1} > \beta$. The choice of α and β smaller than unity is due to the fact that effective Hamiltonians are generally second-order approximations of the original interactions. The solid line follows for $R \to 1.0$, with the respective Hermitian Hamiltonian being a second-order approximation of the original Jaynes-Cummings interaction with a constant coupling $G = \alpha\lambda$, such that $G/\lambda = 10^{-1}$. The dashed line, starting from $G/\lambda = 4.1 \times 10^{-2}$, follows for $R_{\max} \simeq 0.17$. We also consider the dashed-dotted and the dotted lines for $R = 0.1$ and 0.05, which start from $G/\lambda = 3.2 \times 10^{-2}$ and 2.2×10^{-2}, respectively. Therefore, when z is sufficiently far from $z_{\max}$, the effective coupling G is around two orders of magnitude smaller than the original Rabi frequency λ, increasing slowly before reaching the vicinity of $z_{\max}$ ($= \infty$, 1.0, 0.7, 0.47 for $R = 1.0, 0.17, 0.1, 0.05$, respectively) when it presents an abrupt growth through the strong and deep-strong coupling regimes. The atom-field interaction energy thus grows proportionally to G, leading us to conclude that the energy required for engineering H_{eff} must grow as we move away from Hermiticity, decreasing R. In other words, the engineering of H_{eff} for $R \lesssim 0.17$, must demand the action of strong amplification fields to sustain the strength of the atom-field coupling G. In short, Figure 5.1 shows that we can control the atom-field coupling strength by controlling the Hermiticity degree R, at the expense of providing enough energy to engineer the effective interaction H_{eff}.

5.3 A cost-benefit analysis: Sensitive issues of our scheme

We next analyze the cost of this extraordinary gain in the atom-field interaction energy, starting with carrying out the necessary measurements on the observables related to the pseudo-Hermitian system H_{eff}. These observables are computed from those related to the Hermitian system h through the expression $\mathcal{O} = \eta^{-1} o \eta$. Considering, for example, the quadratures of the radiation field, given by $x_1 = \left(a + a^\dagger\right)/2$ and $x_2 = \left(a - a^\dagger\right)/2i$ for the

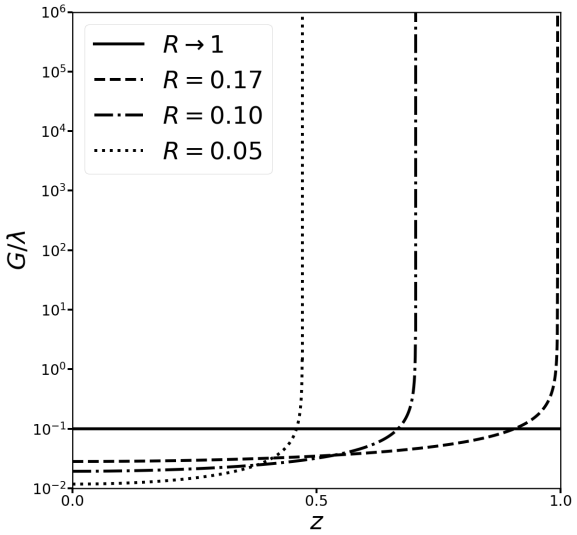

Figure 5.1 – Plot of G/λ against z for $R = 1.0$, 0.17, 0.1 and 0.05, as indicated by solid, dashed, dashed-dotted and dotted lines, respectively, assuming $\alpha = 10^{-1} > \beta$.
Source: By the author.

Hermitian system, we obtain for H_{eff} the transformed observables

$$\mathcal{X}_1 = \eta^{-1} x_1 \eta = \mathcal{A} x_1 + \mathcal{B} x_2, \tag{5.12a}$$

$$\mathcal{X}_2 = \eta^{-1} x_2 \eta = \mathcal{A} x_2 + \mathcal{B} x_1, \tag{5.12b}$$

with coefficients $\mathcal{A} = (\theta \coth \theta + \nu - \mu) \sinh \theta/\theta$ and $\mathcal{B} = (\epsilon - \nu - \mu) \sinh \theta/\theta$, both diverging as $z \to z_{\max}$. Therefore, the knowledge of $\mathcal{X}_1$ and $\mathcal{X}_2$ follows from the simultaneous measurements of the canonically conjugated variables x_1 and x_2, whose accomplishment is discussed in Refs. (110,111). The minimum energy required for performing a measurement of these canonically conjugate variables, over a time interval around $1/G$ and a given error tolerance ε, is estimated to be $E_{\min} \approx \hbar G/\varepsilon$ (112). The higher the Rabi frequencies, the higher the energies required for measuring properties of the radiation field, as higher as the lower the error tolerances.

5.4 The construction of the effective non-Hermitian Hamiltonian

An additional cost for strengthening the atom-field coupling regards the engineering of the non-Hermitian Hamiltonian H_{eff}, which must demand a large supply of energy, as large as that made available by the atom-field interaction G. Consequently, the usual method of engineering Hamiltonians by the adiabatic elimination of fast variables, (53,54)

which requires the amplitudes of the amplification fields to be much smaller than their detunings with the pumped system, should not apply to these cases, as discussed below.

Let us consider the atom-field interactions sketched in Figure 5.2, where the ground ($|g\rangle$) and excited ($|e\rangle$) states are coupled through Raman transitions to N auxiliary adjacent states $|1\rangle$,...,$|N\rangle$, labeled by the frequencies $\tilde{\omega}_\ell$. In Figure 5.2 we only show the adjacent levels $|1\rangle$, $|2\rangle$ and $|3\rangle$. A quantum mode ω and N classical fields ω_ℓ ($\ell = 1, ..., N$) are considered for this purpose. The mode is set to drive the transition $|g\rangle \leftrightarrow |1\rangle$ with strength λ and detuning $\Delta = \tilde{\omega}_1 - \omega$, while the ℓ-th classical field is set to drive the transition $|e\rangle \leftrightarrow |\ell\rangle$ with strength Ω_ℓ and detuning $\Delta_\ell = (-1)^{\delta_{\ell 1}}(\omega_e + \omega_\ell - \tilde{\omega}_\ell)$, setting the energy of the ground state $|g\rangle$ to zero. The Hamiltonian describing the process is given by $H = H_0 + V$, with

$$H_0 = \omega a^\dagger a + \omega_e \sigma_{ee} + \textstyle\sum_\ell \tilde{\omega}_\ell \sigma_{\ell\ell}, \tag{5.13}$$

$$V = \lambda a \sigma_{1g} + \textstyle\sum_\ell \Omega_\ell \sigma_{\ell e} e^{-i\omega_\ell t} + H.c., \tag{5.14}$$

where $a^\dagger$ (a) is the creation (annihilation) operator for the mode and $\sigma_{uv} = |u\rangle\langle v|$ represents pseudo-spin operators, with $u, v = e,g,\ell$. Under the conditions $\Delta \gg \sqrt{\bar{n}}\,|\lambda|$, $\bar{n}$ being the average excitation of the mode, and $\Delta_\ell \gg |\Omega_\ell|$, which imposes severe limitation on the amplitude of the pumping fields, the Hamiltonian in the interaction picture

$$\mathcal{H}(t) = \lambda a \sigma_{1g} e^{i\Delta t} + \textstyle\sum_\ell \Omega_\ell \sigma_{\ell e} e^{-(-1)^{\delta_{\ell 1}} i\Delta_\ell t} + H.c., \tag{5.15}$$

is composed only by highly oscillating terms, enabling, to a good approximation, an effective interaction (49–51, 53, 54, 56, 61, 87, 88, 90, 92)

$$H_{eff} \approx -i\mathcal{H}(t)\int_0^t \mathcal{H}(t)d\tau \approx -\frac{|\lambda|^2}{\Delta} a^\dagger a \sigma_{gg} - \frac{\lambda^*\Omega_1}{\Delta_1} a^\dagger \sigma_{ge} e^{i(\Delta_1-\Delta)t} - \frac{\lambda\Omega_1^*}{\Delta} a \sigma_{eg} e^{-i(\Delta_1-\Delta)t} + \textstyle\sum_\ell (-1)^{\delta_{\ell 1}} \frac{|\Omega_\ell|^2}{\Delta_\ell} \sigma_{ee}.$$

After an unitary transformation using $U(t) = e^{-i\chi\sigma_{ee}t}$, with $\chi = \sum_\ell (-1)^{\delta_{\ell 1}} |\Omega_\ell|^2/\Delta_\ell = \Delta_1 - \Delta > 0$, we finally obtain, for $\beta \gg \bar{n}|\lambda|/\Delta$, the non-Hermitian effective interaction

$$H_{eff} \approx |\lambda|\,\alpha\left(a\sigma_+ + R a^\dagger \sigma_-\right), \tag{5.16}$$

with $\alpha = |\Omega_1|/\Delta$ and $\beta = |\Omega_1|/\Delta_1$. The non-Hermiticity thus follows from the gap $\Delta_1 - \Delta = \chi$ which evidently increases with the number of pumping fields; and that is why

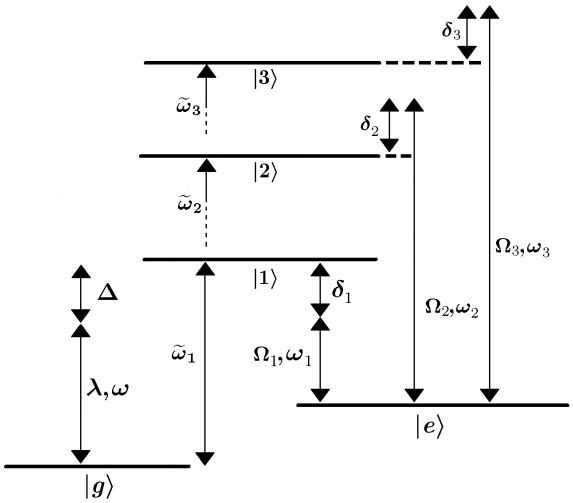

Figure 5.2 – Atomic configuration to engineer the non-Hermitian Jaynes-Cummings interaction.
Source: By the author.

we left this number arbitrary in our scheme. However, as already pointed out, even with an arbitrary number of pumping fields, our adiabatic elimination scheme is not efficient for the construction of far-from-Hermitian interactions, with $R \leq 0.17$, since the pumping amplitudes must be limited by their detunings with the cavity mode.

We stress that although we started from a Hermitian Hamiltonian, the non-Hermiticity results from a second-order approximation in which $\mathcal{H}(t)$ does not in general commute with $\int_0^t \mathcal{H}(\tau)d\tau$. In short, for the regime of parameters we have considered, the originally Hermitian Hamiltonian H reduces to the non-Hermitian second-order approximation H_{eff}. Indeed we verify that the norm of H is no longer conserved under the parameters leading to H_{eff}, indicating that it actually becomes a non-Hermitian operator. In Figure 5.3 we consider the evolution of H to plot $\mathrm{Tr}\,\rho(t)$ against λt, $\rho(t)$ being the evolved atom-field density operator. We start with the field in the vacuum and the atom in the excited state, assuming the parameters given in the caption. The straight, dashed and dot lines refer to $R = 1$, 0.9, and 0.5, respectively, indicating that the norm decreases monotonically for $R = 0.9$ and 0.5. The small deviation from the unit observed for $R = 1$, follows from numerical errors.

In Figure 5.4 we plot the mean excitation $\left\langle a^\dagger a \right\rangle (t)$ against $|\lambda|\, t$ computed from the full Hamiltonian (5.15) (dotted line) and the effective one (5.16) (solid line), starting again with the field in the vacuum, the atom in the excited state and considering the parameters given in the caption. Here we do not consider the metric $\Theta = \eta^\dagger \eta$ to compute the mean value $\left\langle a^\dagger a \right\rangle (t)$ for the non-Hermitian H_{eff}, i.e., we do not follow the prescription in Eq. (5.4), since we only seek to compare the dynamics generated by both Hamiltonians, without

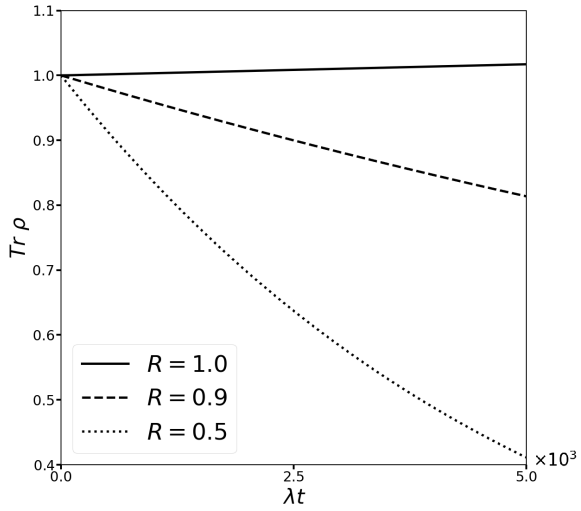

Figure 5.3 – Plot of $\mathrm{Tr}\,\rho(t)$ against λt, for $R = 1.0$, 0.9, and 0.5 as indicated by straight, dashed and dot lines, respectively. We have considered $\alpha = 0.1$ and $\Delta_2 = \Delta_3 = 5 \times 10^3 \lambda$ for all values of R. However, for $R = 1$ we fixed (in units of λ) $\beta = 0.1$, $|\Omega_1| = 9.2$, $|\Omega_2| = |\Omega_3| = 48$ and $\Delta = \Delta_1 = 92$. for $R = 0.9$ we fixed $\beta = 0.09$, $|\Omega_1| = 6.6$, $|\Omega_2| = |\Omega_3| = 141.2$, $\Delta = 66.4$ and $\Delta_1 = 73.8$. Finally, for $R = 0.5$ we fixed $\beta = 0.05$, $|\Omega_1| = 10$, $|\Omega_2| = |\Omega_3| = 501.3$, $\Delta = 100$ and $\Delta_1 = 200$.
Source: By the author.

worrying about norm conservation. In Figs. 5.4(a and b) we consider $R = 0.95$ and 0.9, respectively, to observe that for $R = 0.95$ the effective interaction is a good approximation of the full Hamiltonian for $|\lambda|\, t$ up to around 35. However, when we go to $R = 0.9$, the curves show discrepancies already for $|\lambda|\, t \approx 15$. In both cases the discrepancies are more pronounced in phases than in amplitudes, and increase as we move further away from Hermiticity, decreasing R.

While the engineering enabling $H \to H_{eff}$ follows from the adiabatic elimination method and the map $H_{eff} \to h$ follows from the pseudo-Hermiticity relation, both the adiabatic elimination and the pseudo-Hermiticity must be put together through the energy balance between H and h. The impossibility of such a balance leads us to conclude that another engineering scheme must be developed in which the amplitudes of the pumping fields are not limited by their detunings with the mode.

5.5 Conclusion

The method here proposed for strengthening the Rabi coupling through pseudo-Hermitian Hamiltonians is similar to those for reaching infinite squeezing degree at finite times, (113–115) for the enhancement of Casimir's photon creation, (116) and for the strengthening of the Dicke superradiance intensity. (116) All these achievements rely on the

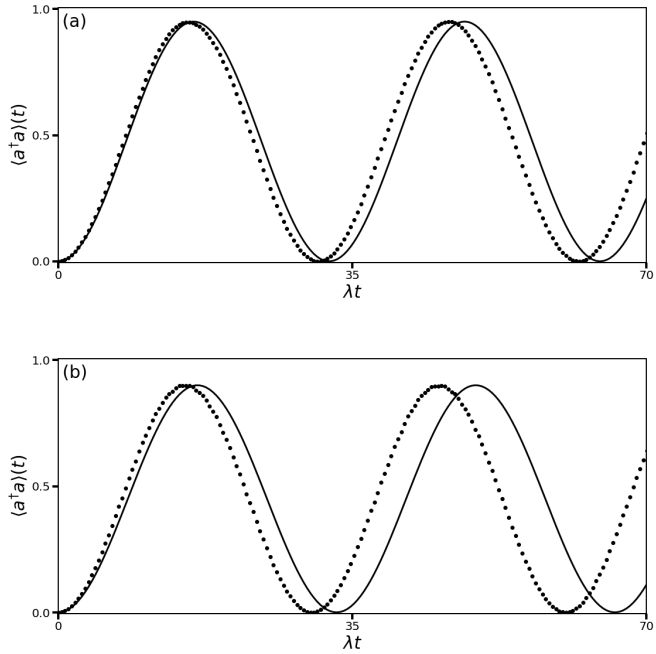

Figure 5.4 – Plot of $\langle a^\dagger a\rangle(t)$ against $|\lambda|\,t$ computed from the full Hamiltonian (5.15) (dotted line) and the effective one (5.16) (solid line), for $R = 0.95$, and 0.9, considering $\alpha = 0.1$ and $\Delta_2 = \Delta_3 = 5 \times 10^3\lambda$ for all values of R. For $R = 0.95$ we fixed (in units of λ) $\beta = 9.5\times10^{-2}$, $|\Omega_1| = 9.3$, $|\Omega_2| = |\Omega_3| = 120$, $\Delta = 92.6$ and $\Delta_1 = 97.5$. For $R = 0.9$ we fixed $\beta = 9 \times 10^{-2}$, $|\Omega_1| = 6.6$, $|\Omega_2| = |\Omega_3| = 141.2$, $\Delta = 66.4$ and $\Delta_1 = 73.8$.
Source: By the author.

engineering of interactions which are far from Hermiticity, a challenge that remains to be accomplished. We stress that the non-Hermitian Hamiltonian (5.2) as well as those introduced in Ref. (113–116), must necessarily be engineered as effective Hamiltonians, since they result in (or leads to) energy gain, which must be provided by high amplitude amplification fields.

It is crucial to underline that the Dyson map η in Eq. (5.5), used to ensure the pseudo-Hermiticity relation (and therefore the conservation of the norm in a new metric $\Theta = \eta^\dagger\eta$), basically implies new observables $\mathcal{O} = \eta^{-1}o\eta$ (67,109) and consequently in the implementation of procedures for measuring canonically conjugated variables. (110,111) Therefore, we stress that the present protocol is perfectly feasible once the engineering of the non-Hermitian Hamiltonian (5.2) is implemented, which is the really sensitive point for its pratical realization.

We have also discussed the energy cost for the remarkable gain in the atom-field coupling, which must be supported by the construction of the non-Hermitian Hamiltonian and by carrying out the measurements of canonically conjugated variables. We finally observe that, apart from the prospects for the implementation of the present method in platforms of radiation-matter interaction, we cannot but speculate on the impacts that

the possible adaptation of the present method would bring to the field of high-energy experimental physics.

CHAPTER 6

CONCLUSIONS AND FUTURE PERSPECTIVES

Summarizing the conclusions presented in the previous chapters, we developed similar protocols for obtaining squeezed vacuum and SCLS lasers, in which the essential concept is based on the building of an effective atom-field interaction as well as the construction of an isomorphism between the algebra of the field operators $\left(a, a^{\dagger}\right)$ acting on the Fock basis $\{|n\rangle\}$ and the generalized field operators, $\left(A, A^{\dagger}\right)$, with the new basis $\{|n\rangle_A\}$, ensuring that the steady state of our effective laser is the coherent state in the generalized vector basis $\{|n\rangle_A\}$. This state can be written in the Fock basis using the relation established between the Fock and generalized bases, producing a state for the laser that depends on the choice for the construction of the generalized operators $\left(A, A^{\dagger}\right)$. In addition, in order to minimize the diffusion due to cavity losses, the effective laser must operate in such a regime that its excitation in the generalized basis approaches zero, i.e. $A|\alpha\rangle_A \to 0$, therefore the laser state in the Fock basis is protected from decoherence. As pointed before, squeezed vacuum states can be useful for optical sensing, metrology, laser spectroscopy and high-resolution interferometry while SCLS can be used to test fundamental phenomena of quantum mechanics and high-precision detection. Regarding to the protocol for strengthening the Rabi coupling through pseudo-Hermitian Hamiltonians, we say that the key for this accomplishment is the engineering of interactions which are far from Hermiticity, which must be constructed as effective Hamiltonians, once they lead to energy gain, which must be provided by high amplitude amplification fields. Moreover we stress here the need for implementation of procedures for measuring canonically conjugated variables, which also demands high energy costs. Finally, the coupling strengthening may be useful in fields such as high-energy experimental physics.

In addition to the works presented here we are also developing two different types

of laser. The first one is based on the construction of an effective interaction, following the protocols of James, (54) using a three level atom and a single mode cavity to build an effective Hamiltonian in the anti-Jaynes-Cummings form: $\mathcal{H}_{eff} = g\left(a^\dagger \sigma_+ + a\sigma_-\right)$. Due to its opposing nature, when comparing to the Jaynes-Cummings Hamiltonian, we have already obtained a stationary state, yet to be characterized. More importantly, we expect to analyse the working regime of this new laser, that might be under the threshold, to compensate the high energy costs — provided by high amplitude amplification fields — to sustain the effective interaction.

The other project deals with a laser with two (or more) cavities in a linear array, with interacting modes in the neighboring cavities, leading to the Hamiltonian: $\mathcal{H}_1 = \omega_a a^\dagger a + \omega_b b^\dagger b + \chi\left(ab^\dagger + a^\dagger b\right)$. By diagonalizing the Hamiltonian that describes this system we obtain a Hamiltonian with the eigenvalues of the normal modes, i.e. $\mathcal{H}_2 = \Omega_A\ A^\dagger A + \Omega_B\ B^\dagger B$. Next we consider a two level atomic sample that resonates only with one of these modes, e.g. the A mode, thus we can neglect the other mode and add the atomic diagonal Hamiltonian and the standard radiation-matter interaction to get $\mathcal{H}_3 = \Omega_A\ A^\dagger A + \frac{\omega_0}{2}\sigma_z + g\left(A\sigma_+ + A^\dagger \sigma_-\right)$. Once we have written the Hamiltonian in the form of Jaynes-Cummings, which leads to the well known master equation for the laser, we can build an isomorphism between our system and the usual laser theory, as already explained through Chapters 3 and 4, so we know that the solution, in the stationary regime, is the coherent state in the normal mode A basis. Using the relation between this basis and the original cavities modes a and b bases to rewrite the coherent state, we finally get the steady state in the original bases. Since the steady state is an entangled state between the cavities, this multicavity laser acts as a source of entanglement. This result would be very interesting, as we would have achieved another steady state for the laser different from the usual coherent state, and since we are not using effective interactions there would be no time validity, meaning that we would not have to restart the system after some certain time.

REFERENCES

1 LEIBFRIED, D. *et al.* Quantum dynamics of single trapped ions. **Reviews of Modern Physics**, APS, v. 75, n. 1, p. 281, 2003.

2 BRUNE, M. *et al.* Observing the progressive decoherence of the "meter" in a quantum measurement. **Physical Review Letters**, APS, v. 77, n. 24, p. 4887, 1996.

3 WINELAND, D. J. Nobel lecture: superposition, entanglement, and raising schrödinger's cat. **Reviews of Modern Physics**, APS, v. 85, n. 3, p. 1103, 2013.

4 HAROCHE, S. Nobel lecture: controlling photons in a box and exploring the quantum to classical boundary. **Reviews of Modern Physics**, APS, v. 85, n. 3, p. 1083, 2013.

5 MONROE, C. *et al.* A "schrödinger cat" superposition state of an atom. **Science**, American Association for the Advancement of Science, v. 272, n. 5265, p. 1131–1136, 1996.

6 YUEN, H. P. Two-photon coherent states of the radiation field. **Physical Review A**, APS, v. 13, n. 6, p. 2226, 1976.

7 MEEKHOF, D. *et al.* Generation of nonclassical motional states of a trapped atom. **Physical Review Letters**, APS, v. 76, n. 11, p. 1796, 1996.

8 LEIBFRIED, D. *et al.* Experimental determination of the motional quantum state of a trapped atom. **Physical Review Letters**, APS, v. 77, n. 21, p. 4281, 1996.

9 BRATTKE, S.; VARCOE, B. T.; WALTHER, H. Generation of photon number states on demand via cavity quantum electrodynamics. **Physical Review Letters**, APS, v. 86, n. 16, p. 3534, 2001.

10 BRUNE, M. *et al.* Quantum rabi oscillation: a direct test of field quantization in a cavity. **Physical Review Letters**, APS, v. 76, n. 11, p. 1800, 1996.

11 KNIGHT, P. Discrete charm of the photon. **Nature**, Nature Publishing Group, v. 380, n. 6573, p. 392–393, 1996.

12 SCHAWLOW, A. L.; TOWNES, C. H. Infrared and optical masers. **Physical Review**, APS, v. 112, n. 6, p. 1940, 1958.

13 MAIMAN, T. H. *et al.* Stimulated optical radiation in ruby. **Nature**, v. 187, p. 493–494, 1960.

14 ULRICH, H.; PROBST, G. J. **Self-organization and management of social systems**: Insights, promises, doubts, and questions. Berlin: Springer, 2012. v. 26.

15 SARGENT, M.; SCULLY, M. O.; LAMB, W. E. **Laser physics**. Massachusetts: Addison-Wesley, 1974. v. 201067196.

16 SCULLY, M. O.; LAMB JUNIOR, W. E. Quantum theory of an optical maser. i. general theory. **Physical Review**, APS, v. 159, n. 2, p. 208, 1967.

17 LAX, M.; LOUISELL, W. Quantum noise. xii. density-operator treatment of field and population fluctuations. **Physical Review**, APS, v. 185, n. 2, p. 568, 1969.

18 BASEIA, B.; NUSSENZVEIG, H. Semiclassical theory of laser transmission loss. **Optica Acta**, Taylor & Francis, v. 31, n. 1, p. 39–62, 1984.

19 GOLUBEV, Y. M.; SOKOLOV, I. Photon antibunching in a coherent light source and suppression of the photorecording noise. **Soviet Physics, JETP**, v. 60, n. 2, p. 234–234, 1984.

20 YAMAMOTO, Y.; MACHIDA, S.; NILSSON, O. Amplitude squeezing in a pump-noise-suppressed laser oscillator. **Physical Review A**, APS, v. 34, n. 5, p. 4025, 1986.

21 HAAKE, F.; TAN, S.; WALLS, D. Photon noise reduction in lasers. **Physical Review A**, APS, v. 40, n. 12, p. 7121, 1989.

22 BERGOU, J. *et al.* Influence of the pumping statistics in lasers and masers. **Optics Communications**, Elsevier, v. 72, n. 1-2, p. 82–86, 1989.

23 PHILLIPS, W. D. Nobel lecture: laser cooling and trapping of neutral atoms. **Reviews of Modern Physics**, APS, v. 70, n. 3, p. 721, 1998.

24 CHU, S. Nobel lecture: the manipulation of neutral particles. **Reviews of Modern Physics**, APS, v. 70, n. 3, p. 685, 1998.

25 COHEN-TANNOUDJI, C. N. Nobel lecture: manipulating atoms with photons. **Reviews of Modern Physics**, APS, v. 70, n. 3, p. 707, 1998.

26 KETTERLE, W. Nobel lecture: when atoms behave as waves: Bose-einstein condensation and the atom laser. **Reviews of Modern Physics**, APS, v. 74, n. 4, p. 1131, 2002.

27 CORNELL, E. A.; WIEMAN, C. E. Nobel lecture: Bose-einstein condensation in a dilute gas, the first 70 years and some recent experiments. **Reviews of Modern Physics**, APS, v. 74, n. 3, p. 875, 2002.

28 ASHKIN, A. Acceleration and trapping of particles by radiation pressure. **Physical Review Letters**, APS, v. 24, n. 4, p. 156, 1970.

29 ASHKIN, A. *et al.* Observation of a single-beam gradient force optical trap for dielectric particles. **Optics Letters**, Optical Society of America, v. 11, n. 5, p. 288–290, 1986.

30 ASHKIN, A.; DZIEDZIC, J. M.; YAMANE, T. Optical trapping and manipulation of single cells using infrared laser beams. **Nature**, Nature Publishing Group, v. 330, n. 6150, p. 769–771, 1987.

31 ASHKIN, A.; DZIEDZIC, J. M. Optical trapping and manipulation of viruses and bacteria. **Science**, American Association for the Advancement of Science, v. 235, n. 4795, p. 1517–1520, 1987.

32 NIELSEN, M. A.; CHUANG, I. **Quantum computation and quantum information**. Maryland: American Association of Physics Teachers, 2002.

33 STRICKLAND, D.; MOUROU, G. Compression of amplified chirped optical pulses. **Optics Communications**, Elsevier, v. 55, n. 6, p. 447–449, 1985.

34 MAINE, P. *et al.* Generation of ultrahigh peak power pulses by chirped pulse amplification. **IEEE Journal of Quantum electronics**, IEEE, v. 24, n. 2, p. 398–403, 1988.

35 DODONOV, V. Nonclassical states in quantum optics: a squeezed review of the first 75 years. **Journal of Optics B**, IOP Publishing, v. 4, n. 1, p. R1, 2002.

36 CAVES, C. M. Quantum-mechanical noise in an interferometer. **Physical Review D**, APS, v. 23, n. 8, p. 1693, 1981.

37 SCULLY, M. O.; MEYSTRE, P. **Quantum optics, experimental gravity, and measurement theory**. New York: Plenum Press, 1983.

38 ABBOTT, B. P. *et al.* Observation of gravitational waves from a binary black hole merger. **Physical Review Letters**, APS, v. 116, n. 6, p. 061102, 2016.

39 SHAPIRO, J. H. Optical waveguide tap with infinitesimal insertion loss. **Optics Letters**, Optica Publishing Group, v. 5, n. 8, p. 351–353, 1980.

40 YONEZAWA, H.; FURUSAWA, A. Continuous-variable quantum information processing with squeezed states of light. **Optics and Spectroscopy**, Springer, v. 108, n. 2, p. 288–296, 2010.

41 UKAI, R. *et al.* Demonstration of unconditional one-way quantum computations for continuous variables. **Physical Review Letters**, APS, v. 106, n. 24, p. 240504, 2011.

42 BRIDA, G.; GENOVESE, M.; BERCHERA, I. R. Experimental realization of sub-shot-noise quantum imaging. **Nature Photonics**, Nature Publishing Group, v. 4, n. 4, p. 227–230, 2010.

43 D'AMBROSIO, V. *et al.* Photonic polarization gears for ultra-sensitive angular measurements. **Nature Communications**, Nature Publishing Group, v. 4, n. 1, p. 1–8, 2013.

44 ASPECT, A.; GRANGIER, P.; ROGER, G. Experimental realization of einstein-podolsky-rosen-bohm gedankenexperiment: a new violation of bell's inequalities. **Physical Review Letters**, APS, v. 49, n. 2, p. 91, 1982.

45 KWIAT, P. G. *et al.* New high-intensity source of polarization-entangled photon pairs. **Physical Review Letters**, APS, v. 75, n. 24, p. 4337, 1995.

46 VOGEL, K.; AKULIN, V.; SCHLEICH, W. P. Quantum state engineering of the radiation field. **Physical Review Letters**, APS, v. 71, n. 12, p. 1816, 1993.

47 ROOS, C. *et al.* Quantum state engineering on an optical transition and decoherence in a paul trap. **Physical Review Letters**, APS, v. 83, n. 23, p. 4713, 1999.

48 VILLAS-BÔAS, C. *et al.* Preparation and control of a cavity-field state through an atom–driven-field interaction: Towards long-lived mesoscopic states. **Physical Review A**, APS, v. 68, n. 5, p. 053808, 2003.

49 PRADO, F. *et al.* Steady fock states via atomic reservoir. **Europhysics Letters**, IOP Publishing, v. 107, n. 1, p. 13001, 2014.

50 ROSSETTI, R. F. *et al.* Slicing the fock space for state production and protection. **Physical Review A**, APS, v. 90, n. 3, p. 033840, 2014.

51 ROSSETTI, R. *et al.* Erratum: Slicing the fock space for state production and protection. **Physical Review A**, APS, v. 93, n. 6, p. 069904, 2016.

52 MORAES NETO, G. *et al.* Steady entanglement in bosonic dissipative networks. **Physical Review A**, APS, v. 90, n. 6, p. 062322, 2014.

53 GAMEL, O.; JAMES, D. F. Time-averaged quantum dynamics and the validity of the effective hamiltonian model. **Physical Review A**, APS, v. 82, n. 5, p. 052106, 2010.

54 JAMES, D.; JERKE, J. Effective hamiltonian theory and its applications in quantum information. **Canadian Journal of Physics**, NRC Research Press Ottawa, Canada, v. 85, n. 6, p. 625–632, 2007.

55 MORAES NETO, G.; PONTE, M. de; MOUSSA, M. Colored channels for high-fidelity information transfer and processing between remote multi-branch quantum circuits. **Europhysics Letters**, IOP Publishing, v. 103, n. 4, p. 43001, 2013.

56 MORAES NETO, G.; PONTE, M. de; MOUSSA, M. Nonlocal dissipative tunneling for high-fidelity quantum-state transfer between distant parties. **Physical Review A**, APS, v. 85, n. 5, p. 052303, 2012.

57 MORAES NETO, G.; PONTE, M. de; MOUSSA, M. Engineering interactions for quasiperfect transfer of polariton states through nonideal bosonic networks of distinct topologies. **Physical Review A**, APS, v. 84, n. 3, p. 032339, 2011.

58 ZHENG, S.-B.; GUO, G.-C. Efficient scheme for two-atom entanglement and quantum information processing in cavity qed. **Physical Review Letters**, APS, v. 85, n. 11, p. 2392, 2000.

59 RODRIGUES, R.; MOUSSA, M.; VILLAS-BÔAS, C. Engineering phonon-photon interactions with a driven trapped ion in a cavity. **Physical Review A**, APS, v. 74, n. 6, p. 063811, 2006.

60 POYATOS, J.; CIRAC, J. I.; ZOLLER, P. Quantum reservoir engineering with laser cooled trapped ions. **Physical Review Letters**, APS, v. 77, n. 23, p. 4728, 1996.

61 PRADO, F. O. *et al.* Nonadiabatic coherent evolution of two-level systems under spontaneous decay. **Physical Review Letters**, APS, v. 102, n. 7, p. 073008, 2009.

62 CELERI, L. *et al.* Switching off the reservoir through nonstationary quantum systems. **Journal of Physics B**, IOP Publishing, v. 41, n. 8, p. 085504, 2008.

63 OZAWA, T. *et al.* Topological photonics. **Reviews of Modern Physics**, APS, v. 91, n. 1, p. 015006, 2019.

64 LO, H.-K.; SPILLER, T.; POPESCU, S. **Introduction to quantum computation and information**. Singapure: World Scientific, 1998.

65 BENDER, C. M.; BOETTCHER, S. Real spectra in non-hermitian hamiltonians having p t symmetry. **Physical Review Letters**, APS, v. 80, n. 24, p. 5243, 1998.

66 BENDER, C. M. Making sense of non-hermitian hamiltonians. **Reports on Progress in Physics**, IOP Publishing, v. 70, n. 6, p. 947, 2007.

67 MOSTAFAZADEH, A. Pseudo-hermiticity versus pt symmetry: the necessary condition for the reality of the spectrum of a non-hermitian hamiltonian. **Journal of Mathematical Physics**, American Institute of Physics, v. 43, n. 1, p. 205–214, 2002.

68 CHITSAZI, M. *et al.* Experimental realization of floquet pt-symmetric systems. **Physical Review Letters**, APS, v. 119, n. 9, p. 093901, 2017.

69 BIESENTHAL, T. *et al.* Experimental realization of pt-symmetric flat bands. **Physical Review Letters**, APS, v. 123, n. 18, p. 183601, 2019.

70 SILVA, L. F. Alves da; DOURADO, R.; MOUSSA, M. Beyond pt-symmetry: Towards a symmetry-metric relation for time-dependent non-hermitian hamiltonians. **SciPost Physics Core**, v. 5, n. 1, p. 012, 2022.

71 SONG, A. Y. *et al.* Pt-symmetric topological edge-gain effect. **Physical Review Letters**, APS, v. 125, n. 3, p. 033603, 2020.

72 MOSTAFAZADEH, A. Pseudo-hermiticity versus pt-symmetry. ii. a complete characterization of non-hermitian hamiltonians with a real spectrum. **Journal of Mathematical Physics**, American Institute of Physics, v. 43, n. 5, p. 2814–2816, 2002.

73 MOSTAFAZADEH, A. Pseudo-hermiticity versus pt-symmetry iii: Equivalence of pseudo-hermiticity and the presence of antilinear symmetries. **Journal of Mathematical Physics**, American Institute of Physics, v. 43, n. 8, p. 3944–3951, 2002.

74 OLIVEIRA NETO, F.; MORAES NETO, G.; MOUSSA, M. H. Y. A squeezed vacuum state laser with zero diffusion from cavity losses. **Annalen der Physik**, Wiley Online Library, v. 534, n. 2, p. 2100072, 2022.

75 ORSZAG, M. **Quantum optics**: including noise reduction, trapped ions, quantum trajectories, and decoherence. Berlin: Springer, 2016.

76 SCULLY, M. O.; ZUBAIRY, M. S. **Quantum optics**. Cambridge: Cambridge University Press, 1997.

77 YAMAMOTO, Y.; IMAMOGLU, A. **Mesoscopic quantum optics**. New Jersey: Wiley, 1999.

78 HEMPSTEAD, R. D.; LAX, M. Classical noise. vi. noise in self-sustained oscillators near threshold. **Physical Review**, APS, v. 161, n. 2, p. 350, 1967.

79 GORDON, J. Quantum theory of a simple maser oscillator. **Physical Review**, APS, v. 161, n. 2, p. 367, 1967.

80 HAKEN, H. Theory of intensity and phase fluctuations of a homogeneously broadened laser. **Zeitschrift für Physik**, Springer, v. 190, n. 3, p. 327–356, 1966.

81 MUSUMBU, D.; GEYER, H.; HEISS, W. Choice of a metric for the non-hermitian oscillator. **Journal of Physics A**, IOP Publishing, v. 40, n. 2, p. F75, 2006.

82 WU, L.-A. *et al.* Generation of squeezed states by parametric down conversion. **Physical Review Letters**, APS, v. 57, n. 20, p. 2520, 1986.

83 WALLS, D.; MILBURN, G. **Quantum optics**. Berlin: Springer, 1994.

84 SLUSHER, R. *et al.* Observation of squeezed states generated by four-wave mixing in an optical cavity. **Physical Review Letters**, APS, v. 55, n. 22, p. 2409, 1985.

85 VILLAS-BOAS, C. *et al.* Squeezing arbitrary cavity-field states through their interaction with a single driven atom. **Physical Review A**, APS, v. 68, n. 6, p. 061801, 2003.

86 ALMEIDA, N. D. *et al.* Engineering squeezed states in high-q cavities. **Physical Review A**, APS, v. 69, n. 3, p. 035802, 2004.

87 SERRA, R. *et al.* Frequency up-and down-conversions in two-mode cavity quantum electrodynamics. **Physical Review A**, APS, v. 71, n. 4, p. 045802, 2005.

88 PRADO, F. *et al.* Bilinear and quadratic hamiltonians in two-mode cavity quantum electrodynamics. **Physical Review A**, APS, v. 73, n. 4, p. 043803, 2006.

89 HUANG, S. *et al.* Precise measurement of ultra-narrow laser linewidths using the strong coherent envelope. **Scientific Reports**, Nature Publishing Group, v. 7, n. 1, p. 1–7, 2017.

90 PRADO, F. O. *et al.* Engineering selective linear and nonlinear jaynes–cummings interactions and applications. **Journal of Physics B**, IOP Publishing, v. 46, n. 20, p. 205501, 2013.

91 ROSADO, W. *et al.* Upper bounded and sliced jaynes–and anti-jaynes–cummings hamiltonians and liouvillians in cavity quantum electrodynamics. **Journal of Modern Optics**, Taylor & Francis, v. 62, n. 19, p. 1561–1569, 2015.

92 ROSSETTI, R. *et al.* Trapped-ion lissajous trajectories by engineering rashba-and dresselhaus-type spin-orbit interactions in a paul trap. **Europhysics Letters**, IOP Publishing, v. 115, n. 5, p. 53001, 2016.

93 BOOZER, A. Theory of raman transitions in cavity qed. **Physical Review A**, APS, v. 78, n. 3, p. 033406, 2008.

94 MUÑOZ, C. S.; JAKSCH, D. Squeezed lasing. **Physical Review Letters**, APS, v. 127, n. 18, p. 183603, 2021.

95 TRAN, M. A.; HUANG, D.; BOWERS, J. E. Tutorial on narrow linewidth tunable semiconductor lasers using si/iii-v heterogeneous integration. **APL Photonics**, AIP Publishing LLC, v. 4, n. 11, p. 111101, 2019.

96 HOROSHKO, D.; KILIN, S. Y. Direct detection feedback for preserving quantum coherence in an open cavity. **Physical Review Letters**, APS, v. 78, n. 5, p. 840, 1997.

97 ASHHAB, S. *et al.* Single-artificial-atom lasing using a voltage-biased superconducting charge qubit. **New Journal of Physics**, IOP Publishing, v. 11, n. 2, p. 023030, 2009.

98 DAO-MING, L.; SHI-BIAO, Z. Scheme for realizing kerr nonlinearity in cavity qed. **Chinese Physics Letters**, IOP Publishing, v. 24, n. 6, p. 1567, 2007.

99 SHOR, P. W. Polynomial-time algorithms for prime factorization and discrete logarithms on a quantum computer. **SIAM Review**, SIAM, v. 41, n. 2, p. 303–332, 1999.

100 AULETTA, G. **Foundations and interpretation of quantum mechanics**: In the light of a critical-historical analysis of the problems and of a synthesis of the results. Singapure: World Scientific, 2000.

101 BENDER, C. M.; BOETTCHER, S.; MEISINGER, P. N. Pt-symmetric quantum mechanics. **Journal of Mathematical Physics**, American Institute of Physics, v. 40, n. 5, p. 2201–2229, 1999.

102 BENDER, C. M. Introduction to pt-symmetric quantum theory. **Contemporary Physics**, Taylor & Francis, v. 46, n. 4, p. 277–292, 2005.

103 CHRISTODOULIDES, D.; YANG, J. *et al.* **Parity-time symmetry and its applications**. Singapore: Springer, 2018. v. 280.

104 BENDER, C. M. *et al.* Faster than hermitian quantum mechanics. **Physical Review Letters**, APS, v. 98, n. 4, p. 040403, 2007.

105 MOSTAFAZADEH, A. Quantum brachistochrone problem and the geometry of the state space in pseudo-hermitian quantum mechanics. **Physical Review Letters**, APS, v. 99, n. 13, p. 130502, 2007.

106 DOVZHENKO, D. *et al.* Light–matter interaction in the strong coupling regime: configurations, conditions, and applications. **Nanoscale**, Royal Society of Chemistry, v. 10, n. 8, p. 3589–3605, 2018.

107 LIBERATO, S. D. Light-matter decoupling in the deep strong coupling regime: The breakdown of the purcell effect. **Physical Review Letters**, APS, v. 112, n. 1, p. 016401, 2014.

108 TEUFEL, J. D. *et al.* Circuit cavity electromechanics in the strong-coupling regime. **Nature**, Nature Publishing Group, v. 471, n. 7337, p. 204–208, 2011.

109 SCHOLTZ, F.; GEYER, H.; HAHNE, F. Quasi-hermitian operators in quantum mechanics and the variational principle. **Annals of Physics**, Elsevier, v. 213, n. 1, p. 74–101, 1992.

110 WÓDKIEWICZ, K. Operational approach to phase-space measurements in quantum mechanics. **Physical Review Letters**, APS, v. 52, n. 13, p. 1064, 1984.

111 LEONHARDT, U.; PAUL, H. Simultaneous measurements of canonically conjugate variables in quantum optics. **Journal of Modern Optics**, Taylor & Francis, v. 40, n. 9, p. 1745–1751, 1993.

112 GEA-BANACLOCHE, J. Minimum energy requirements for quantum computation. **Physical Review Letters**, APS, v. 89, n. 21, p. 217901, 2002.

113 PONTE, M. D. *et al.* All-creation and all-annihilation time-dependent pt-symmetric bosonic hamiltonians: an infinite squeezing degree at a finite time. **Physical Review A**, APS, v. 100, n. 1, p. 012128, 2019.

114 DOURADO, R. *et al.* Erratum: All-creation and all-annihilation time-dependent pt-symmetric bosonic hamiltonians: an infinite squeezing degree at a finite time. **Physical Review A**, APS, v. 102, n. 4, p. 049903, 2020.

115 DOURADO, R. d. A.; PONTE, M. de; MOUSSA, M. H. Y. A time-dependent pseudo-hermitian hamiltonian for a cavity mode with pure imaginary frequency. **Physica A**, Elsevier, v. 581, p. 126195, 2021.

116 CIUS, D. *et al.* Enhancement of photon creation through the pseudo-hermitian dynamical casimir effect. **Physica A**, Elsevier, v. 593, p. 126945, 2022.